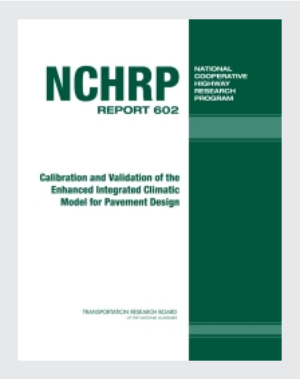

Calibration and Validation of the Enhanced Integrated Climatic Model for Pavement Design

DETAILS

0 pages | | PAPERBACK
ISBN 978-0-309-43602-1 | DOI 10.17226/23098

AUTHORS

NATIONAL COOPERATIVE HIGHWAY RESEARCH PROGRAM

NCHRP REPORT 602

Calibration and Validation of the Enhanced Integrated Climatic Model for Pavement Design

C. E. Zapata AND **W. N. Houston**
ARIZONA STATE UNIVERSITY
Tempe, AZ

Subject Areas
Pavement Design, Management, and Performance

Research sponsored by the American Association of State Highway and Transportation Officials
in cooperation with the Federal Highway Administration

TRANSPORTATION RESEARCH BOARD

WASHINGTON, D.C.
2008
www.TRB.org

NATIONAL COOPERATIVE HIGHWAY RESEARCH PROGRAM

Systematic, well-designed research provides the most effective approach to the solution of many problems facing highway administrators and engineers. Often, highway problems are of local interest and can best be studied by highway departments individually or in cooperation with their state universities and others. However, the accelerating growth of highway transportation develops increasingly complex problems of wide interest to highway authorities. These problems are best studied through a coordinated program of cooperative research.

In recognition of these needs, the highway administrators of the American Association of State Highway and Transportation Officials initiated in 1962 an objective national highway research program employing modern scientific techniques. This program is supported on a continuing basis by funds from participating member states of the Association and it receives the full cooperation and support of the Federal Highway Administration, United States Department of Transportation.

The Transportation Research Board of the National Academies was requested by the Association to administer the research program because of the Board's recognized objectivity and understanding of modern research practices. The Board is uniquely suited for this purpose as it maintains an extensive committee structure from which authorities on any highway transportation subject may be drawn; it possesses avenues of communications and cooperation with federal, state and local governmental agencies, universities, and industry; its relationship to the National Research Council is an insurance of objectivity; it maintains a full-time research correlation staff of specialists in highway transportation matters to bring the findings of research directly to those who are in a position to use them.

The program is developed on the basis of research needs identified by chief administrators of the highway and transportation departments and by committees of AASHTO. Each year, specific areas of research needs to be included in the program are proposed to the National Research Council and the Board by the American Association of State Highway and Transportation Officials. Research projects to fulfill these needs are defined by the Board, and qualified research agencies are selected from those that have submitted proposals. Administration and surveillance of research contracts are the responsibilities of the National Research Council and the Transportation Research Board.

The needs for highway research are many, and the National Cooperative Highway Research Program can make significant contributions to the solution of highway transportation problems of mutual concern to many responsible groups. The program, however, is intended to complement rather than to substitute for or duplicate other highway research programs.

NCHRP REPORT 602

Project 9-23
ISSN 0077-5614
ISBN: 978-0-309-09929-5
Library of Congress Control Number 2008924251

COPYRIGHT PERMISSION

NOTICE

The project that is the subject of this report was a part of the National Cooperative Highway Research Program conducted by the Transportation Research Board with the approval of the Governing Board of the National Research Council. Such approval reflects the Governing Board's judgment that the program concerned is of national importance and appropriate with respect to both the purposes and resources of the National Research Council.

The members of the technical committee selected to monitor this project and to review this report were chosen for recognized scholarly competence and with due consideration for the balance of disciplines appropriate to the project. The opinions and conclusions expressed or implied are those of the research agency that performed the research, and, while they have been accepted as appropriate by the technical committee, they are not necessarily those of the Transportation Research Board, the National Research Council, the American Association of State Highway and Transportation Officials, or the Federal Highway Administration, U.S. Department of Transportation.

Each report is reviewed and accepted for publication by the technical committee according to procedures established and monitored by the Transportation Research Board Executive Committee and the Governing Board of the National Research Council.

The Transportation Research Board of the National Academies, the National Research Council, the Federal Highway Administration, the American Association of State Highway and Transportation Officials, and the individual states participating in the National Cooperative Highway Research Program do not endorse products or manufacturers. Trade or manufacturers' names appear herein solely because they are considered essential to the object of this report.

Published reports of the

NATIONAL COOPERATIVE HIGHWAY RESEARCH PROGRAM

are available from:

Transportation Research Board
Business Office
500 Fifth Street, NW
Washington, DC 20001

and can be ordered through the Internet at:

http://www.national-academies.org/trb/bookstore

Printed in the United States of America

THE NATIONAL ACADEMIES

Advisers to the Nation on Science, Engineering, and Medicine

The **National Academy of Sciences** is a private, nonprofit, self-perpetuating society of distinguished scholars engaged in scientific and engineering research, dedicated to the furtherance of science and technology and to their use for the general welfare. On the authority of the charter granted to it by the Congress in 1863, the Academy has a mandate that requires it to advise the federal government on scientific and technical matters. Dr. Ralph J. Cicerone is president of the National Academy of Sciences.

The **National Academy of Engineering** was established in 1964, under the charter of the National Academy of Sciences, as a parallel organization of outstanding engineers. It is autonomous in its administration and in the selection of its members, sharing with the National Academy of Sciences the responsibility for advising the federal government. The National Academy of Engineering also sponsors engineering programs aimed at meeting national needs, encourages education and research, and recognizes the superior achievements of engineers. Dr. Charles M. Vest is president of the National Academy of Engineering.

The **Institute of Medicine** was established in 1970 by the National Academy of Sciences to secure the services of eminent members of appropriate professions in the examination of policy matters pertaining to the health of the public. The Institute acts under the responsibility given to the National Academy of Sciences by its congressional charter to be an adviser to the federal government and, on its own initiative, to identify issues of medical care, research, and education. Dr. Harvey V. Fineberg is president of the Institute of Medicine.

The **National Research Council** was organized by the National Academy of Sciences in 1916 to associate the broad community of science and technology with the Academy's purposes of furthering knowledge and advising the federal government. Functioning in accordance with general policies determined by the Academy, the Council has become the principal operating agency of both the National Academy of Sciences and the National Academy of Engineering in providing services to the government, the public, and the scientific and engineering communities. The Council is administered jointly by both the Academies and the Institute of Medicine. Dr. Ralph J. Cicerone and Dr. Charles M. Vest are chair and vice chair, respectively, of the National Research Council.

The **Transportation Research Board** is one of six major divisions of the National Research Council. The mission of the Transportation Research Board is to provide leadership in transportation innovation and progress through research and information exchange, conducted within a setting that is objective, interdisciplinary, and multimodal. The Board's varied activities annually engage about 7,000 engineers, scientists, and other transportation researchers and practitioners from the public and private sectors and academia, all of whom contribute their expertise in the public interest. The program is supported by state transportation departments, federal agencies including the component administrations of the U.S. Department of Transportation, and other organizations and individuals interested in the development of transportation. **www.TRB.org**

www.national-academies.org

COOPERATIVE RESEARCH PROGRAMS

CRP STAFF FOR NCHRP REPORT 602

Christopher W. Jenks, *Director, Cooperative Research Programs*
Crawford F. Jencks, *Deputy Director, Cooperative Research Programs*
Edward T. Harrigan, *Senior Program Officer*
Eileen P. Delaney, *Director of Publications*
Hilary Freer, *Senior Editor*

NCHRP PROJECT 9-23 PANEL
Field of Materials and Construction—Area of Bituminous Materials

Larry A. Scofield, *American Concrete Pavement Association, Mesa, AZ* (Chair)
Hussain Bahia, *University of Wisconsin–Madison, Madison, WI*
Luis Julian Bendana, *New York State DOT, Albany, NY*
E. Ray Brown, *US Army Corps of Engineers, Vicksburg, MS*
Dale S. Decker, *Eagle, CO*
Jon A. Epps, *Granite Construction Inc., Sparks, NV*
Eric E. Harm, *Illinois DOT, Springfield, IL*
Dallas N. Little, *Texas A&M University, College Station, TX*
Carl L. Monismith, *University of California–Berkeley, Berkeley, CA*
James A. Musselman, *Florida DOT, Gainesville, FL*
Linda M. Pierce, *Washington State DOT, Olympia, WA*
John Bukowski, *FHWA Liaison*
Thomas Harman, *FHWA Liaison*
Larry L. Michael, *Other Liaison*
Frederick Hejl, *TRB Liaison*

FOREWORD

By Edward T. Harrigan
Staff Officer
Transportation Research Board

This report summarizes the results of research to evaluate, calibrate, and validate the Enhanced Integrated Climatic Model (EICM) incorporated in the original Version 0.7 (July 2004 release) of the *Mechanistic-Empirical Pavement Design Guide* (MEPDG) software with measured materials data from the Long-Term Pavement Performance Seasonal Monitoring Program (LTPP SMP) pavement sections. The report further describes subsequent changes made to the EICM to improve its prediction of moisture equilibrium for granular bases. The report will be of particular interest to pavement design engineers in state highway agencies and industry.

The EICM is a one-dimensional coupled heat and moisture flow model initially developed for the FHWA and adapted for use in the MEPDG developed under NCHRP Projects 1-37A and 1-40. In the MEPDG, the EICM is used to predict or simulate the changes in behavior and characteristics of pavement and unbound materials in conjunction with natural cycles of environmental conditions that occur over many years of service.

The objective of research conducted in NCHRP Project 9-23, "Environmental Effects in Pavement Mix and Structural Design Systems," and reported here was to evaluate, calibrate, and validate the moisture predictive capabilities of the EICM. In particular, the equilibrium moisture condition in the EICM used in the Version 0.7 MEPDG was based on a soil suction model that depends on the water table depth and on a soil-water characteristic curve (SWCC) model that is functionally dependent on simple soil properties. Prior research indicated that sources of error in the prediction of moisture content were primarily derived from the implementation of the Suction Model in the EICM and that a more accurate approach to soil suction computations would be through the use of the Thornthwaite Moisture Index (TMI). With the TMI approach, lateral infiltration is balanced with evaporation for a project-specific climatic region, potentially leading to significant improvement in the prediction of the equilibrium moisture for granular bases.

NCHRP Project 9-23 was specifically aimed at improving the predictive capabilities of the EICM through the analysis of data from the LTPP SMP and other relevant field experiments. The variables required to run and validate the EICM were identified, as well as the variables needed to select the pavement sections for the analysis. A statistically based experiment for the calibration and validation of the EICM was designed, and site investigation and laboratory testing of materials from 30 LTPP sections were completed.

Results of the statistical analysis of the results of the EICM validation confirmed that all its component models and, in particular, the Suction Model needed improvement and calibration. The individual models were calibrated with the best dataset available, gathered from the field sites visited during the project and from the LTPP database. Individual vali-

dation of the models showed improvement in all predictions. Finally, the individual EICM models were revised to incorporate the TMI formalism and then recalibrated and validated. This substantially improved version of the EICM was incorporated in Version 1.0 (June 2007 release) of the MEPDG software developed in NCHRP Project 1-40D.

This report is an abridgement of the contractor's final report for Part II of NCHRP 9-23. The full text of the Part II final report and its six appendixes listed below are available online through a link at http://www.trb.org/TRBNet/ProjectDisplay.asp?ProjectID=959:

1. Appendix A. Detailed Field Information
2. Appendix B. Measured Soil Water Characteristic Curves
3. Appendix C. Measured Moisture And Field Density For Field Sites
4. Appendix D. TDR Moisture Content Data From Database
5. Appendix E. Measured Versus Predicted Water Content—Stage IV Runs
6. Appendix F. Sections With Measured TDR Moisture Content That Do Not Correspond To Equilibrium Conditions.

CONTENTS

CHAPTER 1

Introduction

1.1 Statement of the Problem

The satisfactory design of a layered pavement structure requires the execution of numerous complex tasks and must usually be done iteratively. Two important aspects of this process are (1) the use of a computational model to quantify environmental effects over the design period and (2) the translation of changes in pavement temperature and moisture content into changes in material moduli and other physical properties. Environmental conditions play a significant role in the change in pavement material properties and hence pavement response.

The Enhanced Integrated Climatic Model (EICM) is a one-dimensional coupled heat and moisture flow model initially developed for the FHWA and adapted for use in the *Mechanistic-Empirical Pavement Design Guide* (MEPDG) developed under NCHRP Project 1-37A (software Version 0.7, July 2004 release). In the MEPDG, the EICM is used to predict or simulate the changes in behavior and characteristics of pavement and unbound materials in conjunction with environmental conditions over many years of service.

The objective of research conducted in NCHRP Project 9-23, "Environmental Effects in Pavement Mix and Structural Design Systems," and reported here was to evaluate, calibrate, and validate the moisture predictive capabilities of the EICM. In particular, the equilibrium moisture condition in the EICM is based on a suction model that depends on the water table depth and on a soil-water characteristic curve (SWCC) model that is functionally dependent on simple soil properties. Prior research indicated that sources of error in the prediction of moisture content were primarily derived from the implementation of the Suction model in the EICM and that a more accurate approach to suction computations would be through the use of the Thornthwaite Moisture Index (TMI) in place of the use of the water table depth. With the TMI approach, lateral infiltration is balanced with evaporation for a project-specific climatic region. Although this approach would have an empirical component, it might significantly improve the prediction of the equilibrium moisture for the granular bases, a concern raised by the independent reviewers of the MEPDG in NCHRP Project 1-40A (Brown, 2005).

NCHRP Project 9-23 was specifically aimed at improving the predictive capabilities of the EICM through the analysis of data from the Long-Term Pavement Performance Seasonal Monitoring Program (LTPP SMP) and other relevant field experiments. The variables required to run and validate the EICM were identified, as well as the variables needed to select the pavement sections for the analysis. A statistically based experiment for the calibration and validation of the EICM was designed, and site investigation and laboratory testing of materials from thirty LTPP sections were completed. Finally, based on these results, the individual EICM models were revised, recalibrated, and validated.

Results of the statistical analysis of the results of the EICM validation confirmed that all its component models and, in particular, the suction model, were in need of improvement and calibration. The individual models were calibrated with the best dataset available gathered from the field sites visited during the project and from the LTPP database. Individual validation of the models showed improvement in all predictions. The improved EICM was incorporated in Version 1.0 (June 2007 release) of the MEPDG software developed in NCHRP Project 1-40D.

1.2 Current Knowledge

1.2.1 Enhanced Integrated Climatic Model

Early versions of the EICM comprised three major components:

- The Infiltration and Drainage Model (ID Model) developed at Texas A&M University;

- The Climatic-Materials-Structural Model (CMS Model) developed at the University of Illinois; and,
- The Frost Heave and Thaw Settlement Model (CRREL Model) developed at the United States Army Cold Regions Research and Engineering Laboratory (CRREL).

The EICM output included temperature, moisture content, and freeze/thaw depths throughout the entire pavement profile and was applied to either hot-mix asphalt concrete (HMAC) or Portland cement concrete (PCC) pavements. Modifications to the EICM spanned the final decade of the last century (Lytton et al., 1990; Larson and Dempsey, 1997). In July 1999, the latest version of the EICM was Version 2.1, as developed by Larson and Dempsey at the University of Illinois. Version 2.1 was selected for use in the MEPDG. In 1999, a series of checks of the predictive accuracy of the EICM Version 2.1 was carried out at Arizona State University (ASU) with data for 10 LTPP SMP sites. Agreement between predicted and Time Domain Reflectometry (TDR)-measured moisture contents was judged unsatisfactory, and work began at ASU to increase the predictive accuracy of the EICM. Recommended modifications to Version 2.1 included use of the following:

- New functional fits for the SWCCs;
- New relationships between the SWCCs and material index properties;
- New hydraulic conductivity functions for saturated (k_{sat}) and unsaturated (k_{unsat}) materials; and
- Employment of equilibrium moisture content as an input value.

A finding not fully anticipated was that the seasonal variations in moisture were relatively small compared with the changes in moisture between the initial placement condition and the "equilibrium" or average moisture achieved after a few years of service. The question arose as to whether it was appropriate to input the equilibrium moisture in the general case, because, for example, these equilibrium moisture contents would typically not be known for new pavement construction where instrumentation is unavailable. The ultimate conclusion was that the EICM should, in fact, be required to predict the equilibrium moisture contents. However, the emphasis for the research reported herein was on predicting seasonal oscillations about the equilibrium or mean moisture contents, given that, as stated above, these seasonal oscillations were typically fairly minor, in the absence of open cracks in the pavement.

A further goal of NCHRP Project 9-23 was to evaluate whether or not improvements to the model were adequate and whether or not further improvements would be necessary. Decisions on how to make any needed improvement were to be based on the results of sampling and testing at the LTPP SMP sites.

1.2.2 Moisture Content Changes

Moisture content changes that occur after construction of the pavement section generally fall into three categories:

1. Increase or decrease from the initial condition (typically near optimum) to the equilibrium or *average* condition,
2. Seasonal fluctuation about the average or normal moisture condition due to infiltration of rainfall through cracks in the bound layer(s) and due to fluctuations in the groundwater table (GWT) in the absence of freeze/thaw, and
3. Variations in moisture content due to freeze/thaw.

Witczak et al. (2000) showed that the effect on resilient moduli, M_R, due to Categories 1 and 3 could be quite significant. However, Category 2 results, i.e., seasonal changes in moisture in the absence of freeze/thaw, were found to produce typically insignificant changes in M_R. As a consequence of this finding, it was tentatively decided for the MEPDG to assume that there are no cracks in newly constructed pavements and that the GWT does not fluctuate during the design period. After making these simplifying assumptions, the role of the EICM with respect to moisture content was limited to the prediction of changes under Categories 1 and 3.

The MEPDG research team carried out a limited validation study (Witczak et al., 2000) with data from 10 LTPP SMP sections. However, the comparison between the EICM-predicted and the TDR-measured moisture contents was made in this study before the finding that seasonal changes in moisture content in the absence of freeze/thaw produced negligible changes in M_R had been made. Therefore, these comparisons were repeated as a part of NCHRP Project 9-23. However, the full dataset from all the LTPP SMP sections was now used, and emphasis was placed on prediction of changes from the initial to the equilibrium condition.

The prediction of moisture content is a means, not an end. It is the effect of moisture changes on the mechanical properties of the pavement layers, such as M_R, that is of primary interest. Therefore, in order to decide if a given level of predictive accuracy on moisture content is acceptable or not, it was necessary to translate a typical error in moisture content into a typical error in modulus or another mechanical property and then estimate the effect on performance.

1.2.3 Effects of Temperature

Temperature is the link between the environmental effects on unbound layers and bound layers. Temperature change directly controls freezing and thawing, which in turn produce dramatic changes in the M_R of unbound layers. Moduli of bound layers, particularly HMA layers, are likewise directly controlled by temperature, which also controls thermal crack-

ing of the pavement. Furthermore, the coupling of temperature and time produces aging effects in the pavement layers. Thus, temperature is a key variable in all of these processes, which control the response of pavement sections to traffic loads, and the EICM is required to predict temperature and its seasonal variation over the pavement design life accurately.

1.3 Organization of the Report

This report is an abridgement of the final report for Part II of NCHRP 9-23. Chapter 2 presents the experimental design for calibration and validation of the EICM. The parameters needed to run the models are presented, and the selection process of the sections chosen for site investigation is presented. Chapter 3 summarizes the laboratory and field testing program required to obtain the necessary data for calibration and validation. Chapter 4 discusses the results of the EICM calibration and validation. Chapter 5 presents the development, calibration, and validation of new models required to improve the predictive accuracy of the EICM. Finally, Chapter 6 summarizes the findings and conclusions of the study. The full text of the Part II final report and its six appendices are available online at http://www.trb.org/TRBNet/ProjectDisplay.asp?ProjectID=959.

CHAPTER 2

Experiment Design for Calibration and Validation of the ICM Version 2.6 (EICM)

2.1 Introduction

Preparation of a detailed, statistically based experiment design for the calibration and validation of the EICM began with the identification of data elements needed for its thorough analysis. These data elements fell into three categories:

1. Parameters required to run the EICM;
2. Data required for validation of the EICM; and
3. Data required to select pavement sections for analysis.

Identification of the parameters required to run and validate the EICM was important during the experiment design because pavement sections without these parameters were eliminated from consideration. Variables required for running the EICM included location, pavement profile, HMA or PCC material properties, compacted material properties, and in situ material properties. The parameter required for validation of the EICM was the measured moisture content.

Additional data elements were needed to help select appropriate pavement sections. These included location, climatic condition, and in situ material properties. Examination of pavement cracking data ensured that the pavement sections did not have excessive water flow through the pavement.

The experiment design was divided into two parts. The first part included pavement sections that were analyzed with the results compared with direct, in situ measurements. These sites were visited during the course of the project to obtain the direct measurements. The second part included pavement sections analyzed with the results compared with previously measured values obtained from available databases.

2.2 Parameters Needed for the Calibration and Validation of the EICM

2.2.1 Input Parameters Needed to Run and Evaluate the EICM

A large number of input parameters are needed to run the EICM. The exact number is determined by the level of accuracy desired in the pavement analysis. Three hierarchical levels of analysis are defined in the MEPDG. Level 1 is the most accurate; it requires that a complete set of measured variables be input by the user. Levels 2 and 3 are more approximate; their use requires much less directly measured data. The EICM internally generates values for missing data by using correlations with input data. Some data must be input for each unbound layer. In some cases, this input data may be only index properties, such as gradation and plasticity. In the tables that follow, parameters that can either be input by the user or internally generated by the EICM are shown in bold. The parameters not in bold are internal to the EICM and never require user input.

Table 1 describes the input parameters necessary to initialize the model and define the climatic and boundary conditions. These inputs are required for Levels 1, 2, and 3.

The latitude, longitude, and elevation are used to define the climatic conditions. These parameters trigger the climatic module, which has a database of nearly 800 weather stations throughout the continental Unites States and Canada from the National Climatic Data Center (NCDC). Users may select the station or stations they consider to be the most representative of the site. The weather station files associated with Version 1.0 of the MEPDG software contain approximately 9 years of hourly climatic data; earlier versions were limited to about 4 years. The climatic information available from each station includes the following:

- Hourly air temperature,
- Hourly precipitation,

Table 1. Input parameters for model initialization and climatic/boundary conditions required for Levels 1, 2, and 3.

Parameter	Description/Application
• **Base/subgrade construction completion date** • **Design period**	Input parameters required for model initialization and for controlling the length of the analysis period.
• **Site latitude** • **Site longitude** • **Site elevation**	Input parameters needed to define climatic conditions.
• **Groundwater table depth**	Input parameter needed as a boundary condition.
• **Layer thickness**	Needed to define the pavement system profile. It is required to input the thickness for every layer to be considered.

- Hourly wind speed,
- Hourly percentage sunshine, and
- Hourly relative humidity.

These data are needed by the EICM for several calculations. The air temperature is required by the heat balance equation to calculate long-wave radiation emitted by the air and convective heat transfer from pavement surface to air. In addition to the heat calculations, the temperature data are used to define the freeze-and-thaw episodes within the analysis period.

Heat fluxes resulting from precipitation and infiltration into the pavement structure are not considered in formulating the surface heat flux boundary conditions. The role of the precipitation under these circumstances is not entirely clear, and its incorporation in the energy balance has not been attempted. However, precipitation is needed to compute the amount of snow: the precipitation that falls during a month when the mean temperature is less than the freezing temperature of water is assumed to fall as snow.

Wind speed is required in the computations of the convection heat transfer coefficient at the pavement surface. The percentage sunshine is needed for calculation of heat balance at the surface of the pavement.

The GWT depth was intended to be the best estimate of the annual average depth; its determination from profile characterization borings prior to design was recommended.

Layer thicknesses are assigned to homogeneous layers, i.e., those whose material properties are consistent throughout.

Table 2 lists the required HMA or PCC material input properties. Direct measurements of these parameters are recommended for Level 1 and 2 designs. Use of default values is acceptable—if not desirable—for any level of design, if the entire dataset is not directly measured.

Thermal conductivity, *K,* is the quantity of heat that flows normally across a surface of unit area per unit time and unit temperature gradient normal to the surface. The moisture content affects the thermal conductivity of HMA or PCC. If the moisture content is low, the differences between unfrozen, freezing, and frozen thermal conductivity are small. Only when the moisture content is high (i.e., greater than 10%) does the thermal conductivity vary substantially from unfrozen to freezing to frozen. The thermal conductivity of HMA layers does not vary with varying moisture content as does that of unbound layers.

The heat or thermal capacity is the actual amount of heat energy, *Q*, necessary to change the temperature of a unit mass by one degree.

The surface short wave absorptivity of the pavement depends on pavement composition, color, and texture. The surface short wave absorptivity directly correlates with the amount of available solar energy absorbed by the pavement surface. Generally, the lighter and more reflective the surface is, the lower the short wave absorptivity will be.

Table 3 lists the input parameters for compacted unbound materials. For Level 1 and 2 designs, carefully measured values of maximum dry unit weight (γ_{dmax}), optimum moisture content (w_{opt}), and specific gravity of the solids (G_s) are required for each appropriate layer. All other mass-volume parameters can be precisely computed from these three quantities. If all three of these values cannot be provided, a Level 3 design is rec-

Table 2. Input parameters required for HMAC and PCC material properties.

Level	Required Properties	Options for Determination
1	• **Thermal conductivity** • **Heat capacity** • **Surface short wave absorptivity**	Direct measurements are recommended at this level. However, default property values are available for user convenience.
2	Same as Level 1	Direct measurements or default values can be combined and used.
3	Same as Level 1	Default values are available.

Table 3. Input parameters required for compacted material properties.

Level	Required Parameters	Options for Determination
1	• **Specific Gravity**	Direct measurement required.
	• **Saturated Hydraulic Conductivity**	Direct measurement required.
	• **Maximum Dry Unit Weight**	Direct measurement required.
	• **Dry Thermal Conductivity**	Direct measurement is recommended at this level. However, default values are available for user convenience in case the property is not determined by direct measurements.
	• **Dry Heat Capacity**	Direct measurement is recommended at this level. However, default values are available for user convenience in case the property is not determined by direct measurements.
	• **Plasticity Index**	Direct measurement required.
	• **% Passing #200** • **% Passing #4** • **Diameter D_{60}**	Direct measurement required.
	• **Optimum Gravimetric Water Content**	Direct measurement required.
	• **Soil-Water Characteristic Curve Parameters**	Direct measurement required.
2	• **Specific Gravity**	Direct measurement required.
	• **Saturated Hydraulic Conductivity**	Direct measurement required.
	• **Maximum Dry Unit Weight**	Direct measurement required.
	• **Dry Thermal Conductivity** • **Heat Capacity**	Direct measurements or default values can be combined and used.
	• **Plasticity Index**	Direct measurement required.
	• **% Passing #200** • **% Passing #4** • **Diameter D_{60}**	Direct measurement required.
	• **Optimum Gravimetric Water Content**	Direct measurement required.
3	• Specific Gravity	Direct measurement not required.
	• Saturated Hydraulic Conductivity	Direct measurement not required.
	• Maximum Dry Unit Weight	Direct measurement not required.
	• Dry Thermal Conductivity • Heat Capacity	Default values available.
	• **Plasticity Index**	Direct measurement required.
	• **% Passing #200** • **% Passing #4** • **Diameter D_{60}**	Direct measurement required.
	• Optimum Volumetric Water Content	Direct measurement not required.

ommended. Level 3 design only requires measurement of index properties from the grain size distribution curve, Plasticity Index (*PI*), and percent passing the #200 sieve (P_{200}).

The SWCC is defined as the variation of water storage capacity within the macro- and micro-pores of a soil, with respect to suction (Fredlund et al., 1995). This relationship is generally plotted as the variation of the water content (gravimetric, volumetric, or degree of saturation) with soil suction. Several mathematical equations have been proposed to represent the SWCC and some studies have been conducted to compare the different equations available (Leong and Rahardjo, 1996; Zapata, 1999). The EICM made use of the equation proposed by Fredlund and Xing in 1994 (Fredlund and Xing, 1994), which has shown good agreement with an extended database.

Because of the difficulty surrounding direct measurement of soil suction, only Level 1 design requires input of parameters from direct measurement of SWCC. Level 2 and 3 analyses use the results of recent studies on the SWCC. In these studies, the fitting parameters of the Fredlund and Xing equation were correlated with soil index properties (Zapata, 1999). Therefore, for Levels 2 and 3 the user is required to input simple soil index properties that are internally correlated by the EICM with the SWCC parameters.

Table 4. Input parameters required for natural, in situ material properties for Levels 1, 2, and 3.

Required Properties	Options for Determination
• Specific Gravity	Direct measurement not required.
• Saturated Hydraulic Conductivity	Direct measurement not required.
• Maximum Dry Unit Weight	Direct measurement not required.
• Dry Thermal Conductivity • Heat Capacity	Direct measurements or default values can be combined and used.
• **Plasticity Index**	Direct measurement required.
• **% Passing #200** • **% Passing #4** • **Diameter D_{60}**	Direct measurement required.
• Optimum Gravimetric Water Content	Not required.

Table 4 describes the input parameters for naturally occurring, in situ layers lying below the compacted layers. No distinction is made among Levels 1, 2, and 3. The properties of these lower layers are important to the response to load, but not as important as those of the overlying bound and unbound compacted layers. Therefore, more approximate algorithms are acceptable for the in situ materials, and it is recommended that only *PI*, P_{200}, P_4, and D_{60} be measured for in situ layers.

2.2.2 Variables Needed for the Validation of the EICM

The variables needed to validate the EICM included the following:

- Temperature distribution throughout the pavement profile with time,
- Moisture content measurements throughout the pavement profile with time,
- Frost penetration, and
- California Bearing Ratio (CBR) (desirable for purposes of improving existing correlations, but not necessary).

Temperature is an important factor affecting asphalt binder stiffness and consequently the dynamic modulus (E*) of HMA mixes. Because the modulus of the HMA layers within the pavement structure affect the overall pavement response, it is important to account properly for the temperature as a function of time and depth. The EICM generates a frequency distribution of pavement temperature as a function of time and depth.

Moisture content measurements throughout the pavement profile were likewise needed to compare with moisture contents predicted by the EICM. Moisture content is an important parameter that is required to compute a set of adjustment factors for the resilient modulus M_R, that (1) vary by time and position within the pavement and (2) account for the effects of environmental parameters and conditions such as moisture content changes, freezing, thawing, and recovery from thawing. The unbound material layer adjustment factor, F_{env}, varies with position within the pavement structure and with time throughout the analysis period. F_{env} is a coefficient that is multiplied by the resilient modulus at optimum conditions (M_{Ropt}) to obtain M_R as a function of position and time. The values of M_{Ropt} and thus M_R are calculated in other components of the MEPDG software.

Finally, CBR values were needed for calibrating some of the correlations internal to the EICM.

2.2.3 Variables Needed for Site Selection

In selecting field sites for analysis, additional data were required to ensure acceptable statistical representation. These data included the following:

- Location;
- Climatic conditions,
  - Mean annual air temperature,
  - Annual precipitation;
- Frost penetration depth;
- Subgrade material properties,
  - Gradation,
  - Plasticity; and
- Pavement cracking.

The location referred to here is more general than that described in Section 2.2.1. The state or province of each prospective site was determined in an effort to ensure good geographical distribution, which also ensures a good statistical representation.

A good distribution over the different climatic zones in the United States and Canada was also important to this phase of the project. Mean annual air temperature and annual precipitation data were used as indicators of climatic zones. Both variables were averaged over a 10-year period (1987-1996) to obtain an unbiased estimate. Frost penetration is, of course, related to climatic conditions, but was considered separately, given its relationship with soil type.

A variety of subgrade materials was also desired. Therefore, the subgrade gradation, specifically the percent passing the #200 sieve, was determined for each site. For fine-grained subgrades, plasticity was also examined.

Reported pavement cracking was reviewed to eliminate sites where cracks could allow water flow into the pavement structure. Such flow adds to the moisture content in a way for which the EICM cannot precisely compensate. Using pavement sections with excessive cracking would thus bias the calibration of the EICM.

Cracking information was based on a 500-ft section length. It was assumed that (1) moderate- and high-severity longitudinal, transverse, and fatigue (alligator) cracking contributed the most to infiltration of water through the pavement section profile and (2) longitudinal and fatigue cracking were mostly present in the wheel path, which can be considered approximately 2.5-feet wide. For two wheel paths, the area subjected to cracking within a section would be $500\ \text{ft} \times 2.5\ \text{ft} \times 2 = 2500\ \text{ft}^2$.

Fatigue cracking is measured in units of area, but longitudinal and transverse cracking are measured in units of length. In order to determine a total cracking percentage, the longitudinal and transverse cracking information was converted to an equivalent area by multiplying the length of cracking by a width of 1 foot, assuming that the cracking affects 6 inches on each side of the crack. To combine moderate- and high-severity cracking data into a total cracking percentage, moderate cracking data were given a weighting factor of 0.5. Any section was eliminated if more than 25% of the area subjected to cracking was moderately or severely cracked.

Cracking was considered in the period during which moisture content measurements were made. However, in determining which field sites would be visited for direct measurements, the most recent cracking data available were used.

2.2.4 Available Databases

After the necessary variables were identified, the databases available for use in the project were determined. The search narrowed to the following:

1. LTPP Database,
2. MnRoad,
3. WesTrack, and
4. Arizona Department of Transportation (ADOT) Database

2.2.4.1 LTPP Database

The LTPP program is a 20-year investigation of pavement performance initiated in 1987 as a part of the Strategic Highway Research Program (SHRP). It has been managed by FHWA since 1992. Data characterizing the pavement structure, materials, and performance are being collected for test sections on in-service highways throughout the United States and Canada. Within LTPP, the Seasonal Monitoring Program (SMP) involves a more intensive level of data collection targeted at advancing the understanding of temporal variations in the pavement structure.

2.2.4.2 MnRoad

MnRoad is an experimental test track built by the Minnesota Department of Transportation. The track consists of forty 500-ft-long sections constructed between 1992 and 1994 along I-94, 40 miles northwest of Minneapolis-St. Paul, and loaded with actual highway traffic since that time. MnRoad has evaluated the effects of heavy vehicles on pavements, seasonal changes in paving materials, and improvements in the design and performance of low-volume roads.

2.2.4.3 WesTrack

WesTrack was an experimental road test sponsored by FHWA and located at the National Automotive Test Center near Silver Spring, Nevada. Construction began in 1995 and trafficking in 1996 with driverless trucks. WesTrack consists of 26 HMA pavement sections designed to evaluate the effect of variations in binder content, gradation, and density on the development of permanent deformation and fatigue cracking.

2.2.4.4 ADOT Database

ADOT, in cooperation with FHWA, monitored 37 field sites in Arizona over a period of 5 years in the late 1970s. Temperature, moisture, and deflection data were gathered in addition to material property data. Either temperature *or* moisture content measurements were recorded for any particular site. The study objective was to quantify environmental factors and their relation to the structural characteristics of pavements.

2.2.5 Selection of the Sections for Analysis

Field pavement sections that met the requirements for selection were divided into two groups: those analyzed in the desk analysis and compared with recorded data in the available databases, and those visited to make direct in situ measurements.

Table 5 lists all sites included in the study and indicates to which group the site belongs. Figure 1 presents the location of all field sites.

2.2.5.1 Selection of Sites for Comparison with Previously Recorded Data

A preliminary site selection was made on the basis of the parameters discussed above. Fifty-four sections from the

Table 5. List of selected sites.

Section ID	State	Originating Project	To be Visited	To be Compared to Historical Data
010101	AL	LTPP	Y	Y
010102	AL	LTPP	N	Y
040113	AZ	LTPP	N	Y
040114	AZ	LTPP	N	Y
040215	AZ	LTPP	Y	Y
041024	AZ	LTPP	N	N
052042	AR	LTPP	Y	N
063042	CA	LTPP	N	Y
081053	CO	LTPP	Y	Y
091803	CT	LTPP	Y	Y
100102	DE	LTPP	Y	Y
120107	FL	LTPP	N	N
131005	GA	LTPP	N	Y
131031	GA	LTPP	N	Y
133019	GA	LTPP	Y	Y
161010	ID	LTPP	Y	Y
161021	ID	LTPP	N	N
183002	IN	LTPP	N	Y
204054	KS	LTPP	Y	Y
220118	LA	LTPP	Y	N
231026	ME	LTPP	N	Y
241634	MD	LTPP	N	Y
271018	MN	LTPP	N	N
274040	MN	LTPP	N	Y
281016	MS	LTPP	Y	Y
308129	MT	LTPP	N	Y
310114	NE	LTPP	Y	Y
313018	NE	LTPP	N	Y
320101	NV	LTPP	N	Y
320204	NV	LTPP	Y	Y
331001	NH	LTPP	N	Y
350105	NM	LTPP	Y	N
351112	NM	LTPP	Y	Y
360801	NY	LTPP	N	Y
364018	NY	LTPP	Y	Y
370201	NC	LTPP	N	Y
370205	NC	LTPP	Y	Y
370208	NC	LTPP	N	Y
370212	NC	LTPP	N	Y
371028	NC	LTPP	N	Y
390204	OH	LTPP	Y	Y
404165	OK	LTPP	N	Y
421606	PA	LTPP	N	Y
469187	SD	LTPP	N	Y
481060	TX	LTPP	Y	Y
481068	TX	LTPP	N	Y
481077	TX	LTPP	Y	Y
481122	TX	LTPP	N	Y
483739	TX	LTPP	N	Y
484142	TX	LTPP	N	Y
484143	TX	LTPP	N	Y
491001	UT	LTPP	N	Y
493011	UT	LTPP	N	Y
501002	VT	LTPP	N	Y
510113	VA	LTPP	N	Y
510114	VA	LTPP	Y	Y
533813	WA	LTPP	N	Y
561007	WY	LTPP	N	Y
831801	Manitoba	LTPP	N	Y

(*continued on next page*)

Table 5. (Continued).

Section ID	State	Originating Project	To be Visited	To be Compared to Historical Data
833802	Manitoba	LTPP	N	Y
871622	Ontario	LTPP	N	N
893015	Quebec	LTPP	N	Y
501681	VT	LTPP	Y	N
420603	PA	LTPP	Y	N
416011	OR	LTPP	Y	N
473101	TN	LTPP	BACKUP	N
562020	WY	LTPP	Y	N
562019	WY	LTPP	BACKUP	N
307066	MT	LTPP	Y	N
537322	WA	LTPP	BACKUP	N
531007	WA	LTPP	Y	N
MnRd1	MN	MnRd	Y	Y
MnRd2	MN	MnRd	N	Y
Wstk1	NV	WesTrack	Y	Y
Wstk2	NV	WesTrack	N	Y
ADOT1	AZ	ADOT	N	Y
ADOT14	AZ	ADOT	N	Y
087035	CO	LTPP	Y	N

LTPP database met the criteria and were included in this study. Two sites each at MnRoad and WesTrack and from the ADOT database were included in this study. In total, 60 sites were analyzed and the resulting data were compared with previously recorded data. These 60 sites were representative of the available data, which met all the criteria discussed above.

Figure 2 shows the distribution of these sites with respect to the selection criteria. Sites were located in 31 states and 2 Canadian provinces. Twenty-three sites were in areas with high (greater than 15°C) mean annual air temperature, *Maat*, and 37 sites were in areas with low *Maat*. Nineteen sites were in areas with periods of significant soil freezing. Thirty-two

Figure 1. Map of sites selected to validate the EICM.

					Pavement type			
					HMAC		PCC	
					GWT depth			
					Deep	Shallow	Deep	Shallow
High Maat > 15°C	High Precipitation > 800 mm	Frozen	Coarse Sg					
			Fine Sg	High PI				
				Low PI				
		No freeze	Coarse Sg		1	3		1
			Fine Sg	High PI		3	4	1
				Low PI				1
	Low Precipitation < 800 mm	Frozen	Coarse Sg					
			Fine Sg	High PI				
				Low PI				
		No freeze	Coarse Sg		4	1	1	
			Fine Sg	High PI				
				Low PI	1	1		1
Low Maat < 15°C	High Precipitation > 800 mm	Frozen	Coarse Sg			4		2
			Fine Sg	High PI				
				Low PI				
		No freeze	Coarse Sg			4		2
			Fine Sg	High PI				1
				Low PI	2	1		2
	Low Precipitation < 800 mm	Frozen	Coarse Sg		1	3		2
			Fine Sg	High PI		2		1
				Low PI		3		1
		No freeze	Coarse Sg			4	1	
			Fine Sg	High PI		1		
				Low PI				

Figure 2. Matrix to select sites with recorded data.

sites were in areas with high mean annual precipitation (defined as greater than 800 mm per year) and 28 in areas with low mean annual precipitation.

There was also a good distribution of subgrade conditions. Thirty-four sites had coarse-grained subgrades (defined as less than 50% passing the #200 sieve); 26 sites had fine-grained subgrades. Of these 26 sites, 13 had high plasticity index, *PI* (defined as greater than 20) and 13 had low *PI*.

Thirty-nine sites were HMA pavements; 21 were PCC.

2.2.5.2 Selection of Sites Visited and Compared with Directly Measured Values

Thirty sites were selected for field visits. Twenty of these sites were used to validate the recorded data found in the databases. Based on the criteria discussed above, 10 new sites were chosen to provide additional data where needed. Figure 3 shows the distribution of these sites with respect to the selection criteria.

The 20 validation sites were chosen from the 60 sites selected for comparison with historical data. First, the original 60 sites were examined with regard to the dates of the historical data. Only sites where data collection concluded in 1998 or later were considered for a site visit. Next, the most recent cracking data were examined to best determine the present condition of the pavement. A total cracking percentage was calculated as described previously, and only sites with less than 25% cracking were considered for a site visit.

From the remaining sections, selection was completed in order to represent the original distribution. In particular, the distributions of low and high *Maat*, low and high precipitation, frozen soil and non-frozen soil, coarse and fine subgrade, high and low plasticity index, and HMA and PCC concrete in the validation sections were kept as close as possible to those of the original 60 sections.

Based on the conditions described above, 10 new sections were chosen to provide additional data where needed. Since the original 60 had a rather large proportion of PCC sections (35%), all 10 new sections selected were HMA pavements.

					Pavement type			
					HMAC		PCC	
					GWT depth			
					Deep	Shallow	Deep	Shallow
High Maat > 15°C	High Precipitation > 800 mm	Frozen	Coarse Sg					
			Fine Sg	High PI				
				Low PI				
		No freeze	Coarse Sg		1	1		
			Fine Sg	High PI	1	1	1	
				Low PI		1		1
	Low Precipitation < 800 mm	Frozen	Coarse Sg					
			Fine Sg	High PI				
				Low PI				
		No freeze	Coarse Sg		1		1	
			Fine Sg	High PI	1			
				Low PI		1		
Low Maat < 15°C	High Precipitation > 800 mm	Frozen	Coarse Sg		1	1		1
			Fine Sg	High PI				
				Low PI				
		No freeze	Coarse Sg		1	1		
			Fine Sg	High PI	1			1
				Low PI	1			1
	Low Precipitation < 800 mm	Frozen	Coarse Sg		1	1		
			Fine Sg	High PI		1		
				Low PI	1	1		
		No freeze	Coarse Sg			1	1	
			Fine Sg	High PI	1	1		
				Low PI	1			

Figure 3. Matrix to select sites to be visited.

CHAPTER 3

Field and Laboratory Sampling and Testing

3.1 Field Sampling and Testing

Sites originally selected for field visits included 28 LTPP sites, the MnRoad test facility, and the WesTrack test facility for a total of 30 sites. Because of rainfall, very shallow groundwater, and saturated layers encountered at the time of the field visit, no sampling was performed at the site in Delaware, Ohio. Out of the remaining 29 sites, 18 had TDR instrumentation.

In general, three locations, 3 feet apart, located along the center of the outer lane of the highway were cored, and soil samples were collected representing each unbound layer beneath the pavement. At the 18 LTPP SMP sites, the three locations were cored near the TDR instrumentation hole just outside the respective test section, in the transition zone either at the start or end of the section. At non-SMP sites, there was no TDR instrumentation and, therefore, sampling was performed in one of the two transition zones approximately 8 to 10 feet from the section. Because of reconstruction, resurfacing, or decommissioning of the SMP, TDR instrumentation could not be physically located at several sites. In such cases, the former TDR location was located with data in the LTPP database. This database provided the coordinates of the TDR with respect to the section and the outer edge of the lane.

Typically, three sand cone tests and samples from the granular base and six tube samples from the subgrade were obtained from each site. In addition, a tube sample or a grab sample was collected from the side of the highway away from the shoulder. If cracks were present in the pavement, one of the three locations (or a fourth location) was chosen next to a crack.

3.1.1 Gathering Initial Site Information

For non-SMP sites, one of the transition zones of the test section was selected to perform the sampling and testing. If the TDR location was not visible, it was located with the help of the weather instrumentation post located on the side of the road and the coordinates of the instrumentation hole obtained from the LTPP database.

A site description was recorded on a field data sheet with a sketch of the site details. The site information included site identification, exact site location, name of the highway, pavement type (HMA or PCC), pavement condition (cracking and rutting), condition of the shoulders, median and sides (grassy or gravelly slopes), side drainage features, general topography in the site vicinity, and special features (e.g., hills, water ponds, water in the side drains, vegetation, and land use). Photographs were taken showing the site identification signs, general site vicinity, sampling locations on the pavement, and any special features. Also, included in the site description were the weather conditions for temperature, sky, and wind.

3.1.2 Pavement Coring

The pavement was cored in at least three locations along the centerline of the outer lane. The coring locations were marked on the pavement approximately 3 feet apart.

Prior to drilling the first core, a random location on the pavement, at least 10 feet from the actual sampling locations, was drilled with a 2-inch-diameter coring bit to assess the thickness of the bound layer at the site. With this information, the sample locations were cored with a 10-inch core bit to a depth such that 1 inch of the pavement was left intact and then the coring bit was retracted. This action was carefully executed to prevent the contamination of the unbound layers beneath the pavement with drilling water. The water in the cut was removed and the cut cylinder was detached at its base by driving flat steel wedges into the crack. The removed HMA cores were labeled and stored in 5-gallon plastic buckets for transportation back to ASU for testing. The remaining inch of material in the bottom of the hole was then removed using a jackhammer. The coring procedure was repeated for the other two holes. If a treated base was encountered, it was removed using the jackhammer.

3.1.3 Sand Cone Tests on Granular Base

Granular base materials do not permit tube sampling. Therefore, sand cone tests were performed on granular base layers to determine in situ moisture content and dry density. After coring exposed the granular base layer, less than 1 inch of the base material was removed and a leveled surface was prepared inside the hole. The specially prepared cylindrical base plate was placed on the leveled surface, and the cylinder was secured in place by driving wood wedges around it. A 6-inch-diameter, 7- to 8-inch-deep hole was excavated within the base plate, and all the material removed from the hole was carefully collected in a plastic container to prevent moisture loss from evaporation. The container was tightly sealed, weighed, labeled, and stored in a plastic tub for transporting. The preweighed sand cone apparatus filled with sand was placed on the base plate covering the excavated hole and the sand was allowed to run into the hole by opening the valve on the neck of the sand cone apparatus. Once the sand flow stopped the valve was closed and the final weight of the apparatus was recorded. The difference between the initial and final weights gave the amount of sand in the funnel and the hole.

The sand cone was calibrated in the laboratory prior to the fieldwork using the same sand used in the field. Sand from the same source was used throughout the project. The calibration included determining the volume of sand required to fill the funnel and the density of sand when allowed to free fall from the apparatus. These values were used in the dry density computations. The weight of soil removed from the hole provided the in situ moist weight and the amount of sand in the hole and density of sand were used to calculate the volume of the hole. The moist density was obtained using the moist weight and volume of the hole. The sample was oven dried in the laboratory to obtain the dry weight and hence the dry density.

Once the sand cone test was completed, the hole was cleaned free of sand, widened, and deepened until the subgrade was exposed. The procedure was repeated at each hole.

3.1.4 Tube Sampling

Most of the subgrade materials found at the 29 sites were cohesive soils that permitted tube sampling. However, a few sites containing granular subgrades required sand cone testing on the subgrades.

Once the subgrade was exposed, sample tubes were driven into the subgrade to collect material. Two types of tubes were used: 1.8-inch diameter by 6-inch long and 2.8-inch diameter by 12-inch long. The small 1.8-inch-diameter tubes were driven to a depth of 4 inches while the large 2.8-inch-diameter tubes were typically driven to a depth of 8 inches. A slide hammer was used to drive the tubes into the soil. Two slotted wood plates placed on the pavement against the pipes maintained the verticality of the sampling rods during the driving. The starting depth of the sample was recorded. The sample tube was retracted from the ground by extracting the tube and the pipes with a jack.

Each sample tube was stamped for identification, with its weight, height, and internal diameter recorded. The retrieved sample was separated from the sampling rod, and the sample was carefully trimmed to have smooth flat surfaces on both ends. The distance to the soil surface from each edge of the tube was measured. Ten locations along the perimeter of the tube were measured on each edge to obtain two distances, ΔL_1 and ΔL_2. With ΔL_1, ΔL_2, and the length of the tube, the length of the sample was determined for volume calculations. The tube containing the trimmed sample was weighed, capped with plastic lids on both sides, taped, labeled, and stored in a plastic tub for transportation. In this way, all data needed for the calculation of the moist density was gathered in the field.

3.1.5 Side Samples and Disturbed Samples

A sample was collected from the roadside at each site to allow comparison of the conditions of uncovered soil with the covered material. Often the roadside soils were fine-grained, permitting tube sampling. However, there were occasions when the sand cone procedure was required on the roadside because of the presence of granular material.

A representative disturbed sample was collected for index testing from around each sand cone hole and each tube sample. These samples were collected into plastic bags, labeled, and placed in a plastic tub for transportation. Table 6 lists the samples collected at each site. Table 7 summarizes the site information.

3.1.6 Moisture Content near Cracks

When cracks were present on the pavement, soil samples were obtained from the unbound layers near a crack by coring a hole about 2 inches from a selected crack. Twelve sites were sampled near cracks. The moisture contents of the samples near cracks were compared with the average moisture content of the samples obtained from other holes, located away from the crack. The comparison indicated that the average difference in moisture contents was +0.38% with a minimum of −1.72% and a maximum of +2.61%. The standard deviation of this difference was ±0.81%. The positive sign indicates the moisture near the crack was higher than the moisture away from the crack.

It is apparent from this comparison that the moisture content near cracks was not significantly higher than that away from cracks. This suggests that the cracks were not providing avenues for water penetration, perhaps because they were typically filled with dust and fine particles.

Table 6. Samples collected from sites visited.

#	Section	General Location	Highway	Layer Information[1]	HMAC Cores	Sand Cone Tests	Tube Samples
1	010101	Opelika, AL	US-280, WB	7.5" HMAC; 7.5" GB; Clayey SG	4	4	6
2	040113	Chloride, AZ	US-93, NB	4.5" HMAC; 7.5" GB; Granular SG	4	9	0
3	040215	Buckeye, AZ	I-10, EB	11" PCC; 7" GB; Granular SG	—	6	1
4	052042	Crossette, AR	US-82, WB	7" HMAC; 7" TB; 1.5" GB; Clayey SG	4	0	9
5	063042	Thornton, CA	I-5, SB	8.5" PCC; 4.5" TB; 8" Comp. SG; Clayey/Silty SG	—	0	10
6	081053	Delta, CO	US-50, NB	7" HMAC; 6" GB; 30" SB; Clayey SG	3	6	5
7	087035	Aurora, CO	I-70, EB	6" HMAC; 8.5" PCC; 4.5" GB; 29.5" SB; Clayey SG	3	3	8
8	091803	Groton, CT	ST-117, NB	9" HMAC; 12" GB; Rocky SG	3	6	0
9	204054	Junction City, KS	I-70, WB	9.5" PCC; 4" TB; 2.5" GB; Clayey SG	—	0	6
10	220118	Moss Bluff, LA	US-171, NB	10.5" HMAC; 4" & 8.5" TBs; Clayey SG	3	0	7
11	281016	Collins, MS	ST-35, WB	9.5" HMAC; 33" GB; Clayey SG	3	1	10
12	307066	Big Timber, MT	I-90, WB	10.5" HMAC; 3" GB; 15.5" SB; Clayey SG	3	5	6
13	310114	Hebron, NE	US-81, SB	7" HMAC; 12" GB; Clayey SG	3	3	7
14	320204	Battle Mountain, NV	I-80, EB	11.5" PCC; 6.5" GB; 20.5" SB; TB; Unknown SG	—	6	0
15	350105	Rincon, NM	I-25, NB	10" HMAC; 3" GB; Clayey SG	3	0	6
16	364018	Otego, NY	I-88, EB	9.3" PCC; Granular SG	—	6	0
17	370205	Lexington, NC	US-52, SB	8.5" PCC; 7.5" CTB; Clayey SG	—	0	7
18	416011	Harrisburg, OR	I-5, SB	13" HMAC; 12"+ GB; GWT @ 25"; Unknown SG	2	1	0
19	420603	Milesburg, PA	I-80, WB	4" HMAC; 10.5" PCC; 8" GB; 29.5" SB; Rocky SG	3	7	0
20	473101	Auburntown, TN	ST-96, EB	5.5" HMAC; 7" open graded HMAC; 4" CTB; Clayey SG	3	0	7
21	481060	Vidaurri, TX	US-77, NB	7""HMAC; 10" TB; 7" GB; Clayey SG	3	3	7
22	481077	Estelline, TX	US-287, SB	2" HMAC; 12" TB; 12" GB; Granular SG	3	4	6
23	484143	Beaumont, TX	US-90, EB	10.5" PCC; 4" TB; 10" Compacted SB; Clayey SG	—	1	5
24	501681	Charlotte, VT	US-7, NB	7" HMAC; 3.5" TB; 21.5" GB; 12" SB; Clayey/Silty SG	3	4	7
25	537322	Pullman, WA	US-195, NB	10" HMAC; 9" GB; Clayey SG	3	3	7
26	562019	Gillette, WY	ST-59, SB	8" HMAC; 11" CTB; 11" SB; Clayey SG	4	0	8
27	562020	Sheridan, WY	I-90, WB	7" HMAC; 12.5" CTB; Clayey SG	3	0	7
28	MnRoad	Albertville, MN	I-94, WB	8.5" HMAC; Compacted Clayey SG	13	0	9
29	WesTrack	Silver Springs, NV	Test Loop	6" HMAC; 11.5" GB; 12" Eng. Fill; 6" Compacted Clayey SG	8	6	14

[1]HMAC = Asphalt concrete; GB = Granular base; SG = Subgrade; PCC = Portland cement concrete; CTB = Cement treated base; TB = Treated base; SB = Subbase

Table 7. Summary of site information.

No.	Section ID	Abbr ID	City	State	Date of field Work		Highway	Latitude North	Longitude West	Elev. (ft)	Pave Type	TDR	Cracks
1	010101	1-3	Opelika	AL	Nov 7	2001	US-280 WB	32.6061	85.2512	151	HMAC	Yes	None
2	040113	2-3	Chloride	AZ	Dec 3,4	2001	US-93 NB	35.3920	114.2550	3580	HMAC	Yes	Severe
3	040215	4-1	Buckeye	AZ	Dec 18,19	2001	I-10 EB	33.4570	112.7400	1100	PCC	Yes	None
4	052042	1-5	Crossette	AR	Nov 15	2001	US-82 WB	33.1342	91.8384	140	HMAC	No	Minor
5	063042	8-3	Thornton	CA	Jun10,11,12	2001	I-5 SB	38.2389	121.4403	11	PCC	Yes	Mod
6	081053	7-5	Delta	CO	May 22	2002	US-50 NB	38.6979	108.0263	5140	HMAC	Yes	None
7	087035	7-4	Aurora	CO	May 20	2002	I-70 EB	39.7431	104.7378	5500	HMAC/ PCC	No	Mod
8	091803	6-1	Groton	CT	Apr 16	2002	ST-117 NB	41.3950	72.0270	165	HMAC	Yes	Minor
9	204054	5-3	Junction City	KS	Apr 1,2	2002	I-70 WB	38.9670	97.0910	1190	PCC	Yes	Mod
10	220118	3-1	Moss Bluff	LA	Dec 10	2001	US-171 NB	30.3342	93.1983	27	HMAC	No	None
11	281016	1-4	Collins	MS	Nov 13	2001	ST-35 WB	33.1342	89.4200	1549	HMAC	Yes	None
12	307066	7-1	Big Timber	MT	May 13	2002	I-90 WB	45.8134	110.0024	4072	HMAC	No	Mod
13	310114	5-4	Hebron	NE	Apr 3	2002	US-81 SB	40.0710	97.6239	1611	HMAC	Yes	Mod
14	320204	8-2	Battle Mtn	NV	June 5	2002	I-80 EB	40.7210	117.0380	4550	PCC	Yes	Mod
15	350105	1-1	Rincon	NM	Oct 29	2001	I-25 NB	32.6783	107.0707	4117	HMAC	No	None
16	364018	6-3	Otego	NY	Apr 22	2002	I-88 EB	42.3780	75.1920	1070	PCC	Yes	Mod
17	370205	5-1	Lexington	NC	Mar 25, 26	2002	US-52 SB	35.8700	80.2660	742	PCC	Yes	Mod
18	416011	2-2	Harrisburg	OR	Nov 30	2001	I-5 SB	44.2946	123.0612	323	HMAC	No	None
19	420603	6-4	Milesburg	PA	Apr 24	2002	I-80 WB	40.9745	77.7914	1360	HMAC/ PCC	No	None
20	473101	5-2	Auburntown	TN	Mar 28	2002	ST-96 EB	35.9412	86.1223	770	HMAC	No	None
21	481060	3-3	Vidaurri	TX	Dec 13	2001	US-77 NB	28.5098	97.0583	78	HMAC	Yes	None
22	481077	1-2	Estelline	TX	Nov 1,2	2001	US-287 SB	34.5387	100.4352	1835	HMAC	Yes	None
23	484143	3-2	Beaumont	TX	Dec 11,12	2001	US-90 EB	28.5098	94.3710	42	PCC	Yes	None
24	501681	6-2	Charlotte	VT	Apr 18	2002	US-7 NB	44.3081	73.2456	255	HMAC	Yes	Mod
25	537322	8-1	Pullman	WA	Jun 3	2002	US-195 NB	46.7299	117.2235	2545	HMAC	No	None
26	562019	7-3	Gillette	WY	May 16	2002	ST-59 SB	44.1652	105.4460	4577	HMAC	No	Minor
27	562020	7-2	Sheridan	WY	May 14	2002	I-90 WB	44.9386	107.1974	4022	HMAC	No	Minor
28	MnRd	6-5	Albertville	MN	May 2,3	2002	I-94 WB	45.2400	93.6500	-	HMAC	Yes	Severe
29	WesTr	2-1	Silver Springs	NV	Nov 26, 27	2001	Test Loop	39.4200	119.2200	-	HMAC	Yes	Minor

3.2 Data Collection from Existing Databases

The following databases were searched for sites appropriate for a desk engineering analysis:

1. LTPP,
2. MnRoad,
3. WesTrack, and
4. ADOT.

For sites where adequate data existed, the data needed for preliminary runs of the EICM were extracted. These data included those required to (1) run the EICM and (2) validate the EICM.

3.2.1 Parameters Required to Run the EICM

The types of data required to run the EICM are summarized below. The list presented is based on nomenclature used by LTPP, which includes particular Section Identification numbers and State codes.

Analysis Conditions

- Section
- State Code

- SHRP Identification Number
- State
- Project Type
- Pavement Type
- Construction Number
- Unbound Layers Preparation Completion Date
- Asphalt Construction Completion Date
- Traffic Opening Date
- Date of Another Event
- Event
- TDR/Thermistor Installation Date
- Design Period
- Sites Already Visited
- Lab ID

Pavement Lane Properties

- Pavement Type
- Lane Width
- Pavement Slope
- Thermal Conductivity
- Heat Capacity
- Surface Short Wave Absorptivity

Environmental/Climatic

- Latitude (degrees and minutes)
- Longitude (degrees and minutes)
- Elevation
- Groundwater Table Depth

Pavement Structure

- Layer Number
- Layer Type
- Layer Description
- Representative Thickness
- Material Description
- Bedrock Information

Atterberg Limits

- State Code and SHRP ID Number
- Construction Number
- Layer Number and Layer Type
- Liquid Limit, Plastic Limit, and Plasticity Index
- Source of Information

Gradation Parameters

- State Code and SHRP ID Number
- Layer Number and Layer Type
- Percent Passing #200 Sieve
- Percent Passing #4 Sieve
- Diameter D_{60}

Optimum Moisture Content and Maximum Dry Unit Weight

- State Code and SHRP ID Number
- Layer Number and Layer Type
- Optimum Moisture Content
- Maximum Dry Unit Weight
- Source of Information

Unbound Materials Gradation

- State Code and SHRP ID Number
- Layer Number and Layer Type
- Test Number
- Test Date
- Gradation Analysis from Passing 3″ Sieve to Passing 1/2″ Sieve
- Gradation Analysis from Passing 3/8″ to Passing #200 Sieve
- Hydrometer Analysis
- Percentage > 2 mm
- Percentage of Coarse Sand
- Percentage of Fine Sand
- Percentage of Silt
- Percentage of Clay
- Source of Information

Unbound Materials Classification

- AASHTO Soil Classification (Test 1 and Test 2 when applicable)
- Unified Soil Classification (Test 1 and Test 2 when applicable)
- Dry Thermal Conductivity
- Heat Capacity

3.2.2 Parameters Required to Validate the EICM

The data required to validate the EICM are time histories of moisture content measurements throughout the pavement profile. TDR measurements were obtained for the sites selected from the databases.

3.2.2.1 LTPP DATABASE

Parameters Required to Run the EICM. The data required to run the EICM were extracted for 67 test sections from the LTPP SMP database. Fifty-five of the 67 sections were used for the Stage IV runs and analysis described in Chapter 4. Twenty-eight sites were used for the Stage II and III runs and analysis; these were the sites where field visits were made to data for the Stage I runs and analysis. TDR data were found in the LTPP database.

Missing Data. Several pieces of data were missing from the LTPP database. These data were requested from the LTPP

regional offices and the individual state DOTs. In some cases, however, reasonable estimates were made to complete the database.

Unbound Layers Preparation Completion Date. This information was not found in the LTPP database in many cases. When necessary, the completion date was assumed to be 2 months prior to the Asphalt Construction Completion date.

Design Period. The design period was chosen based on the time history of TDR and thermistor measurements available in the database.

Pavement Slope. A value of 1.5% was assumed for all sections.

Dry Thermal Conductivity. Reasonable values of thermal conductivity for HMA pavements range from 0.44 to 0.81 BTU/hr-ft-°F. A default value of 0.67 BTU/hr-ft-°F was assumed for all sections. For PCC pavements, the values range from 0.47 to 0.67 BTU/hr-ft-°F; a value of 0.57 BTU/hr-ft-°F was assumed. The dry thermal conductivity of the unbound materials was not available in the database. The EICM uses default values that are a function of the AASHTO soil classification. The thermal conductivity default values were taken from Tye (1969), Larsen (1982), Yaws (1997), and Farouki (1982).

Heat Capacity. Reasonable values of heat capacity for HMA pavements range from 0.22 to 0.40 BTU/lb-°F. A default value of 0.22 BTU/hr-ft-°F was assumed for all sections. For PCC pavements, the values range between 0.15 and 0.25 BTU/lb-°F. A value of 0.15 BTU/lb-°F was assumed. Soil heat capacities were not available in the LTPP database. A recommended value of 0.18 BTU/lb-°F is used in the EICM for every material type (Robertson and Hemingway, 1995).

Surface Short Wave Absorptivity. Reasonable values of surface short wave absorptivity for weathered (gray) HMA range from 0.80 to 0.90. A default value of 0.85 was assumed for all of the HMA sections. For PCC pavements, the values range between 0.70 and 0.90. A value of 0.80 was assumed (Moats, 1994).

GWT Depth. Information not found in the LTPP database was taken from Von Quintus (2001). Von Quintus gathered these data from Soil Conservation Service reports and maps. Additional data were gathered from the U.S. Geological Survey records, state DOTs, and LTPP boring logs and comments. The National Water Information System website displayed groundwater levels based on the input of a site's longitude and latitude. These groundwater level data were considered adequate when the wells identified in the search were reasonably close to the site and the data were recently recorded. However, for some sites, the available data could not be considered recent, the distance between the site and the well was too large, or both. In such cases, environmental consultants in the area were contacted for in-house data, if available, or direction to appropriate state agencies. State agencies typically provided groundwater data through their websites. For example, the Texas Water Development Board (TWDB) maintains a good groundwater database for the entire state on its website.

For several sites, no groundwater table depth information was available from any source. In these cases, a conservative estimate of the groundwater table level was obtained from the borehole depth provided in the LTPP boring log. Some sites are believed to have a deep groundwater table, far below the borehole depth, but this situation should not strongly affect the prediction of moisture content variations at shallow depths.

Layer Type. In all cases, the subgrade (SS) was reported to be an uncompacted layer; therefore the top 12 inches of the subgrade was assumed to be compacted material. This compacted "sublayer" was not included in the pavement structure for the site.

Bedrock Information. In most cases, records of depth to bedrock were not found in the LTPP database. In order to complete this information, the following sources were used:

1. Soil Conservation Service reports and maps (Von Quintus, 2001).
2. Data from the US Geological Survey and state DOTs.
3. State DOT records.
4. LTPP boring log information and comments.

Lime-Treated or Cement Aggregate Material. Several sections have either lime-treated soil or cement-aggregate material. The EICM was incapable of dealing with these types of materials. Furthermore, there is no data available in the LTPP database for these layers. These sections were run by making assumptions about plasticity reduction and gradation changes.

3.2.2.2 Minnesota Road Research Project (MnRoad) Data

The Minnesota Department of Transportation (MnDOT) constructed forty, 500-foot-long asphalt, concrete, and gravel-surfaced pavement test sections (known as test cells) from 1992 to 1994. This site, known as MnRoad, consists of 3 miles of two-lane interstate I-94 (known as Mainline cells) as well as 2.5 miles of closed-loop, low-volume test track (known as low-volume cells). The I-94 traffic, an estimated 14,000 vehicles per day (15% trucks), generally uses the Mainline facility where 23 heavily instrumented test cells are

subjected to live traffic loads. The low-volume facility with 17 test cells is subjected to controlled loading by a single vehicle circling the two-lane test track. The Mainline portion is divided into two parts, referred to as the 5-Year Mainline (5-year design life) and 10-Year Mainline (10-year design life) (U. of Minnesota, 1997).

For the EICM desk engineering analysis, two MnRoad sections, cells 4 and 21 from the Mainline road, were selected.

LTPP instrumentation packages for measurement of moisture, temperature, and frost penetration in pavement sections were installed at MnRoad. Moisture content was recorded with TDR probes, with data recorded at 2-week intervals. In addition to moisture measurements, pavement temperature was measured with temperature probes and electrical resistivity probes were installed to measure frost penetration.

3.2.2.3 WesTrack Data

WesTrack was an experimental test road facility constructed at the Nevada Automotive Test Center (NATC) near Fernley, Nevada, under the FHWA project "Accelerated Field Test of Performance-Related Specifications for Hot-Mix Asphalt Construction." WesTrack was constructed as a 2.9-km oval loop consisting of twenty-six 70-m-long experimental sections on the two tangents. Construction was completed in October 1995. Trafficking was carried out between March 1996 and February 1999.

WesTrack Sections 12, 15, and 25 were selected for the EICM desk analysis. Most of the required information was taken from *NCHRP Report 455: Recommended Performance-Related Specification for Hot-Mix Asphalt Construction: Results of the WesTrack Project* (Epps et al., 2002).

An LTPP SPS-type weather station was installed at WesTrack near the vehicle and staging and maintenance area. The equipment recorded the following information hourly:

- Air temperature,
- Relative humidity,
- Wind speed,
- Wind direction,
- Solar radiation, and
- Precipitation (water equivalent).

Instrumentation packages developed by LTPP for measurement of moisture, temperature, and frost penetration in pavement sections were placed at the edge of the test lane in Sections 12 and 25. The following sensors were placed at each of these locations:

- 10 TDR probes,
- 18 probes to measure pavement surface temperature, and
- 35 electrical resistivity probes to measure frost penetration.

Data from the temperature and resistivity probes were continuously recorded, while data from TDR probes were recorded at approximately 2-week intervals. Readings were monitored continuously at 0.5 in. intervals in the pavement. The TDR data was presented in *NCHRP Report 455*.

Piezometer observation wells were installed near the SPS instrumentation packages adjacent to Sections 12 and 25 to monitor the depth of the groundwater table. The average depths for the south and north tangents were found to be about 10.8 ft. and 11.2 ft. below the pavement surface, respectively. This relatively high water table was attributed to high water flow in the Carson River, which resulted from the wet winter of 1994-95 in the Sierra Nevada Mountains.

3.2.2.4 ADOT Sites

Two test sites (1 and 14) from ADOT were selected for the EICM desk engineering analysis. Site 1 is in Avondale, at the intersection of Buckeye Rd. and 91st Avenue. Its original construction was completed in 1936. In December 1956, the road was widened, and new subgrade and subbase layers were constructed. Site 14 is in Flagstaff, between mileposts 337 and 336 on I-17. Construction was completed in August 1960.

The information required for the desk analysis was taken from the FHWA/AZ Report 80/157, *Environmental Factor Determination from In-Place Temperature and Moisture Measurements under Arizona Pavements*, September 1980 (Way, 1980).

Instrumentation packages for measurement of moisture and temperature were placed at the edge of the side lane for Sites 1 and 14. The following sensors were placed at each of these locations:

- Four TDRs to measure moisture and
- Six thermistors to measure pavement temperature.

Data from the thermistor probes were recorded monthly, while data from the TDR probes were recorded in uneven periods ranging from a few days to 1 year.

The groundwater table was not monitored at these sites during the time of the experiments. Therefore, approximate groundwater depths were determined using USGS data. The average water table for Site 1 was found to be about 68.1 ft below the pavement surface at a location 0.067 miles from the site. The groundwater table for Site 14 was determined to be about 1002 ft below the pavement surface, with measurements made at two locations, 0.164 and 0.180 miles away from the test site.

3.3 Laboratory Testing Program

Table 8 lists the laboratory tests conducted on the soil samples taken at the field sites. Hydraulic conductivity tests were

Table 8. Laboratory tests performed for NCHRP 9-23 project.

Test	Sample	Number
Moisture Content	All Sand Cone and Tube Samples	257
Dry Density	All Sand Cone and Tube Samples	251
Gradation	Composite Samples Representing Each Layer	144
Atterberg Limits (Liquid Limit and Plastic Limit)	Composite Samples Representing Each Layer	148
Specific Gravity	Composite Samples Representing Each Layer	104
Saturated Hydraulic Conductivity	Selected Granular Base and Subgrade Samples	64
SWCC Testing	Selected Granular Base, Subgrade, and Side Samples	85
Hydraulic Conductivity on HMAC Cores	Cores from HMAC Pavements	22

performed on one of the HMA cores obtained from each HMA pavement site.

3.3.1 Moisture Content and Dry Density

The in situ moisture content and dry density of granular bases and subgrades provided valuable data for determining the equilibrium moisture contents beneath the pavements. The moisture contents at the time of the site visit were regarded as the equilibrium moisture content or very close to the equilibrium moisture content since all the pavements were constructed more than 5 years before the measurements were made. Seasonal fluctuation could be a factor influencing this assumption. However, based on the TDR moisture content data, the seasonal fluctuation appeared to be significant only in the cold regions where freeze and thaw conditions occur. Also, if the groundwater table is within 2 feet of the ground surface, the soil may become fully saturated. The design moisture contents derived from the data obtained in this study are most applicable when these two conditions are unlikely to occur.

3.3.1.1 Moisture Content of Sand Cone Samples

Sand cone samples were collected in plastic containers in the field. The total moist weight of the sample was determined by weighing the sample plus the container and subtracting the weight of the container. The moist soil in the container was transferred to a drying pan in a 110°C oven; the dry weight of the soil was obtained after holding the soil in the oven for at least 24 hours. The moist weight and dry weight were used to calculate the moisture content of the sample. Care was taken to prevent drying of the sample after opening its container; however, this procedure gives an accurate moisture content and dry density determination, even if some inadvertent drying occurs.

The above procedure used the total sample because a supplemental undisturbed sample collected from around the sand cone hole was available for the Atterberg limit and specific gravity tests that required samples in a natural state. However, when a supplemental sample was not available, a portion of the sand cone sample was separated for other tests. Once the other tests were completed, the dry weight of the separated sample was obtained and the moisture content of the total sample was computed.

3.3.1.2 Moisture Content of Tube Samples

Tube samples containing moist soil were weighed in the field and the weight, length, and diameter of each tube were recorded. These measurements and the recess of the trimmed sample from each end provided information to compute the moist density of the sample. The samples were extruded from the tubes in the laboratory and oven dried for moisture content determination.

If a portion of the sample was required for saturated hydraulic conductivity and SWCC tests, partial moisture content was obtained as described in the previous section. The moisture content based on the total sample was then obtained after completing all tests.

3.3.1.3 Dry Density

The field measurements of both sand cone samples and tube samples provided the moist densities. Once the moisture content of a sample was determined the dry density was obtained by

$$\gamma_{dry} = \gamma_{moist}/(1 + w) \quad (1)$$

where

γ_{dry} = dry density
γ_{moist} = moist density
w = moisture content

3.3.2 Grain Size Distribution

Results of the grain size distribution (GSD) or the gradation test were of great importance in developing the moisture

prediction models and the modification of the family of SWCCs. In the moisture prediction models, the percentage of the material passing the #200 sieve (P_{200}) was used as one of the two correlation parameters. In the SWCC modifications, most of the correlation parameters were derived from the gradation curve: D_{10}, D_{20}, D_{30}, D_{90}, C_c, C_u, and P_{200}.

The GSD of a sample was obtained by a washed sieve analysis of an oven-dried sample of the P_{200} material, using a standard set of ASTM sieves. In some instances, samples from the same layer were combined for GSD analysis.

The GSD data for each sample was subjected to curve fitting using a commercially available software package that is primarily designed for handling unsaturated soil properties. The software contains a four-parameter curve-fitting feature that is capable of fitting sigmoidal curves to GSD as well as SWCCs. This feature was extensively used in this study. The four parameters associated with the sigmoidal fit are designated a, b, c, and h_r.

Specifically, the curve fitting parameters for GSD were designated a_g, b_g, c_g, and h_{rg}. Once the parameters were known for the GSD of a given soil, the equation of the GSD was expressed as, Percent Passing = f (Particle Diameter, a_g, b_g, c_g, h_{rg}) or

$$\text{Percent Passing} = \frac{\left[1-\left\{\frac{\ln\left(1+\frac{h_{rg}}{\text{Diameter}}\right)}{\ln\left(1+\frac{h_{rg}}{1\times10^{-5}}\right)}\right\}^{7}\right]}{\left[\ln\left[\exp(1)+\left(\frac{a_g}{\text{Diameter}}\right)^{b_g}\right]\right]^{c_g}} \qquad (2)$$

This equation permitted the calculation of the values of D_{10} through TD_{90} for each curve. When the curve fitting was for the SWCC, the parameters were designated a_f, b_f, c_f, and h_{rf}. SWCC curve fitting is discussed in detail later in this chapter.

3.3.3 Atterberg Limits

Atterberg limits specifically, Liquid Limit (LL) and Plastic Limit (PL), were determined on individual samples as well as composite samples. The plasticity index (PI) was calculated from PI = LL – PL. The values of LL, PL, and PI were used as correlation parameters in moisture prediction models and SWCC modifications.

3.3.4 Specific Gravity

Specific gravity of individual and composite samples was determined using standard test procedures. Typically, the samples were sieved through a No. 4 sieve and the fraction passing the No. 4 sieve was used for the test.

3.3.5 Saturated Hydraulic Conductivity

Undisturbed samples from subgrades and reconstituted samples from granular bases were subjected to saturated hydraulic conductivity tests. Samples representing each layer encountered at the sites were selected. Typically, two tests were carried out for each site. The saturated hydraulic conductivity was determined using the falling-head permeability test method. Testing was conducted in 2.8-inch-diameter, 12-inch-long stainless steel tubes.

The tube containing the sample was placed vertically in a 5-gallon bucket and the tube was filled with water. The initial and final heights of the water levels inside and outside the sample tube along with the elapsed time between readings were recorded. The test time was dependent on the soil type. Reconstituted granular materials took a couple of hours, while fine-grained samples took several days.

3.3.5.1 Sample Extrusion

Tube samples selected for hydraulic conductivity tests were carefully extruded leaving about a 2- to 3-inch length of soil in the tube. A manually operated hydraulic jack and a steel frame were used in the extrusion process. The extruded soil was used for partial moisture content determination.

3.3.5.2 Calculation of Saturated Hydraulic Conductivity

The hydraulic conductivity was calculated using the following equation:

$$k_{sat} = \frac{aL}{At}\ln\left(\frac{H_i}{H_f}\right) \qquad (3)$$

where

k_{sat} = saturated hydraulic conductivity,
a = area of the water surface above the sample,
L = length of the soil sample,
A = area of the soil sample,
t = elapsed time between initial and final readings,
H_i = initial head,
H_f = final head.

3.3.5.3 Reconstitution of Granular Samples

Granular base samples were reconstituted in 2.8-inch-diameter tubes for hydraulic conductivity testing. Only the portion of the sample passing the No. 4 sieve was used in the reconstitution process. To obtain a representative minus No. 4 sample from the main sample, the distribution of minus No. 4 sample between the No. 4 and No. 10 sieves, No. 10 and No. 40 sieves, and passing the No. 40 sieve was calculated

based on the GSD of the total sample. Then the individual masses passing and retained on respective sieves were weighed separately and combined prior to compaction. The same sample reconstitution procedure was used in preparation of granular samples for SWCC testing.

3.3.6 Hydraulic Conductivity on Asphalt Cores

One HMA core from each site was subjected to the hydraulic conductivity test to determine the infiltration of the HMA layers in the field. The HMA core was first waterproofed on the sides with paint and then a mini-dam was formed on the top from silicone. The core was then placed inside a 5-gallon bucket on a bed of dry sand. The top of the core was filled with water and the weight of water added was recorded. The water was allowed to permeate the core for 24 hours with the water level in the mini-dam kept constant. The weight of the bucket and dry sand before and after the test was recorded. The difference between the weight measurements indicated the amount of water passed through the core during the test. The test was started with dry sand and the bucket was tightly closed with a lid to prevent any evaporation. The percentage of water passed through the HMA cores was computed.

Twenty-two cores were tested in this manner. Of the 22 tests, 20 did not indicate significant water permeation through the HMA. The two tests that did show measurable permeation through the cores belonged to the WesTrack site in Nevada and the Big Timber site in Montana.

3.3.7 Soil-Water Characteristic Curves

SWCC determination played a very important role in this study. The SWCC describes the relationship between the matric suction and the moisture content of a given soil. A key objective of this research was to improve an existing family of SWCCs by correlating parameters derived from GSD and index properties. A large number of experimentally determined SWCCs were required to accomplish this objective. This project provided more than 90 soil samples well distributed over the entire country, which was considered an excellent representation of the soil conditions throughout the continental United States.

Samples were selected for SWCC testing from each of the 29 sites to represent each layer encountered during field sampling. In addition, the samples collected from the roadside were selected for SWCC testing. Therefore, each site contributed at least three samples.

A total of 85 SWCCs were generated from 33 granular or nonplastic samples and 52 fine-grained samples. In addition, SWCCs were determined for 9 fabricated granular samples, increasing the total number of SWCCs to 94. The fabricated samples were prepared by mixing 1%, 10%, and 20% of nonplastic fines with fine, medium, and coarse sand samples, respectively. A new suction measurement device was developed as part of this research and the abovementioned samples were tested using this new device. High air-entry ceramic discs (rated up to 1,500 kPa) were used in the device.

3.3.7.1 Typical SWCC Data Points

SWCC testing provided values of applied pressure, volume tube readings, and height measurements. The degree of saturation corresponding to applied suction was computed using the water content, dry density, and specific gravity of the sample.

3.3.7.2 Observations on SWCCs

Figure 4 shows a typical SWCC for a granular sample. Several observations were made regarding the shape of the SWCCs:

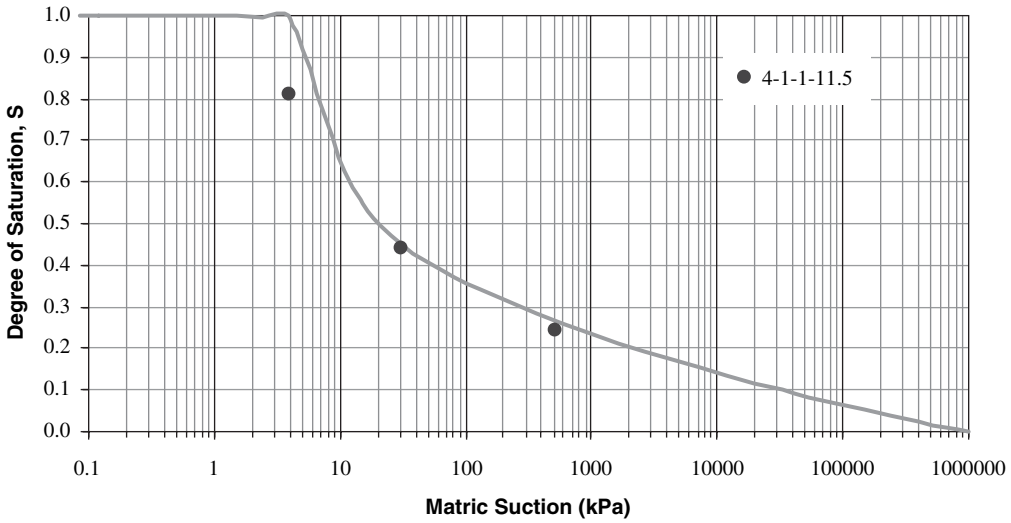

Figure 4. Typical SWCC for a granular sample.

1. Data points generated for nonplastic curves were plotted with the existing family of curves. When the soil contained very little or no fines, i.e., a P_{200} of less than 2%, the measured curves appeared to agree with the existing curves. However, when the value of P_{200} was higher than 2%, the measured curves deviated from the family of curves, by assuming a less steep path.
2. The shape of the GSD curve played a role in deciding the shape of the SWCC, as has been shown by researchers in the past.
3. For plastic soils, the density correction greatly influenced the curve. As the testing progressed, the density increased and the void ratio decreased as a result of drying of the sample. As void ratio decreased, the degree of saturation increased. Therefore, the new data points showed an upward trend deviating from the existing curves.
4. The Fredlund and Xing equation restricted the projection of SWCC to 1,000,000 kPa at zero degree of saturation. However, the new curves associated with highly plastic soils seemed to project pass this limiting value.
5. One fabricated sample that contained coarse sand and 20% of fines demonstrated that, toward the end of the test, the fine particles traveled to the bottom of the sample through the voids of the gap-graded coarse sand and created a silt barrier prohibiting further movement of water.

CHAPTER 4

Evaluation of the Enhanced Integrated Climatic Model

4.1 Introduction

Verification and validation of the EICM was carried out with the data from LTPP, MnRoad, WesTrack, and ADOT sections.

In the first iteration of the analysis, the EICM was used in its original form (i.e., Version 2.6 developed for the NCHRP 1-37A project and implemented in Version 0.7 of the MEPDG software) for prediction. Based on the results of this iteration, the EICM predictive accuracy was judged to be unacceptable, and all available information and research findings were then applied to the development of modifications to improve the accuracy of the program results. Overall, the process was broken into the following steps:

1. Gather data.
2. Run the EICM.
3. Compare measured and EICM-predicted values.
4. Modify the EICM.
5. Repeat the EICM runs.
6. Continue iterations until acceptable accuracy was achieved.

4.2 Gathering Data

The data needed to validate the EICM were summarized in Chapter 3. Data from the LTPP database, MnRoad, WesTrack, and ADOT were extracted, assembled, and input into the EICM. These data, along with the field information collected from the 29 LTPP sites visited were used for the validation of the 2.6 version of the EICM.

In addition to the data collected from the 29 LTPP site visits and 60 sections currently available in the LTPP database, WesTrack reports were reviewed and the data for three sections were extracted. Additional data were collected from two MnRoad sections and two from ADOT.

4.3 EICM Runs

Four sets of EICM runs (termed Stages I, II, III, and IV) were conducted to validate the different models and algorithms used for predicting moisture content. This process allowed for the checking of individual models in isolation from other models.

4.3.1 Stage I Runs

The Stage I EICM runs were conducted for the sites visited by the project team; directly measured index properties were input to the EICM. All input data were obtained from laboratory testing done on the samples collected at each field site, and, therefore, the dataset was the best available to the project. The dataset included the SWCCs, saturated hydraulic conductivity, specific gravity, gradation analysis, and Atterberg limits measured for each sample collected at different depths at every site. The laboratory testing did not include development of compaction curves, so the optimum water content and the maximum dry density were extracted from the data available from LTPP, MnRoad, and WesTrack databases.

The Stage I runs were completed at five different levels of input parameters for a total of 150 runs. The statistical analysis is discussed later in this chapter.

4.3.2 Stage II Runs

Stage II runs were conducted to measure the accuracy and the level of confidence of index properties cataloged in the databases developed through the desk analyses. Thus, the field-measured values of percent passing #200 and plasticity index were replaced by values from the databases. These runs quantified errors in moisture content caused by errors in the index properties derived from the databases; the runs were conducted for a subset of the Stage I sites.

4.3.3 Stage III Runs

Stage III runs were conducted for the sites included in Stages I and II. However, the input data were exclusively taken from the databases developed from the desk analyses. The TDR values reported in the databases were used as the measured values. Thus, any added error between the Stage II and Stage III results was primarily due to error in the TDR values themselves.

4.3.4 Stage IV Runs

Stage IV runs included the field sites visited by the project team and those identified for desk analysis, with input data derived only from the databases. This permitted comparison of TDR moisture values with those predicted by the EICM Version 2.6.

4.4 EICM Runs Within the MEPDG Hierarchical Levels of Analysis

As currently implemented, three hierarchical levels of analysis have been defined in the MEPDG. The level of analysis determines the set of parameters required for input by the user. For instance, substantially more input parameters are needed for MEPDG Level 1. On the other hand, if Level 3 analysis is desired, fewer input values are needed, and these will be less accurate or default parameters. The level selected determines the accuracy of the input and thus, also, the output; however, the analytical procedure is the same, regardless of the level selected.

This hierarchical concept applies equally to the use of the EICM within the MEPDG. Table 9 summarizes the input parameters required to run the EICM for each level of analysis. This table shows that it was not possible to validate Level

Table 9. Input required by the EICM by level of analysis.

Parameter	Application	Level of Analysis		
		1	2	3
Model Initialization				
Base/Subgrade construction date	Required for model initialization	√	√	√
Climatic/Boundary Conditions				
Latitude	To define weather station	√	√	√
Longitude	To define weather station	√	√	√
Elevation	To define weather station	√	√	√
Groundwater Table Depth	Annual average			√
	Seasonal values	√	√	
Pavement Structure				
Layer thickness		√	√	√
Material type		√	√	√
Asphalt Concrete and PCC Materials				
Thermal conductivity	Default value		√	√
	Direct measurement	√		
Heat capacity	Default value		√	√
	Direct measurement	√		
Unbound Materials (Compacted or natural)				
Atterberg limits	Direct measurement	√	√	√
Sieve analysis	Direct measurement	√	√	√
Soil classification	To correlate with resilient modulus			√
Resilient modulus or CBR or R-value or Layer coefficient a_i at optimum condition			√	
k_1, k_2, k_3 values	To calculate the resilient modulus at optimum conditions	√		
Specific gravity of solids	Direct measurement	√	√	
Saturated hydraulic conductivity	Direct measurement	√	√	
Maximum dry unit weight	Direct measurement	√	√	
Optimum moisture content	Direct measurement	√	√	
Dry thermal conductivity	Direct measurement	√	√	
	Default value		√	√
Heat capacity	Direct measurement	√		
	Default value		√	√
Soil-water characteristic curve parameters	From direct suction measurements	√		
Drainage and Surface Properties				
Surface short wave absorptivity	Default value		√	√
	Direct measurement	√		
Infiltration	Choose from Negligible, Minor, Moderate, or Extreme	√	√	√
Drainage path length	Only if infiltration is considered	√	√	√
Pavement cross slope	Only if infiltration is considered	√	√	√

1 analysis in Stage IV due to the lack of information. Specifically, the LTPP database lacks the following parameters:

- Seasonal values of the GWT depth for several sections, and
- Direct measurements of thermal conductivity, heat capacity, specific gravity of solids, saturated hydraulic conductivity (except for a few sections), suction measurements, and surface short wave absorptivity.

Level 2 analyses were completed for some sections for which values of the following parameters were available:

- Seasonal variation of the GWT depth,
- Saturated hydraulic conductivity,
- Maximum dry unit weight,
- Optimum moisture content, and
- CBR option to estimate the resilient modulus at optimum condition.

Level 3 analyses were completed for all desk analysis sites. A key parameter at this level is infiltration allowed into the pavement structure. The EICM permits selection from four infiltration cases:

1. Negligible: 0% of rainfall allowed to infiltrate the pavement system. EICM assumes 0 ft of cracking.
2. Minor: 10% of rainfall allowed to infiltrate the pavement system. EICM assumes 10 ft of cracks per 100 ft of survey length.
3. Moderate: 50% of rainfall allowed to infiltrate the pavement system. EICM assumes 100 ft of cracks per 100 ft of survey length.
4. Extreme: 100% of rainfall allowed to infiltrate the pavement system. EICM assumes 1,000 ft of cracks per 100 ft of survey length.

Stage IV runs only considered the case of negligible infiltration. No comparisons were made considering minor, moderate, or extreme infiltration. The infiltration model developed by the University of Illinois (based on edge drains measurements) considers pavement cracking as the way water flows into the pavement structure. Based on the type of pavement, an infiltration rate is assumed based on the ratios shown above. After a rain, water is added to the moisture content of the base coarse in proportion to the amount of rainfall and the infiltration rate. The research team that developed the flexible pavement design procedure in NCHRP Project 1-37A determined that the infiltration model was in need of revision and, hence, the EICM in the original Version 0.7 of the MEPDG software was calibrated with the assumption of *no infiltration* due to rainfall. For this reason, the selection of the sections to validate the EICM in the present study was based on pavements for which cracking was reported to be low to none.

When cracks were present on a field pavement section visited by the project team, soil samples were obtained from the unbound layers near a crack by coring one of the holes about 2 inches from a selected crack. Such samples were taken at 12 sites. The moisture contents of the samples near cracks were compared with the average moisture content of the samples obtained from other holes located away from the crack. The comparison indicated that the average difference in moisture contents was +0.38%, with a minimum of –1.72% and a maximum of +2.61%. The standard deviation of this difference was 0.81. The positive sign indicated that the moisture near the crack was higher than the moisture away from the crack. These results suggest that the moisture content near the cracks was not significantly higher than that away from them and that the cracks were not providing avenues for water penetration, perhaps because the cracks were typically filled with dust and fine particles.

4.5 Statistical Analysis

The data obtained from the EICM runs described above were statistically analyzed. Conclusions were drawn from the following statistical parameters: (1) the adjusted coefficient of determination, R^2; (2) the standard error of the estimate divided by the standard deviation, S_e/S_y; (3) the algebraic mean error, e_{alg}; and (4) the absolute mean error, e_{abs}. The algebraic mean error, e_{alg} is given by

$$e_{a\lg} = \frac{100\sum_{i=1}^{n}\frac{(y_i - \hat{y}_i)}{y_i}}{n} \tag{4}$$

where

y_i = measured moisture content
$\hat{y}_i$ = predicted moisture content
n = number of data points

and the absolute mean error, e_{abs}, by

$$e_{abs} = \frac{100\left|\sum_{i=1}^{n}\frac{(y_i - \hat{y}_i)}{y_i}\right|}{n} \tag{5}$$

The adjusted coefficient of determination, R^2, provides a measure of the accuracy of prediction of the model. R^2 is calculated as a function of the ratio S_e/S_y by the following equation:

$$R^2 = 1 - \left(\frac{S_e}{S_y}\right)^2 \tag{6}$$

where

R^2 = Adjusted coefficient of determination
S_e = Standard error of estimate
S_y = Standard deviation

The formulas used to calculate S_e and S_y are given below:

$$S_e = \sqrt{\frac{\sum_{i=1}^{n}(\hat{y}_i - y_i)^2}{n-p}} \quad (7)$$

$$S_y = \sqrt{\frac{\sum_{i=1}^{n}(y_i - \overline{y}_i)^2}{n-1}} \quad (8)$$

where

y_i = measured moisture content
$\hat{y}_i$ = predicted moisture content
$\overline{y}_i$ = average of y_i
n = number of data points
p = number of unknown parameters

Table 10 summarizes the possible sources of error for the four stages of analysis.

The possible sources of error will be explained in detail in the following sections.

4.5.1 Stage I Analysis

In the Stage I analysis, 89 measured moisture content values were compared with the predicted results. The Stage I runs were considered at five different levels of accuracy:

- Stage I-Level 1
- Stage I-Level 2a
- Stage I-Level 2b
- Stage I-Level 2c
- Stage I-Level 3

This stepwise analysis allowed for the quantification of the contribution to the error of each of the models included in the EICM to predict the moisture content, considering the input parameters were not sources of error for this Stage (see Table 10). More importantly, this analysis allowed for the calibration of the current version of the EICM moisture prediction.

The Stage I-Level 1 analysis comprised the moisture prediction for the field pavement sections visited by the project team. Information gathered in the field is considered the best available dataset; the error found in the prediction was primarily due to the Suction Model in the EICM. The Suction Model refers to the process used to calculate the equilibrium suction, h, in the field. This parameter is calculated by the following equation:

$$h = y \cdot \gamma_{water} \quad (9)$$

where

y = distance from groundwater table
γ_{water} = unit weight of water

The Stage I-Level 2a analysis included the same sites used in the Stage I-Level 1 analysis, but SWCC parameters were not input. The EICM automatically calculated the SWCC parameters, allowing estimation of the error due to the SWCC model built into the program. The SWCC model refers to the set of correlations used to calculate an equilibrium moisture content based on soil suction and soil index properties such as Passing #200 (P_{200}), Diameter 60 (D_{60}), and Plasticity Index (PI). The SWCC model is given by the Fredlund and Xing equation:

$$\theta_w = C(h) \times \left[\frac{\theta_{sat}}{\left[\ln\left[EXP(1) + \left(\frac{h}{a_f} \right)^{bf} \right] \right]^{cf}} \right] \quad (10)$$

Table 10. Possible sources of error.

Sources of Error	Stage I					Stage II	Stage III	Stage IV
Level of Analysis	**1**	**2a**	**2b**	**2c**	**3**	**1**	**1**	**3**
Suction model	√	√	√	√	√	√	√	√
SWCC model		√	√	√	√			√
k-sat model			√	√	√			√
Gs model				√	√			√
Compaction model					√			√
TDR measurements							√	√
Input parameters:								
SWCC parameters		—	—	—	—			—
Saturated permeability			—	—	—			—
Specific gravity				—	—			—
Optimum water content					—			—
Maximum dry density					—			—
Atterberg limits						√	√	√
Gradation						√	√	√

with

$$C(h)=\left[1-\frac{\ln\left(1+\frac{h}{h_\varepsilon}\right)}{\ln\left(1+\frac{1.45\times10^{5}}{h_\varepsilon}\right)}\right] \quad (11)$$

where

θ_w = Volumetric moisture content, in %
a_f, b_f, c_f, and h_ε = SWCC fitting parameters

In the MEPDG, the SWCC parameters are correlated with soil index properties using the following equations:

For plastic unbound materials ($P_{200}PI > 0$)

$$a_f=\frac{0.00364(P_{200}PI)^{3.35}+4(P_{200}PI)+11}{6.895} \quad \text{(psi)} \quad (12)$$

$$\frac{b_f}{c_f}=-2.313(P_{200}PI)^{0.14}+5 \quad \text{(dimensionless)} \quad (13)$$

$$c_f=0.0514(P_{200}PI)^{0.465}+0.5 \quad \text{(dimensionless)} \quad (14)$$

$$\frac{h_\varepsilon}{a_f}=32.44e^{0.0186(P_{200}PI)} \quad \text{(dimensionless)} \quad (15)$$

For granular nonplastic materials ($P_{200}PI = 0$)

$$a_f=\frac{0.8627(D_{60})^{-0.751}}{6.895} \quad \text{(psi)} \quad (16)$$

$$\overline{b}_f=7.5 \quad \text{(dimensionless)} \quad (17)$$

$$c_f=0.1772\ln(D_{60})+0.7734 \quad \text{(dimensionless)} \quad (18)$$

$$\frac{h_\varepsilon}{a_f}=\frac{1}{D_{60}+9.7e^{-4}} \quad \text{(dimensionless)} \quad (19)$$

The Stage I-Level 2b analysis estimated the error due to the k-sat Model built into the EICM. These runs were for the same sites and with the same data used in the Stage I-Level 2a analysis, but the saturated hydraulic conductivity was automatically calculated by the EICM. The k-Sat Model is a set of correlations used to calculate the saturated hydraulic conductivity from soil index properties such as Passing #200 (P_{200}), Diameter 60 (D_{60}), and Plasticity Index (PI). The k-sat Model is defined by the following relationships:

For granular nonplastic and very low plastic materials ($0 \le P_{200}PI < 1$)

$$k_{sat}=118.11\times10^{\left[-1.1275(\log D_{60}+2)^2+7.2816(\log D_{60}+2)-11.2891\right]} \text{ (ft/hr)} \quad (20)$$

The above equation is valid for D_{60} less than 20 mm. If D_{60} is greater than 20 mm, the EICM sets D_{60} = 20 mm.

For plastic unbound materials ($P_{200}PI > 1$)

$$k_{sat}=118.11\times10^{\left[0.0004(P_{200}PI)^2-0.0929(P_{200}PI)-6.56\right]} \text{ (ft/hr)} \quad (21)$$

The Stage I-Level 2c analysis estimates the error due to the Gs Model built into the EICM. The Gs Model is a correlation used to calculate the specific gravity of soils based on the Passing #200 (P_{200}) and Plasticity Index (PI). These runs used the same sites and data as for the Stage I-Level 2b analysis except that, in this case, the specific gravity, G_s, was automatically calculated by the EICM. The Gs Model is defined by the following relationship:

$$G_s=0.041(P_{200}PI)^{0.29}+2.65 \quad (22)$$

The Stage I-Level 3 analysis estimated the error due to the Compaction Model built into the EICM. The Compaction Models are correlations used to estimate the optimum water content and the dry unit weight for cases where this information is not available. The correlations are based on Passing #200 (P_{200}), Diameter 60 (D_{60}), and Plasticity Index (PI). These runs used the same sites and data used in Stage I-Level 2c analysis except that, in this case, the compaction parameters were estimated by the EICM. The Compaction Model carries out the following steps:

1. Identify the layer as a compacted base course, compacted subgrade, or natural in situ subgrade.
2. Calculate the optimum degree of saturation, S_{opt}:
   $$S_{opt}=6.752\ (P_{200}PI)^{0.147}+78 \quad (23)$$
3. Compute the optimum gravimetric moisture content, w_{opt}:
   a) If $P_{200}PI > 0$ (plastic materials):
      $$w_{opt}=1.3\ (P_{200}PI)^{0.73}+11 \quad (24)$$
   b) If $P_{200}PI = 0$ (granular, nonplastic materials):
      $$w_{opt\,(T99)}=8.6425\ (D_{60})^{-0.1038} \quad (25)$$
      i. If layer is not a base course
         $$w_{opt}=w_{opt\,(T99)} \quad (26)$$
      ii. If layer is a base course
         $$\Delta w_{opt}=0.0156[w_{opt(T99)}]^2-0.1465w_{opt(T99)}+0.9 \quad (27)$$
         $$w_{opt}=w_{opt\,(T99)}-\Delta w_{opt} \quad (28)$$
4. Compute $\gamma_{d\,max}$ for compacted materials, $\gamma_{d\,max\,comp}$
   $$\gamma_{d\max comp}=\frac{G_s\gamma_{water}}{1+\frac{w_{opt}G_s}{S_{opt}}} \quad (29)$$
5. Compute $\gamma_{d\,max}$
   a) If layer is a compacted material
      $$\gamma_{d\max}=\gamma_{d\max comp} \quad (30)$$
   b) If layer is a natural in situ material
      $$\gamma_d=0.90\gamma_{d\max comp} \quad (31)$$
      EICM uses γ_d for $\gamma_{d\,max}$.

6. Compute the volumetric water content, θ_{opt}

$$\theta_{opt} = \frac{w_{opt}\gamma_{d\,\max}}{\gamma_{water}} \quad (32)$$

Table 11 and Figures 5 through 10 present the measured versus predicted moisture contents from the Level 1 analysis runs. Table 12 summarizes the statistical analysis.

With the EICM in Version 0.7 (July 2004 release) of the MEPDG software, predicted water contents were lower than measured water contents, particularly for soils with low PI and nonplastic materials, at all levels of the analysis. This conclusion was based on the algebraic error, which was positive for analysis levels. Possible explanations of this finding are given below:

- The Suction Model, which predicts suction by $y\gamma_w$, overpredicts suction—the absolute error associated with this model was found to be 31%, which is equivalent to an R^2 of 65%. (Note that the R^2 for the Stage I – Level 1 runs, which analyzed the accuracy of the Suction Model, is 65%). This is considered a substantial error.
- The SWCC models contributed minor error to the overall prediction of moisture content. This error was calculated as the difference of the absolute error found for Stage I – Level 2a runs and the error found for the Stage I – Level 1 runs. The change in absolute error was found to be 10% (from 31% to 41%), which is equivalent to a change in the R^2 statistic from 65% to 58%. Further analysis of the moisture content prediction showed that this contribution to the error mostly arose from the prediction for nonplastic granular materials as shown in Figure 10.
- The inclusion of the *k-sat* Model in the prediction of moisture content did not add substantial error to the estimate. The R^2 dropped from 58.2% to 57.5%; and the absolute error improved to 36% from 41%. It was noted that, once freezing occurs, nonplastic granular soils dry up, the unsaturated hydraulic conductivity, k_{unsat}, trends to zero, and water does not have enough time to get back in before freezing occurs again. This phenomenon would explain in part the underpredicted moisture content results.
- The accuracy of the *Gs Model* was analyzed in the Stage I – Level 2c runs. The error did not increase when the *Gs Model* was used in place of field-measured specific gravities. The absolute error was 35.4%, which compares with the error found in the previous run of 35.5%. Of interest, the R^2 value increased to 64%, which indicates less scatter in the overall prediction of moisture content, but not necessarily a better one.
- Stage I – Level 3 analysis checked the added error when the Compaction Model was incorporated in the analysis. The absolute error slightly increased from 35.4% to 35.7%. The scatter, as measured by the R^2 statistic, was marginally larger, decreasing from 64% to 60%.

Based on the results of the Stage I analyses, with the EICM underpredicting the moisture content in the unbound materials, it was evident that the Suction and SWCC models needed improvement. The prediction of moisture content for the plastic materials was found to be better than the prediction for the granular materials. In addition, it appeared that there were limitations or problems with the modeling of post-freezing moisture contents under certain conditions, which might be related to the *k-sat* Model. A solution for this problem was also pursued.

Note that $y\gamma_w$ may typically overestimate suction because, in real-life situations, suction may be depressed by a more or less steady influx of water from condensation of water vapor, which is not considered in the current model. Further, the presence of small undetected lenses of perched water, which are believed to be prevalent, would lead to overestimation of the suction.

4.5.2 Stage II Analysis

Stage II analysis made use of the databases available for the sites visited, with the material properties available in the different databases used as input parameters into the EICM program. This process allowed the research team to evaluate the validity of the parameters found in the databases as well as the sensitivity of the models to key parameters when used for moisture prediction purposes.

The databases available (i.e., LTPP, MnRoad, and WesTrack) provided material gradation, Atterberg limits, optimum water content, and maximum dry unit weight. Data such as SWCCs, hydraulic conductivity, and specific gravity are rarely cataloged in such databases. However, compaction data were not part of the laboratory program of this project, so only the validity of the gradation and Atterberg limits data, which were considered to be fundamental information in the prediction process, was checked.

Forty-nine points of measured moisture content were extracted from the LTPP and MnRoad databases. The information was compared with data points predicted by the EICM. Table 13 presents the predicted moisture content, along with the site identification; Table 12 summarizes the statistical analysis.

These results showed that the model underpredicted the moisture content. Figure 11 shows the measured versus predicted values. The algebraic error went from 8% for the runs with actual measurements to 34% for the runs with data from databases. The R^2 statistics went from 65% to 48% as the scatter increased. The results showed that prediction of the moisture content of the unbound material with the EICM models is very sensitive to the gradation and Atterberg limits of the

Table 11. Measured versus predicted moisture content – Stage I analysis.

Section ID	State	Lab ID	Sample Type	Layer	Measured Grav. w (%)	Level 1 EICM Predicted Grav. w (%)	Level 2a EICM Predicted Grav. w (%)	Level 2b EICM Predicted Grav. w (%)	Level 2c EICM Predicted Grav. w (%)	Level 3 EICM Predicted Grav. w (%)
10101	**AL**	1-3-(7.5-10)	Grab (SC)	GB	9.80	5.96	9.51	10.80	7.16	6.67
		1-3-(14.5-15)	Tube	SS	23.43	22.47	24.10	22.91	22.78	22.60
		1-3-(23)	Tube	SS	18.81	20.34	21.81	20.73	20.62	20.45
40113	**AZ**	2-3-(5.5-6.5)	Grab (SC)	GB	3.19	5.10	0.00	0.00	0.00	0.00
		2-3-(12-13.5)	Grab (SC)	SS	7.52	8.23	0.00	0.00	0.00	0.00
40215	**AZ**	4-1-(11.5)	Grab (SC)	GB	5.21	2.75	7.19	7.19	7.19	0.00
		4-1-(18-18.5)	Tube	SS	7.49	14.46	9.99	10.48	10.38	7.18
52042	**AR**	1-5-(13-14)	Grab	GB	19.83	17.52	17.28	15.23	15.76	18.52
		1-5-(18.5)	Tube	SS	18.16	18.01	17.77	15.65	16.20	19.04
		1-5-(15-15.5)	Tube	SS	18.01	17.28	17.05	15.02	15.54	18.26
		1-5-(23-24)	Tube	SS	16.96	17.84	18.14	18.14	18.56	24.72
63042	**CA**	8-3-(13-14)	Tube	Comp SS	18.93	21.07	18.68	18.68	18.62	13.03
		8-3-(20-21)	Tube	SS	16.56	19.68	17.98	17.93	17.60	16.67
		8-3-(28-29)	Tube	SS	16.54	19.46	18.88	18.83	18.48	17.51
81053	**CO**	7-5-(7.5)	Grab (SC)	GB1	3.68	2.70	0.00	0.00	0.00	0.00
		7-5-(13.5-14)	Grab (SC)	GB2	5.19	3.84	0.00	0.00	0.05	0.05
		7-5-(43)	Tube	NatSS	22.96	23.55	24.10	24.28	23.91	23.97
		7-5-(50)	Tube	NatSS	23.46	23.80	24.52	24.52	23.86	27.40
87035	**CO**	7-4-(14.5)	Grab (SC)	GB	3.31	1.66	0.00	2.47	2.47	2.37
		7-4-(19)	Tube	SB	6.64	0.22	1.41	7.69	7.96	8.61
		7-4-(37)	Tube	SB	9.73	0.21	1.39	7.58	7.84	8.48
		7-4-(48)	Tube	SS	19.98	18.91	19.55	19.14	19.14	20.48
91803	**CT**	6-1-(10-12.5)	Grab (SC)	GB	5.03	2.84	0.00	0.00	0.00	0.00
		6-1-(20-21)	Grab (SC)	SS	7.13	6.56	0.00	0.00	0.00	0.00
204054	**KS**	5-3-(16-16.5)	Tube	SS	22.02	20.87	21.90	21.96	21.90	23.72
		5-3-(22)	Tube	SS	21.17	20.42	21.43	21.49	21.43	23.21
		5-3-(27)	Tube	SS	17.12	19.10	20.30	20.51	19.88	22.60

Table 11. (Continued).

Section ID	State	Lab ID	Sample Type	Layer	Measured Grav. w (%)	Level 1 EICM Predicted Grav. w (%)	Level 2a EICM Predicted Grav. w (%)	Level 2b EICM Predicted Grav. w (%)	Level 2c EICM Predicted Grav. w (%)	Level 3 EICM Predicted Grav. w (%)
220118	**LA**	3-1-(24)	Tube	SS	16.62	13.27	12.97	12.97	13.03	17.48
		3-1-(29)	Tube	SS	16.83	13.06	12.77	12.77	12.83	17.20
		3-1-(32)	Tube	SS	21.45	13.23	12.94	12.94	13.00	17.43
		3-1-(34)	Tube	SS	22.63	20.60	17.68	17.50	17.80	17.98
281016	**MS**	1-4-(9.5-10.5)	Grab (SC)	GB	10.10	7.18	1.46	5.93	5.83	6.08
		1-4-(18-19)	Tube	GB	10.34	7.30	1.48	6.03	5.92	6.18
		1-4-1-27	Tube	GB	7.59	15.06	13.08	13.41	13.30	17.82
		1-4-(40-42)	Tube	SS	16.68	15.60	13.55	13.89	13.78	18.46
307066	**MT**	7-1-(10-10.5)	Grab (SC)	GB	5.94	5.75	0.00	0.00	0.00	4.10
		7-1-(13-13.5)	Grab (SC)	SB	5.39	5.97	0.00	0.00	0.00	4.27
		7-1-(29-30)	Tube	SS	13.86	13.84	11.70	6.73	6.57	12.71
		7-1-(38-39)	Tube	SS	14.52	12.92	13.72	13.72	13.12	18.69
310114	**NE**	5-4-(7.5-9)	Grab (SC)	GB	2.37	4.06	0.00	0.00	0.00	0.00
		5-4-(19)	Tube	SS	26.27	18.69	24.65	24.21	24.21	24.21
		5-4-(25-28)	Tube	SS	24.56	18.39	24.25	23.82	23.82	23.82
320204	**NV**	8-2-(12)	Grab (SC)	GB	5.08	8.02	0.00	0.00	0.00	0.00
		8-2-(18-19)	Grab (SC)	SB	5.94	12.43	0.00	0.00	0.00	0.00
		1-1-(10-13)	Tube	SS	20.45	19.39	23.58	23.87	23.87	20.90
		1-1-(22)	Tube	SS	22.03	19.97	25.04	25.35	25.35	22.20
364018	**NY**	6-3-(10-10.5)	Grab (SC)	SS	5.29	7.58	0.00	0.00	0.00	0.00
		6-3-(18-19)	Grab (SC)	SS	5.07	7.83	0.00	0.00	0.00	0.00
370205	**NC**	5-1-(16)	Tube	SS	31.44	17.21	15.88	15.88	15.81	19.87
		5-1-(24)	Tube	SS	28.01	20.62	21.49	21.49	21.49	20.02
420603	**PA**	6-4-(15-17)	Grab (SC)	GB	3.81	0.18	0.00	3.10	0.00	6.47
		6-4-(22.5-23)	Grab (SC)	ComSS	10.35	0.20	9.07	9.68	8.71	9.01
473101	**TN**	5-2-(17)	Tube	SS	32.76	24.19	25.29	21.72	21.65	20.28
		5-2-(20)	Tube	SS	36.10	25.23	26.38	22.66	22.59	21.16
		5-2-(24-26)	Tube	SS	35.21	24.88	27.98	25.72	25.65	29.32
481060	**TX**	3-3-(17)	Grab (SC)	GB	8.40	8.80	11.34	11.34	10.55	9.64
		3-3-(23-24)	Tube	SS	19.15	20.89	20.51	20.51	20.07	20.89

(*continued on next page*)

Table 11. (Continued).

Section ID	State	Lab ID	Sample Type	Layer	Measured Grav. w (%)	Level 1 EICM Predicted Grav. w (%)	Level 2a EICM Predicted Grav. w (%)	Level 2b EICM Predicted Grav. w (%)	Level 2c EICM Predicted Grav. w (%)	Level 3 EICM Predicted Grav. w (%)
		3-3-(26)	Tube	SS	17.83	19.24	16.19	16.19	16.31	20.12
		3-3-(32-34)	Tube	SS	21.37	19.28	16.22	16.22	16.34	20.16
481077	**TX**	1-2-(15-16)	Grab (SC)	GB	3.29	5.43	2.29	4.26	4.03	2.06
		1-2-(22)	Tube	SS	9.07	13.79	2.95	5.48	5.18	2.65
		1-2-(30.5-31)	Tube	SS	11.26	17.97	3.14	5.69	5.46	3.62
484143	**TX**	3-2-1-15	Grab (SC)	Comp SB	25.55	14.87	17.37	17.37	17.37	22.98
		3-2-(25)	Tube	SS	19.67	17.56	17.79	17.62	17.62	21.06
		3-2-(35-36)	Tube	SS	19.97	19.56	18.52	18.52	18.05	18.75
501681	**VT**	6-2-(11.5)	Grab (SC)	GB	2.99	1.14	0.00	1.33	0.24	0.00
		6-2-(13)	Grab (SC)	GB	2.85	1.12	0.00	3.75	0.45	6.03
		6-2-(17-20)	Grab (SC)	GB	3.58	1.16	0.00	9.31	5.05	8.48
		6-2-(33-35)	Tube	SB	9.39	2.11	0.05	9.77	8.88	10.70
		6-2-(44)	Tube	SS	12.55	10.67	11.56	13.14	14.13	17.55
537322	**WA**	8-1-(10-11)	Grab (SC)	GB	5.05	3.14	0.00	0.09	0.09	0.09
		8-1-(20-22)	Tube	SS	21.37	21.44	20.57	21.13	21.13	22.06
		8-1-(29-31)	Tube	SS	20.57	20.49	19.66	20.19	20.19	21.08
562019	**WY**	7-3-(19-19.5)	Tube	SB	14.23	12.20	1.24	0.17	5.62	0.17
		7-3-(30)	Tube	SS	19.68	14.95	1.39	0.17	8.37	0.17
		7-3-(39)	Tube	SS	22.33	16.03	19.31	17.45	18.07	21.97
		7-3-(46)	Tube	SS	23.22	17.28	20.19	18.25	18.90	22.98
562020	**WY**	7-2-(20-21)	Tube	SS	14.74	0.21	13.67	13.67	12.27	16.68
		7-2-(29-30)	Tube	SS	14.67	10.48	10.23	10.23	9.17	12.90
MnRoad 4	**MN**	6-5-(9-12)	Tube	Comp SS	14.44	17.05	15.13	15.13	15.02	14.32
		6-5-(19-20)	Tube	Comp SS	13.66	17.71	15.11	15.05	15.38	18.36
		6-5-(15-17)	Tube	Comp SS	14.38	16.94	15.03	15.03	14.92	14.23
Wstk 12	**NV**	2-1-(6.5-8)	Grab (SC)	GB	7.06	8.39	4.36	7.53	6.82	6.21
		2-1-(17.5-18)	Tube	Eng. Fill	18.27	14.23	18.97	17.44	18.09	20.08
		2-1-(30)	Tube	Comp SS	20.97	17.32	18.83	18.01	18.08	19.95
		2-1-1-39	Tube	SS	14.99	15.84	15.96	15.96	15.73	15.01
Wstk 15	**NV**	2-1-(6.5-8)	Grab (SC)	GB	7.24	8.44	1.42	7.41	6.89	6.09
		2-1-(18)	Tube	Eng. Fill	22.55	15.15	17.38	15.09	14.16	19.85
		2-1-(30)	Tube	Comp SS	22.06	13.21	18.38	16.31	16.38	22.28

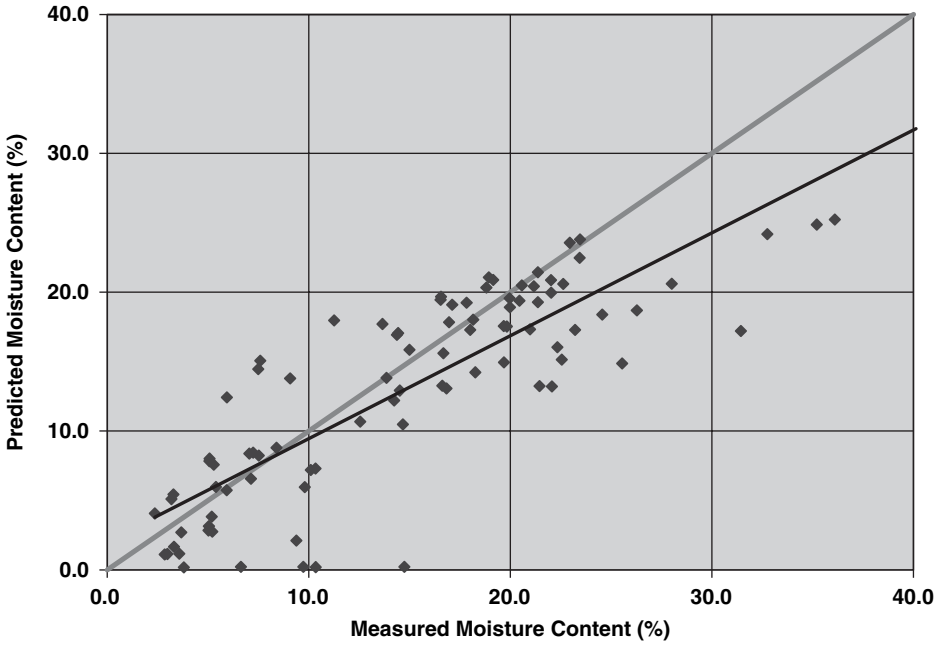

Figure 5. Comparison of measured and predicted moisture contents – Stage I-Level 1 runs.

soil, emphasizing the need to use measured gradation and Atterberg Limits with the MEPDG whenever possible in lieu of estimated values.

4.5.3 Stage III Analysis

Stage III analysis was similar to that in Stage II, except that the moisture predictions were compared with the TDR moisture data from the databases. This allowed quantification of the errors associated with TDR data, which is crucial for future predictive capabilities.

The TDR-measured volumetric moisture contents for LTPP SMP sites were obtained from the LTPP database (LTPP, 2003). Typically, TDR instrumentation included 10 probes installed at 10 different depths starting from the granular base and reaching well into the subgrade. The database

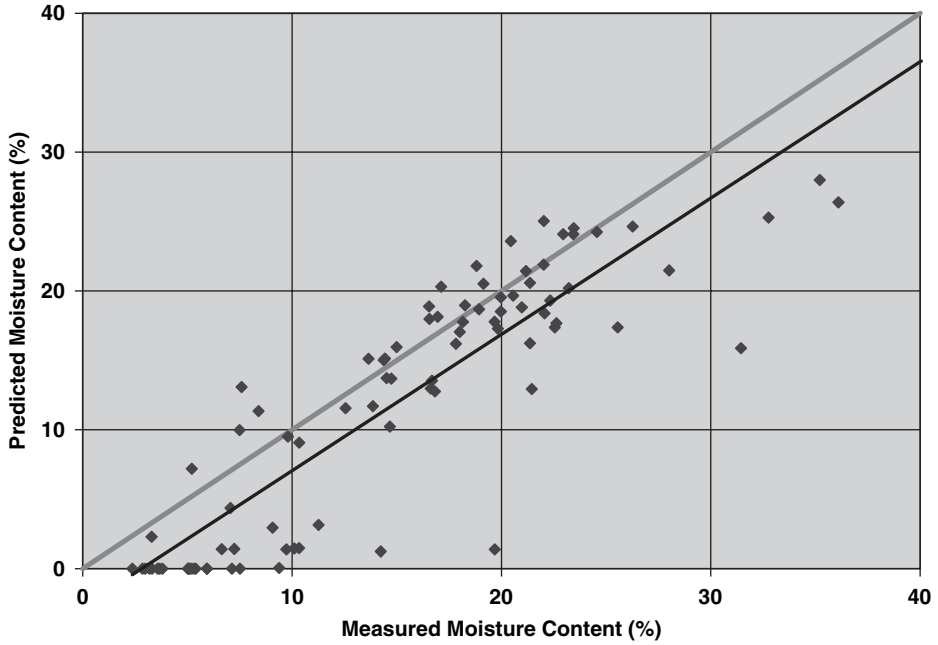

Figure 6. Comparison of measured and predicted moisture contents – Stage I-Level 2a runs.

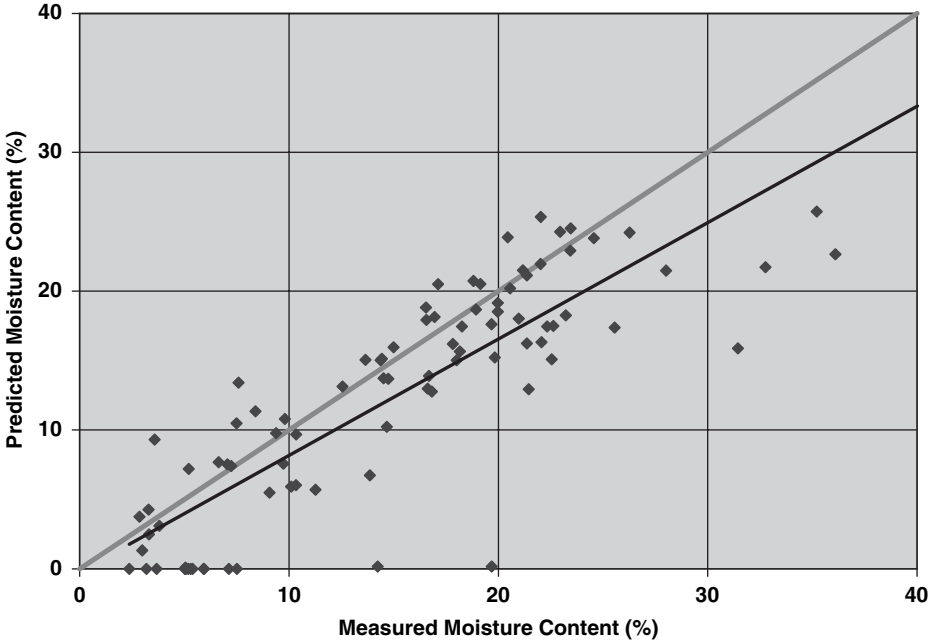

Figure 7. Comparison of measured and predicted moisture contents – Stage I-Level 2b runs.

recorded the depth of each probe. For comparison, data from the probes corresponding to the sample depth were extracted from the database and plotted versus time. Figure 12 shows a typical plot of TDR volumetric water content versus time for the LTPP SMS site in Opelika, Alabama. (Plots for all the sites are presented in Appendix D on the project web page).

In general, TDR data indicate that moisture content fluctuates around an average value with higher moisture contents in the spring. The fluctuation was most prominent for sites in cold weather regions. For this study, the average moisture content was computed by excluding the unusually low moisture contents recorded during winter months. These unusual readings result from the presence of frozen water. The TDR probe measures the dielectric constant of the soil water surrounding the probe. The moisture content is then computed from the dielectric constant, using functions developed through calibrations for fine-grained and coarse-grained materials. However, the TDR can detect only the unfrozen or

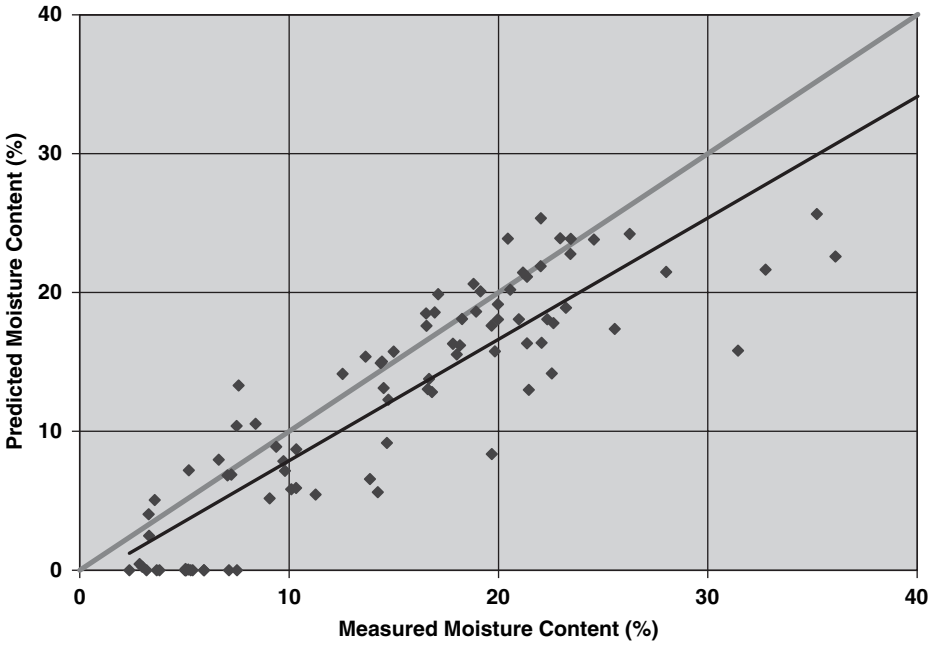

Figure 8. Comparison of measured and predicted moisture contents – Stage I-Level 2c runs.

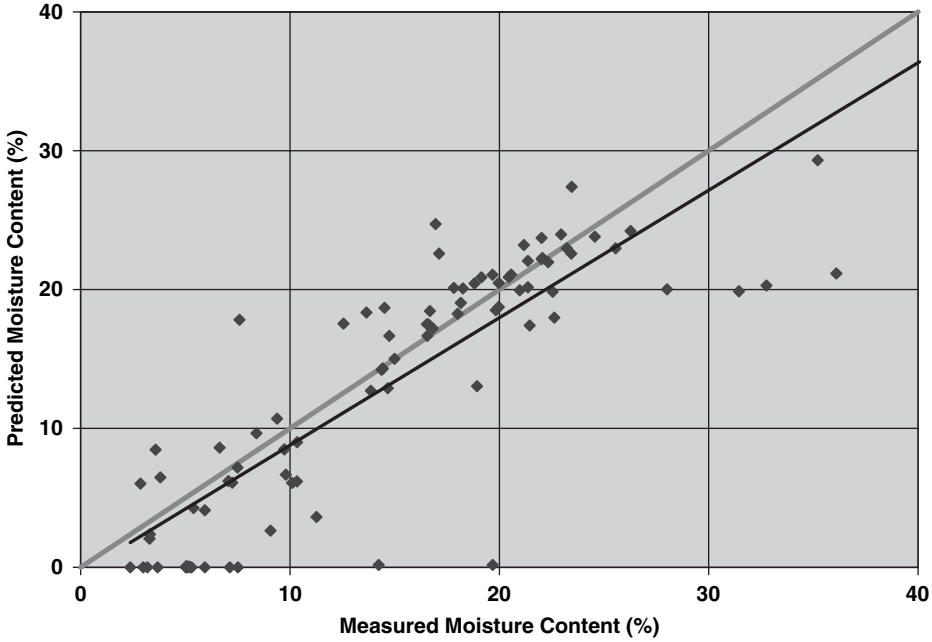

Figure 9. Comparison of measured and predicted moisture contents – Stage I-Level 3 runs.

free water; when water freezes, the readings will indicate erroneously low values of moisture content.

Forty-three data points were used in the comparison shown in Figure 13; the data for each point are presented in Table 14. The statistics in Table 12 represent the error associated with the TDR measurements, as well as the error associated with the use of gradation and Atterberg limits from the databases. These data indicate that the TDR-measured values were generally higher than field-measured values.

To use the TDR data in subsequent analysis, the average TDR-measured moisture contents along with the corresponding field-measured moisture contents for the best 23 sites were compared to obtain a correction factor for the TDR readings that would allow better comparisons in the future. The 23 sites were those with a history of more stable readings and a minimum of data from freeze-thaw cycles. Table 15 presents these TDR and field volumetric moisture contents. The data, as expected from previous results, indicated that the TDR-measured values were generally higher than the field-measured values. The TDR versus field-measured moisture content plot is shown in Figure 14 along with a curve fitted to the data, from which a correction factor was determined.

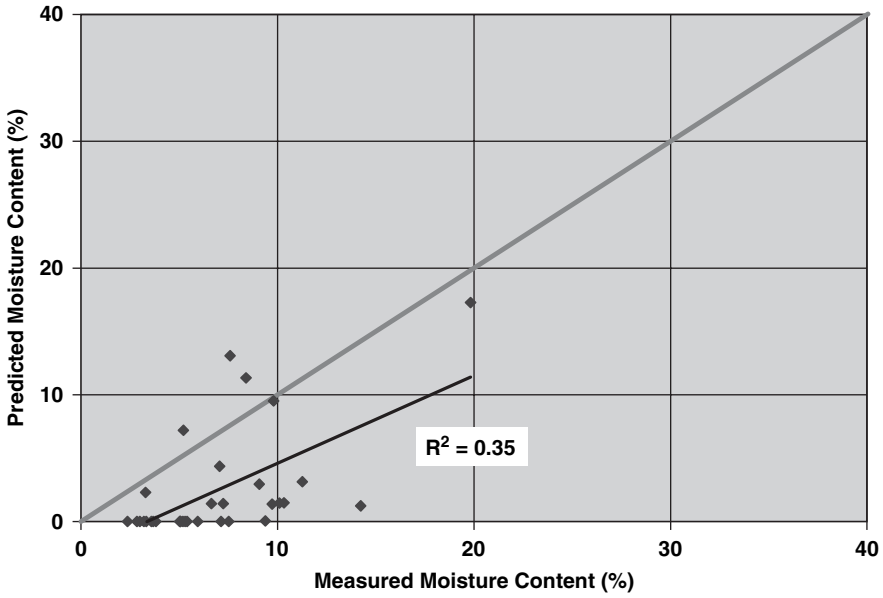

Figure 10. Measured versus predicted gravimetric moisture content Stage I - Level 2a runs for nonplastic granular materials.

Table 12. Statistical parameters for runs at different stages of analysis.

Analysis	n	Unknown Parameters	Degrees Freedom	S_e	S_y	S_e/S_y	R^2	e_{alg} (%)	e_{abs} (%)
Stage I – Level 1	89	0		4.8216	8.1707	0.590	0.652	8.8	31.1
Stage I – Level 2a	89	4	85	5.2802	8.1707	0.646	0.582	34.1	41.4
Stage I – Level 2b	89	5	84	5.3282	8.1707	0.652	0.575	22.2	35.5
Stage I – Level 2c	89	6	83	4.9299	8.1707	0.603	0.636	26.5	35.4
Stage I – Level 3	89	8	81	5.1756	8.1707	0.633	0.599	16.9	35.7
Stage II	49	0		5.5182	7.6696	0.719	0.482	34.3	42.3
Stage III	43	8	35	7.8344	6.7690	1.157	-0.340	36.5	45.9

Table 13. Measured versus predicted moisture content – Stage II analysis.

Site No.	Section ID	State	Sample ID	Layer	Average Grav. Moisture Content (%)	Predicted Vol. Eq. Moisture Content EICM (%)	Predicted Grav. Eq. Moisture Content EICM (%)
1	**10101**	**AL**	1-3-1-15	SS	23.4	16.4	10.2
			1-3-1-23	SS	18.8	26.0	14.7
2	**40113**	**AZ**	2-3-1-5.5	GB	3.2	0.0	0.0
			2-3-1-13.5	SS	7.5	0.0	0.0
3	**40215**	**AZ**	4-1-1-11.5	GB	5.2	14.2	6.5
			4-1-1-18.5	SS	7.5	11.4	5.6
4	**63042**	**CA**	8-3-1-13	Comp SS	18.9	11.9	6.9
			8-3-1-20	SS	16.6	23.1	12.6
			8-3-1-28	SS	16.5	31.4	18.0
5	**81053**	**CO**	7-5-1-7.5	GB1	3.7	0.1	0.0
			7-5-1-14	GB2	5.2	0.0	0.0
			7-5-1-43	NatSS	23.0	36.4	22.0
			7-5-1-50	NatSS	23.5	43.8	26.3
6	**91803**	**CT**	6-1-1-11	GB	5.0	0.0	0.0
			6-1-1-20	SS	7.1	2.3	1.1
7	**204054**	**KS**	5-3-2-16.5	SS	22.0	29.6	18.0
			5-3-2-27	SS	17.1	34.3	17.9
			5-3-3-22	SS	21.2	29.6	17.6
8	**281016 A**	**MS**	1-4-1-9.5	GB	10.1	1.6	0.8
			1-4-1-19	GB	10.3	20.1	10.3
			1-4-1-27	GB	7.6	26.1	14.4
			1-4-2-42	SS	16.7	26.9	15.4
9	**281016 B**	**MS**	1-4-1-9.5	GB	10.1	1.6	0.8
			1-4-1-19	GB	10.3	1.7	0.9
			1-4-1-27	GB	7.6	2.7	1.5
			1-4-2-42	SS	16.7	3.7	2.1
10	**310114**	**NE**	5-4-1-9	GB	2.4	0.0	0.0
			5-4-1-19	SS	26.3	41.6	26.1
			5-4-1-27	SS	24.6	41.6	25.7
11	**364018**	**NY**	6-3-1-10.5	SS	5.3	0.0	0.0
			6-3-1-19	SS	5.1	0.0	0.0
12	**370205**	**NC**	5-1-1-16	SS	31.4	31.6	23.3
			5-1-1-24	SS	28.0	33.6	22.4
13	**481060 A**	**TX**	3-3-2-17	GB	8.4	0.0	0.0
			3-3-1-24	SS	19.1	24.0	15.1
			3-3-3-26	SS	17.8	24.6	14.4
			3-3-1-34	SS	21.4	24.6	14.5
14	**481060 B**	**TX**	3-3-2-17	GB	8.4	15.8	8.4
			3-3-1-24	SS	19.1	27.0	17.0
			3-3-3-26	SS	17.8	29.6	17.4
			3-3-1-34	SS	21.4	29.6	17.4
15	**481077**	**TX**	1-2-1-16	GB	3.3	7.4	3.5
			1-2-1-22	SS	9.1	7.4	4.5
16	**484143**	**TX**	3-2-1-15	Comp SB	25.6	34.4	23.2
			3-2-1-25	SS	19.7	38.8	22.3
			3-2-1-35	SS	20.0	38.8	22.5
17	**MnRoad 4**	**MN**	6-5-1-12	Comp SS	14.4	28.3	15.1
			6-5-1-20	Com	13.7	28.3	15.3
			6-5-3-15	Com	14.4	28.3	15.0

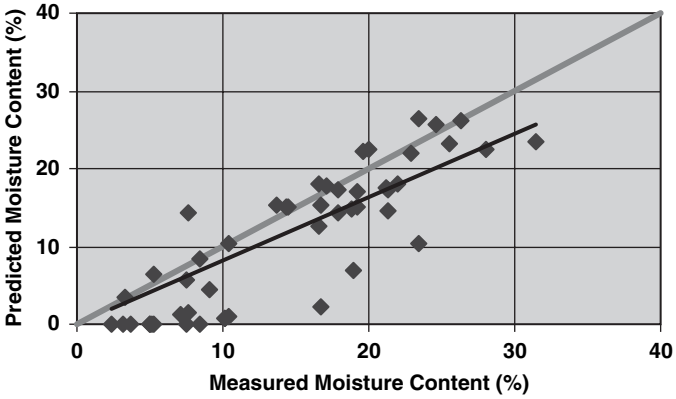

Figure 11. Comparison of measured and predicted moisture contents - Stage II runs.

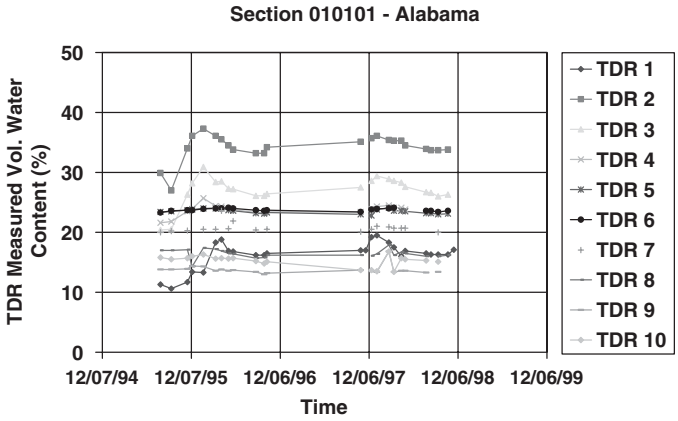

Figure 12. TDR data for Alabama site.

Figure 15 presents the correction factor curve; Figure 16 shows corrected data.

4.5.4 Stage IV Analysis

Stage IV runs comprised all sites, the visited and the desk analysis sites; input data were derived from the databases only. TDR moisture values were compared with the predicted moisture contents from the EICM Version 2.6 output files. Figure 17 shows the measured versus predicted moisture contents for the Alabama site as an example of the data obtained. The legend indicates the depth of the TDR device in inches. (A complete set of plots is presented in Appendix E on the project web page).

Once the runs were completed, the possible sources of error in the measured data obtained from the databases were determined, and data points were eliminated that did not fit into the category of "equilibrium" conditions needed for an unbiased estimate. (Appendix F on the project web page shows the plots for the sections with these data eliminated.) The primary sources of discrepancies between measured and predicted data were as follows:

1. Frozen water, causing much lower moisture content measured in the field than predicted by the EICM;
2. Water content measurements performed during thawing seasons, causing measured water contents not at equilibrium and generally higher than those predicted by the EICM; and
3. TDR malfunction, causing erratic recorded data.

Models needing revisions were determined by inspection, without detailed error analysis. Sources of error were (1) errors in the input index values, (2) errors in the SWCCs, (3) errors in the groundwater table position, (4) errors in the material profile, and (5) errors in the TDR values themselves.

The systematic method used to discover and quantify these potential errors showed that all models needed refinement, particularly the Suction model. The next chapter deals with the development of improved models based on the extensive field collected database, which allowed significant improvement in the prediction capabilities of EICM Version 2.6.

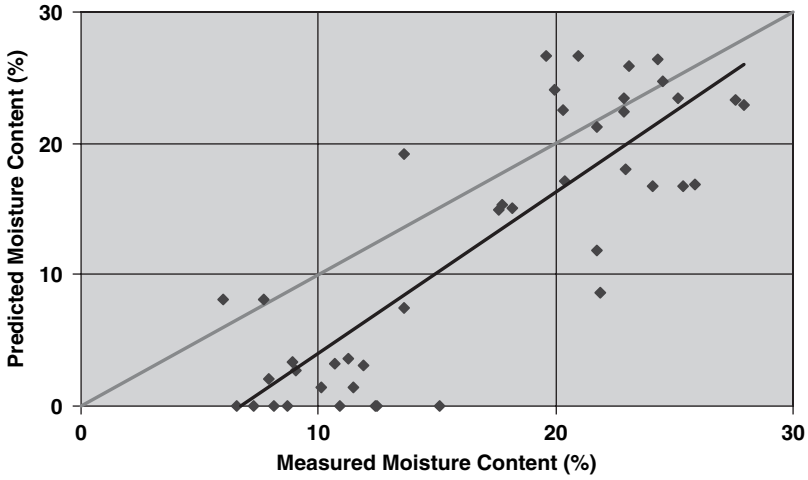

Figure 13. Comparison of measured and predicted moisture contents - Stage III runs.

Table 14. Measured versus predicted moisture content – Stage III analysis.

Site No.	Section ID	State	Sample ID	Layer	Average TDR Grav. Moisture Content (%)	Predicted Vol. Eq. Moisture Content EICM (%)	Predicted Grav. Eq. Moisture Content EICM (%)
1	10101	AL	1-3-1-10	GB	7.67	18.3	8.1
			1-3-1-15	SS	21.75	33.9	21.2
			1-3-1-23	SS	13.59	33.9	19.2
2	40113	AZ	2-3-1-5.5	GB	8.15	0.0	0.0
			2-3-1-13.5	SS	6.55	0.0	0.0
3	40215	AZ	4-1-1-11.5	GB	12.42	0.0	0.0
			4-1-1-18.5	SS	13.63	15.3	7.5
4	52042	AR	1-5-2-13.5	GB	A	26.7	15.7
			1-5-1-18.5	SS	A	26.7	16.1
			1-5-2-15	SS	A	26.7	15.5
			1-5-1-23	SS	A	26.7	16.0
5	63042	CA	8-3-1-13	Comp SS	21.71	20.3	11.8
			8-3-1-20	SS	20.39	31.4	17.2
			8-3-1-28	SS	22.96	31.4	18.0
6	81053	CO	7-5-1-7.5	GB1	5.96	18.1	8.1
			7-5-1-14	GB2	8.94	6.4	3.3
			7-5-1-43	NatSS	22.85	38.9	23.5
			7-5-1-50	NatSS	19.59	44.4	26.7
7	87035	CO	7-4-1-14.5	GB	A	5.0	2.4
			7-4-1-19	SB	A	16.2	8.8
			7-4-1-37	SB	A	16.2	8.6
			7-4-1-48	SS	A	36.4	21.1
8	91803	CT	6-1-1-11	GB	8.68	0.0	0.0
			6-1-1-20	SS	12.45	0.0	0.0
9	204054	KS	5-3-2-16.5	SS	25.17	38.6	23.4
			5-3-2-27	SS	19.93	46.2	24.1
			5-3-3-22	SS	27.96	38.6	22.9
10	220118	LA	3-1-1-24	SS	A	22.3	13.2
			3-1-1-34	SS	A	40.4	24.5
			3-1-2-29	SS	A	22.3	13.0
			3-1-3-32	SS	A	22.3	13.2
11	281016	MS	1-4-1-9.5	GB	10.11	2.8	1.4
			1-4-1-19	GB	11.50	2.8	1.4
			1-4-1-27	GB	11.90	5.6	3.1
			1-4-2-42	SS	10.69	5.6	3.2
12	307066	MT	7-1-1-10	GB	A	10.8	4.7
			7-1-1-13.5	SB	A	10.8	4.8
			7-1-1-30	SS	A	14.5	7.7
			7-1-1-39	SS	A	34.2	17.2
13	310114	NE	5-4-1-9	GB	7.28	0.0	0.0
			5-4-1-19	SS	24.31	42.0	26.3
			5-4-1-27	SS	23.12	42.0	25.9
15	350105	NM	1-1-1-13	SS	A	41.1	23.9
			1-1-1-22	SS	A	41.1	25.4
16	364018	NY	6-3-1-10.5	SS	10.89	0.0	0.0
			6-3-1-19	SS	15.10	0.0	0.0
17	370205	NC	5-1-1-16	SS	27.58	31.5	23.3
			5-1-1-24	SS	22.85	33.6	22.4
19	420603	PA	6-4-1-17	GB	A	0.0	0.0
			6-4-1-23	ComSS	A	0.0	0.0
20	473101	TN	5-2-1-17	SS	A	33.2	22.8
			5-2-3-20	SS	A	33.2	23.7
			5-2-1-25	SS	A	33.2	23.4

Table 14. (Continued).

Site No.	Section ID	State	Sample ID	Layer	Average TDR Grav. Moisture Content	Predicted Vol. Eq. Moisture Content EICM	Predicted Grav. Eq. Moisture Content EICM
					(%)	(%)	(%)
21	**481060**	**TX**	3-3-2-17	GB	21.89	16.3	8.6
			3-3-1-24	SS	25.86	26.9	16.9
			3-3-3-26	SS	24.11	28.5	16.7
			3-3-1-34	SS	25.39	28.5	16.8
22	**481077**	**TX**	1-2-1-16	GB	7.90	4.4	2.1
			1-2-1-22	SS	9.08	4.4	2.6
			1-2-1-31	SS	11.26	6.1	3.6
23	**484143**	**TX**	3-2-1-15	Comp SB	24.53	36.5	24.7
			3-2-1-25	SS	20.32	39.2	22.5
			3-2-1-35	SS	20.96	45.9	26.6
24	**501681**	**VT**	6-2-1-11.5	GB	**A**	2.0	1.0
			6-2-1-20	GB	**A**	15.5	7.2
			6-2-3-13	GB	**A**	5.7	2.5
			6-2-2-35	SB	**A**	21.8	10.7
			6-2-1-44	SS	**A**	29.8	15.7
25	**537322**	**WA**	8-1-1-11	GB	**A**	0.2	0.1
			8-1-1-20	SS	**A**	0.3	0.2
			8-1-1-29	SS	**A**	36.0	21.3
26	**562019**	**WY**	7-3-1-19.5	SB	**A**	0.2	0.1
			7-3-1-30	SS	**A**	0.3	0.2
			7-3-4-39	SS	**A**	3.6	2.2
			7-3-4-46	SS	**A**	3.6	2.3
27	**562020**	**WY**	7-2-1-20	SS	**A**	21.2	11.0
			7-2-1-29	SS	**A**	19.5	9.8
28	**MnRoad 4**	**MN**	6-5-1-12	Comp SS	18.14	28.2	15.1
			6-5-1-20	Comp SS	17.75	28.2	15.3
			6-5-3-15	Comp SS	17.63	28.2	15.0
A	No TDR data (or site was not visited)						

Table 15. TDR and field volumetric moisture content.

Site	Sample ID	Depth (in)	Layer	Field Measured θ_w%	TDR-Measured θ_w%
AL	1-3-1-15	15	SS	36.79	34.33
AZ1	2-3-2-13	13	SS	11.85	11.49
AZ2	4-1-1-18.5	18.5	SS	13.58	26.10
CA	8-3-3-21	21	SS	30.22	37.10
CA	8-3-1-28	28	SS	24.27	37.56
CO1	7-5-1-43	43	SS	38.10	43.00
CT	6-1-1-20	20	SS	12.70	25.57
KS	5-3-2-16.5	16.5	SS	35.47	39.15
MS	1-4-2-42	42	SS	28.90	20.71
NE	5-4-2-25	25	SS	38.62	41.46
NV	8-2-3-18	18	SB	12.78	21.10
NY	6-3-1-19	19	SS	11.16	18.69
NC	5-1-2-24	24	SS	43.57	36.60
TX1	3-3-2-23	23	SS	30.44	39.81
TX2	1-2-1-22	22	SS	15.41	19.40
TX3	3-2-1-15	15	C SS	37.80	36.47
TX4	3-2-2-25	25	SS	33.55	38.31
TX5	3-2-1-35	35	SS	34.19	39.86
MnR	6-5-3-15	15	C SS	27.88	28.33
MnR	6-5-1-20	20	C SS	27.54	29.76
WTr	2-1-2-18	18	Fill	32.02	37.30
WTr	2-1-2-30	30	C SS	30.76	33.80
MS	1-4-3-18	18	SB	21.23	19.97

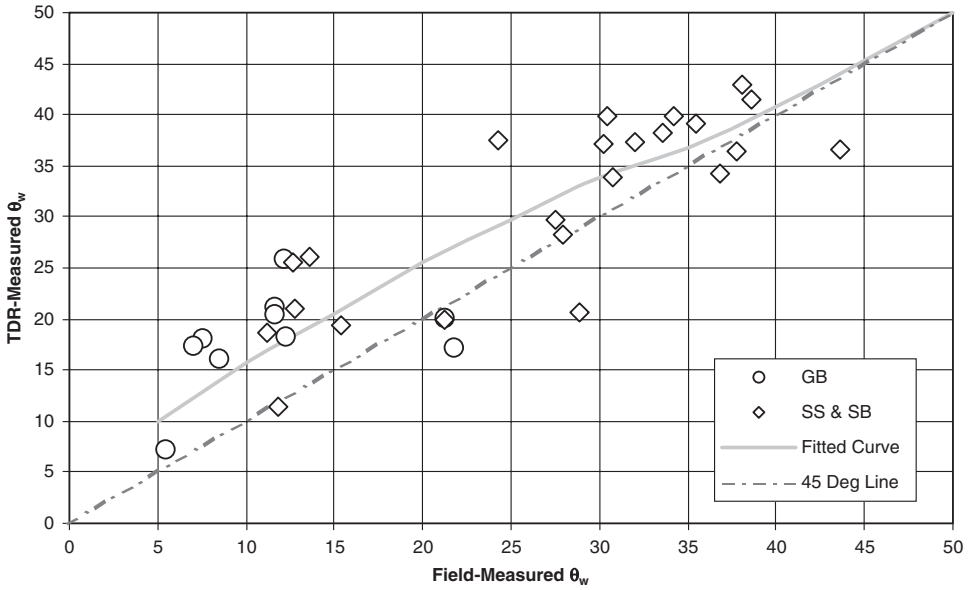

Figure 14. TDR-measured versus field-measured moisture content.

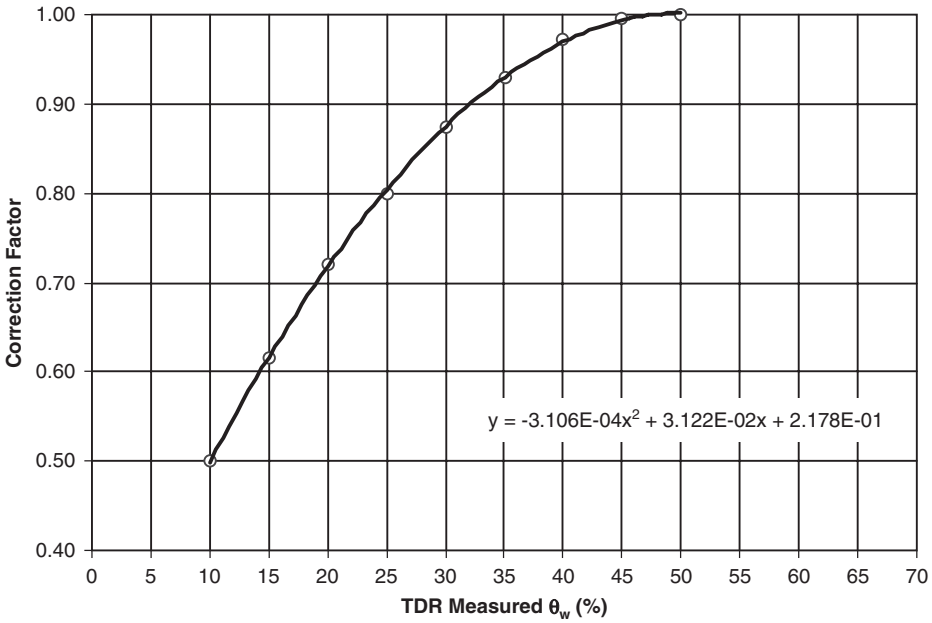

Figure 15. Correction factor for TDR-measured moisture content.

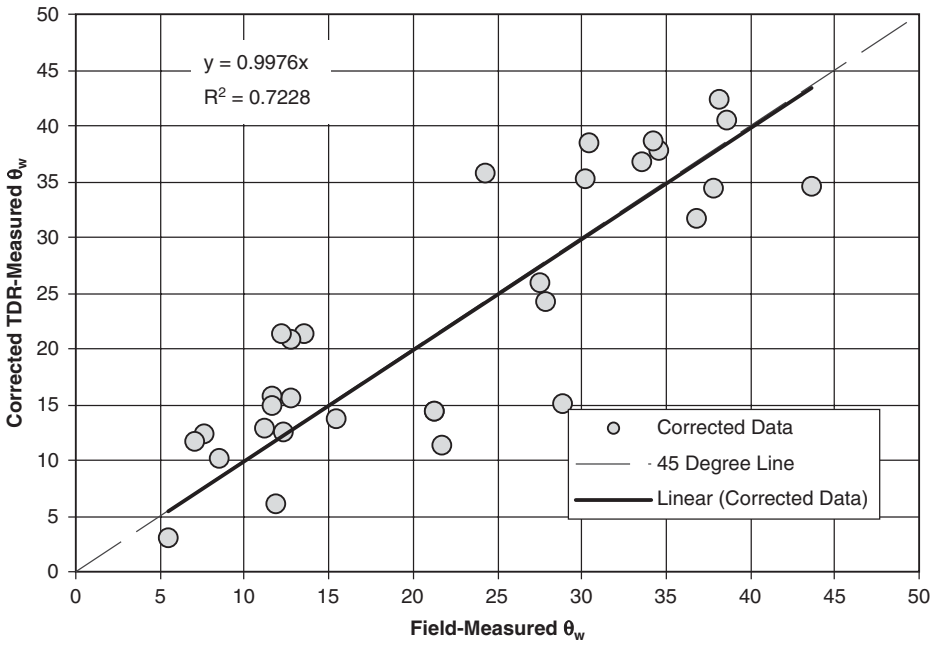

Figure 16. Corrected TDR data versus field measured data.

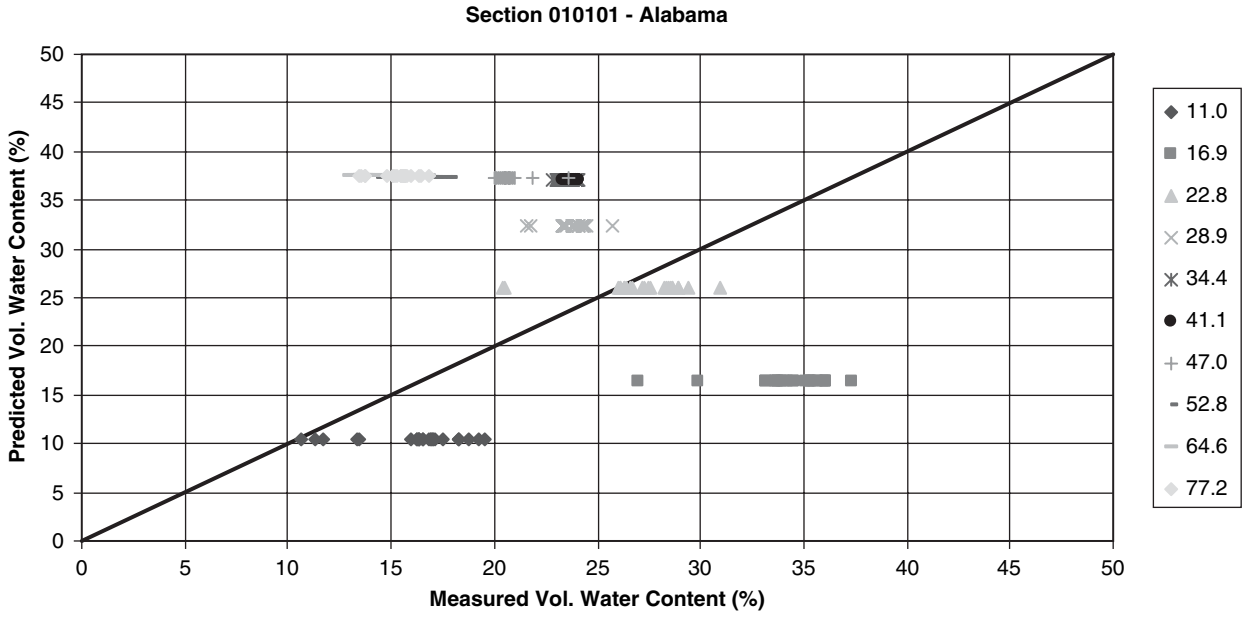

Figure 17. LTPP section 010101 – Stage IV run.

CHAPTER 5

Calibration of the Enhanced Integrated Climatic Model

5.1 SWCC Model Calibration

5.1.1 Background

The relationship between soil suction and moisture content is commonly known as the soil water characteristic curve (SWCC). Knowledge of this relationship is important when modeling unsaturated flow and predicting moisture contents for pavement design purposes. In the SWCC, the soil moisture can be expressed as gravimetric water content, volumetric water content, or degree of saturation. The shape of SWCC is dependent on the soil type. Typical SWCCs for sand, silt, and clay are shown in Figure 18. The amount of fines and the plasticity index of the soil highly influence the SWCC (Zapata, 1999).

The most direct way of obtaining the SWCC for a given soil is to measure the suction of a representative sample in the laboratory using filter paper, pressure plate, or other available method. Several suction-moisture content data pairs are determined to obtain a complete curve. This process may take several days to a couple of weeks, depending on the type of soil being tested. The drying curve may differ from the wetting curve, introducing a hysteresis to the characteristics. If the hysteresis is not significant, it may be ignored, with a single curve used for both drying and wetting cases.

Solute suction does not seem to be sensitive to the changes in the soil water content. As a result, change in the total suction is usually represented by the change in matric suction. Therefore, matric suction measurements are important and typically presented in SWCCs (Fredlund and Rahardjo, 1993).

Since the determination of SWCCs involves special testing devices and difficult procedures, it is not very widely performed in common engineering practice compared with other well-known tests. For example, the direct shear test is commonly used to obtain the soil strength parameters, cohesion, and angle of friction for pavement design purposes. Also, consolidation tests are used to determine the settlement and expansive characteristics of soils. Yet, determination of soil suction is a very important task in the field of unsaturated soil mechanics. Therefore, many researchers have suggested methods of obtaining the SWCC using grain size distribution (GSD) and other soil properties without direct measurements of the SWCC. These methods can be grouped into three categories (Zapata, 1999):

1. Statistical estimation of water contents at selected matric suction values. This process generally requires a regression analysis and a curve fitting procedure.
2. Correlation of soil properties with the fitting parameters of an analytical equation that represents the SWCC.
3. Estimation of SWCC using a physics-based conceptual model.

Comparison of different models can be found in van Genuchten and Leij (1992); Williams and Ahuja (1992); Kern (1995); Nandagiri and Prasad (1997); and Zapata (1999). In this study, the second approach was adopted. Researchers that have adopted the second approach include Ghosh (1980); Williams et al. (1983); Ahuja et al. (1985); Rawls et al. (1992); Cresswell and Paydar (1996); Tomasella and Hodnett (1998); and Zapata (1999).

Zapata (1999) developed a family of SWCCs by correlating simple soil properties: D_{60} and *wPI*. D_{60} refers to the diameter in mm corresponding to 60% passing by weight; *wPI* is the weighted Plasticity Index, *PI* ($wPI = P_{200} \times PI$), and P_{200} is the percent passing the #200 sieve.

The fitting parameters of a sigmoidal curve described by the Fredlund and Xing equation were correlated to D_{60} and *wPI*. The Fredlund and Xing (1994) equation is shown below:

$$\theta = C(h) \times \left[\frac{\theta_s}{\left[\ln\left[\exp(1) + \left(\frac{h_s}{a} \right)^b \right] \right]^c} \right] \tag{33}$$

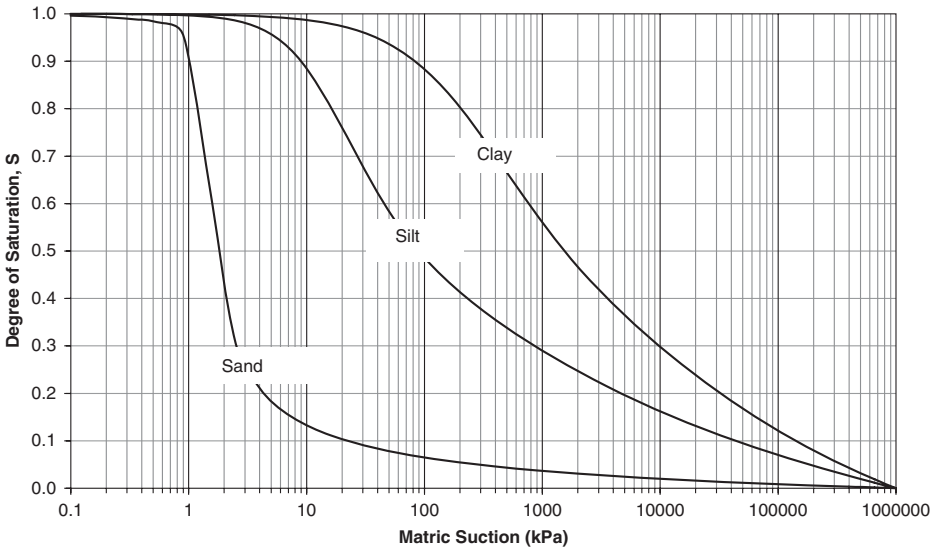

Figure 18. Typical SWCCs.

$$C(h)=\left[1-\frac{\ln\left(1+\frac{h_s}{h_r}\right)}{\ln\left(1+\frac{10^6}{h_r}\right)}\right] \tag{34}$$

where

a = a soil parameter which is primarily a function of the air entry value of the soil in kPa.
b = a soil parameter which is primarily a function of the rate of water extraction from the soil, once the air entry value has been exceeded.
c = a soil parameter which is primarily a function of the residual water content.
h_r = a soil parameter which is primarily a function of the suction at which the residual water content is reached in kPa.

The SWCC curves determined for this study (more than 90 SWCCs) were also evaluated by correlating various parameters to the fitting parameters used in Equation 33. The correlation parameters included the soil properties: D_{10}, D_{20}, D_{30}, D_{60}, D_{90}, C_c, C_u, *LL*, *PL*, *PI*, P_{200}, *wPI*, and the unit surface area of soil. In addition to these parameters, four parameters identified as a_g, b_g, c_g, and h_{rg} were included in the analysis. These four fitting parameters were computed by fitting the GSD of each soil to a sigmoidal curve available in the SoilVision® software package, which handles unsaturated soil properties. Based on the results, a new method to obtain SWCCs was developed and is presented in the next sections.

5.1.2 Existing SWCC Models

The existing family of SWCCs referred to in this study as the SWCC model was the family of SWCCs developed by Zapata (1999). Zapata investigated the uncertainty in SWCC and its effects on unsaturated shear strength predictions. A database containing 180 experimentally obtained SWCCs was analyzed in developing the family of curves. In the analysis, nonplastic and plastic soils were treated separately and two sets of SWCCs were developed.

The SWCC Model implemented in the EICM Version 2.6 is given by the Fredlund and Xing equation:

$$\theta_w = C(h)\times\left[\frac{\theta_{sat}}{\left[\ln\left[EXP(1)+\left(\frac{h}{a_f}\right)^{bf}\right]\right]^{cf}}\right] \tag{35}$$

with

$$C(h)=\left[1-\frac{\ln\left(1+\frac{h}{h_\varepsilon}\right)}{\ln\left(1+\frac{1.45\times10^5}{h_\varepsilon}\right)}\right] \tag{36}$$

where

h = Matric suction, in psi
θ_w = Volumetric moisture content, in %
a_f, b_f, c_f, and h_ε = SWCC fitting parameters

The SWCC parameters were correlated with soil index properties as explained below.

5.1.2.1 For Granular Nonplastic Materials (wPI = 0)

Soils with plasticity equal to zero fall into this group. In Zapata's analysis, parameters derived from the GSD of each

soil were analyzed in search of a correlation with the SWCC. In order to obtain correlation parameters associated with the SWCC, each set of data points was fitted with the Fredlund and Xing equation using SoilVision® to generate four fitting parameters: a_f, b_f, c_f, and h_ε. The four parameters were correlated with the parameters derived from the respective GSD. In the case of nonplastic soils, D_{60} correlated best with a_f, b_f, c_f, and h_ε. The correlations are represented by the following equations:

$$a_f = \frac{0.8627(D_{60})^{-0.751}}{6.895}, \text{ psi} \quad (37)$$

$$\bar{b}_f = 7.5 \quad (38)$$

$$c_f = 0.1772\ln(D_{60}) + 0.7734 \quad (39)$$

$$\frac{h_\varepsilon}{a_f} = \frac{1}{D_{60} + 9.7e^{-4}} \quad (40)$$

These correlations generate a family of curves based on D_{60} values ranging from 0.1 mm to 1.0 mm as shown in Figure 19.

5.1.2.2 For Plastic Unbound Materials (wPI > 0)

Soils that exhibit plasticity fall into this group. In the case of plastic soils, parameters, a_f, b_f, c_f, and h_ε correlated with the *wPI* value ($P_{200}PI$) as follows:

$$a_f = \frac{0.00364(wPI)^{3.35} + 4(wPI) + 11}{6.895}, \text{ psi} \quad (41)$$

$$\frac{b_f}{c_f} = -2.313(wPI)^{0.14} + 5 \quad (42)$$

$$c_f = 0.0514(wPI)^{0.465} + 0.5 \quad (43)$$

$$\frac{h_\varepsilon}{a_f} = 32.44e^{0.0186(wPI)} \quad (44)$$

Therefore, another family of curves was generated based on the *wPI* values ranging from 0.1 to 50 as shown in Figure 20.

Both families of curves were combined and presented as one family of curves as shown in Figure 21 (Zapata et al., 2000). Based on recommendations by other experts, all SWCCs were forced through a suction of 10^6 kPa for 0% saturation.

5.1.3 Method Adopted in Developing a New Set of SWCCs

The SWCCs available from other sources used in Zapata's analysis originated from tests where volume change was not taken into consideration. In the past, SWCCs were determined by testing slurry samples with no tracking of volume change. Therefore, no corrections were applied with respect to the volume change in computing the degree of saturation. This procedure leads to errors, especially near the tail end (high suction) of SWCCs for plastic soils. In the case of determining drying SWCCs, the density of the soil sample tends to increase as the test progresses. The density change could be significant when highly plastic, compressible soils are involved. Because the degree of saturation increases with the density of the material, the tail end of a SWCC might be actually located higher than the position of the uncorrected curve.

The pressure plate device developed and used in this project provided the necessary data to apply volume change corrections. The density of the sample was calculated for each point and used in the computation of degree of saturation, producing a set of SWCCs that captured the volume-change correction.

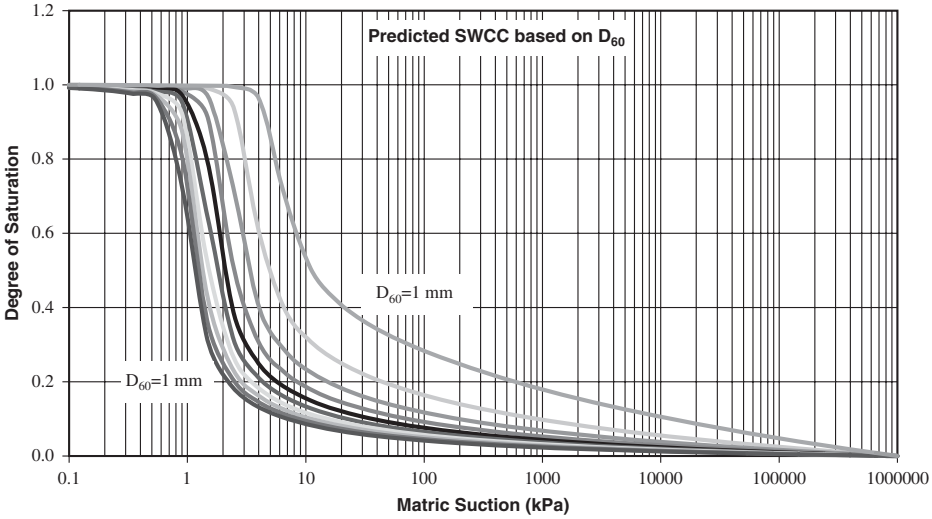

Figure 19. Family of existing SWCCs for nonplastic soils.

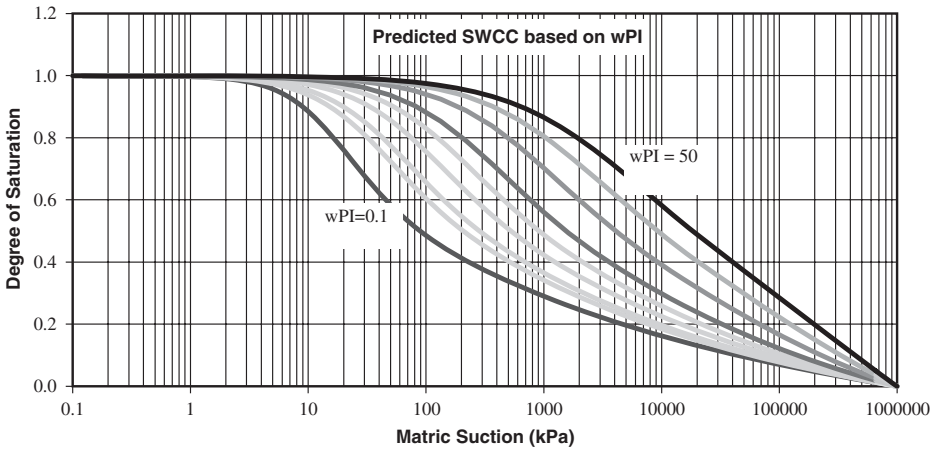

Figure 20. Family of existing SWCCs for plastic soils.

The availability of 180 SWCCs from the previous study proved useful because they were combined into the analysis, statistically enhancing the database. Approximate volume-change corrections were applied to each of the curves associated with plastic soils before pooling the data together as described later.

The method for obtaining the correlations developed in this study was similar to the method used by Zapata (1999); however, more parameters or parameter combinations were considered.

5.1.4 Correlation Parameters and Curve Fitting Procedure

The procedure followed to find a new set of SWCCs was as follows:

1. The GSD curves for all soils with SWCCs were developed.
2. Values of D_{10} through D_{90} were obtained from the GSD.
3. *Cc*, *Cu*, P_{200}, *LL*, *PL*, *PI*, *wPI*, and the estimated surface area were found for each soil.
4. Possible combinations of the above parameters were obtained. For example, relations such as D_{90}/D_{10}, $P_{200} \times D_{90}/D_{10}$, $(D_{90}D_{60}D_{10})/3$, and D_0 were estimated by projecting the two extremes of the GSD curve on to the Percent Passing = 0 and 100% lines, respectively, as illustrated in Figure 22.
5. SoilVision® software was used to fit Fredlund and Xing equations to the experimental data points of each SWCC, and the fitting parameters a_f, b_f, c_f, and h_ε for nonplastic soils and a_{fh}, b_{fh}, c_{fh}, and h_{rfh} fitting parameters for plastic soils were found.
6. By means of statistical non-linear regression analyses, the best correlations between a_f, b_f, c_f, h_ε, a_{fh}, b_{fh}, c_{fh}, h_{rfh} and the soil index parameters were found.
   a. The fitting parameters were expressed in terms of best correlating soil index parameters, and the values of a_f, b_f, c_f, h_ε, a_{fh}, b_{fh}, c_{fh}, and h_{rfh} for each soil using the respective function were found.
   b. The parameter-based curves, along with the experimental data points for each soil, were compared.
   c. New correlations were acceptable if there was good agreement between the experimental data points and the parameter-based curve.

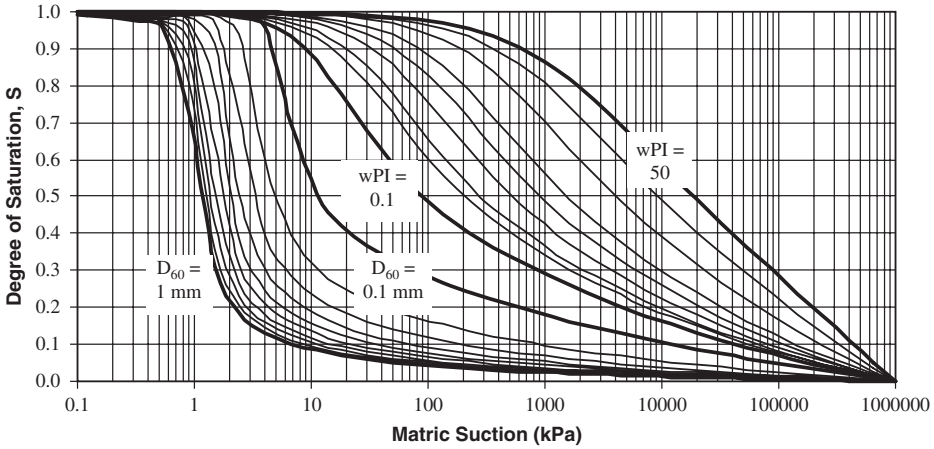

Figure 21. Family of existing SWCCs.

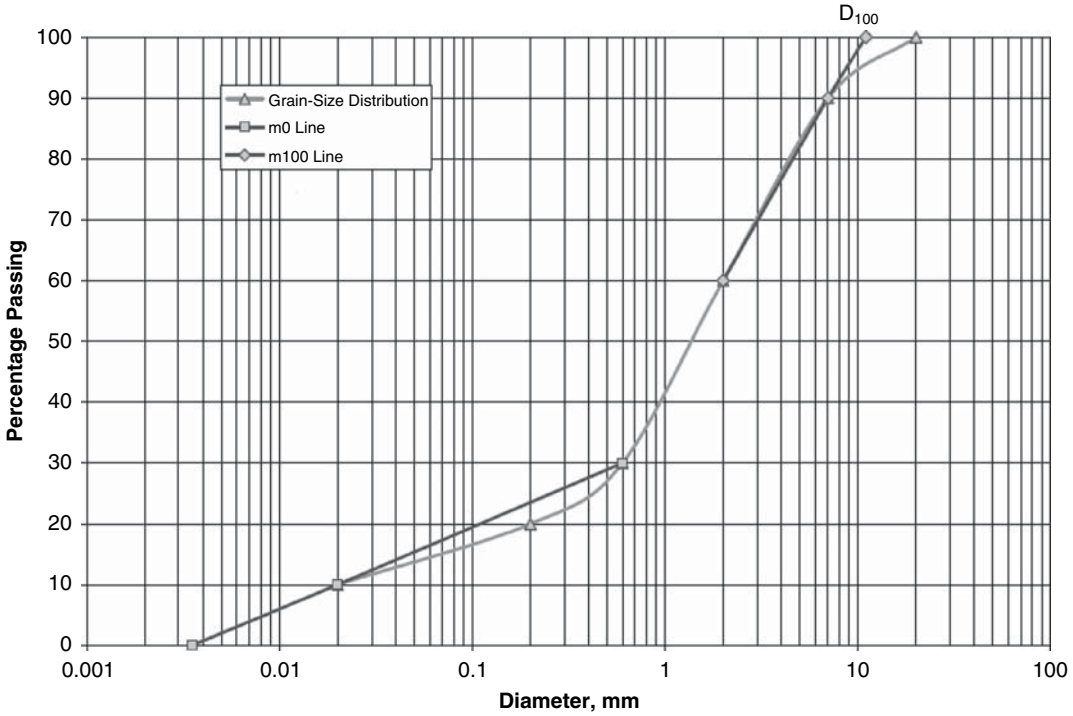

Figure 22. Projection of GSD to obtain D0 and D100.

5.1.5 Application of Volume-Change Correction

The required correction factors were derived from the SWCC testing results for the samples gathered at the project field sites as follows:

1. Fifty-two new SWCCs, measured on soils that exhibited plasticity, were considered.
2. Using the sample height measurement at each data point, the vertical strain of the sample, ε, corresponding to the matric suction was computed as follows:

$$\varepsilon = \Delta H/Ho \quad (45)$$

where
ΔH = Change in sample height
Ho = Initial sample height

3. The strain versus matric suction relationships corresponding to the 52 samples were plotted and analyzed to find any trends.
4. Based on the plots, a set of correction curves was developed using *wPI* as the variable soil property. The curves are shown in Figure 23.
5. Three widely spaced data points representing each SWCC to be corrected were selected from the uncorrected curve and the corresponding ε values were determined using Figure 23 based on suction and *wPI*.
6. The strain values were converted to change in void ratio using the following:

$$\varepsilon = \frac{\Delta e}{1 + e_o} \quad (46)$$

where
Δe = Change in void ratio
e_o = Initial void ratio

7. The change in void ratio, Δe, was subtracted from e_o to obtain the corrected void ratio e_1.
8. Using the volumetric water content θ_w, and γ_d of the original data, gravimetric water content, w, was back-calculated using the following equation:

$$w = \frac{\theta_w \gamma_w}{\gamma_d} \quad (47)$$

9. The corrected volumetric water content, $\theta_{w\text{-}corr}$ was calculated for each point:

$$\theta_{w\text{-}corr} = \frac{G_s w}{1 + e} \quad (48)$$

10. A modified Fredlund and Xing curve was fitted to the corrected data points to obtain the four fitting parameters: a_{fh}, b_{fh}, c_{fh}, and h_{rfh}.

5.1.6 Databases Used in SWCC Model Calibration

For the analysis, the soils with a weighted PI of less than 1.0 were categorized as nonplastic (NP) soils. The weighted PI

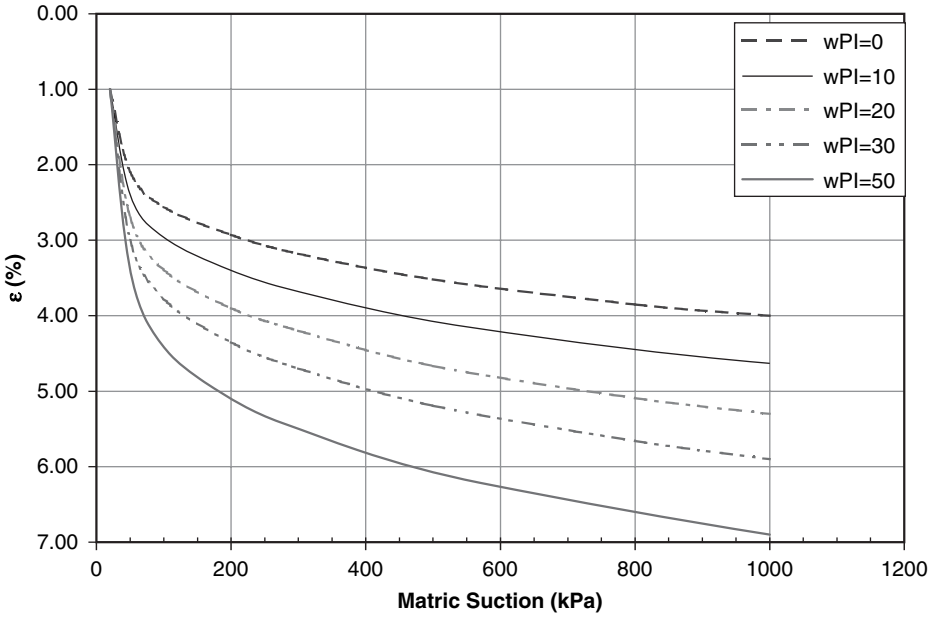

Figure 23. Volume change correction curves.

(*wPI*), is expressed as the product of P_{200} (expressed as a decimal) and the *PI* of the soil. Soils that exhibited *wPI* greater than or equal to 1.0 were categorized as plastic (*PI*) soils.

A database containing 180 experimentally obtained SWCCs collected from the published literature was used in Zapata's analyses in developing the family of SWCC curves that was implemented in the EICM Version 2.6 model in MEPDG software Version 0.7. Of these SWCCs, the best 134 curves were pooled with the 83 curves determined in this project. The number of soils used in the analysis from each database is summarized in Table 16.

Following a regression analysis, two sets of correlations were derived for nonplastic soils and plastic soils, respectively. The following sections present the set of correlation equations derived for each soil type.

5.1.7 Correlation Equations for Nonplastic Soils

$$a_f = 1.14a - 0.5 \tag{49}$$

where

$$a = -2.79 - 14.1\log(D_{20}) - 1.9\times10^{-6}P_{200}^{4.34} + 7\log(D_{30}) + 0.055D_{100} \tag{50}$$

$$D_{100} = 10^{\left[\frac{40}{m_1}+\log(D_{60})\right]} \tag{51}$$

$$m_1 = \frac{30}{[\log(D_{90}) - \log(D_{60})]} \tag{52}$$

Note: Extreme cases may exist where the computed value of a_f is negative, which will lead to erroneous results. Therefore, the value of a_f was limited to 1.0.

$$b_f = 0.936b - 3.8 \tag{53}$$

where

$$b = \left\{5.39 - 0.29\ln\left[P_{200}\left(\frac{D_{90}}{D_{10}}\right)\right] + 3D_0^{0.57} + 0.021P_{200}^{1.19}\right\}m_1^{0.1} \tag{54}$$

$$D_0 = 10^{\left[\frac{-30}{m_2}+\log(D_{30})\right]} \tag{55}$$

$$m_2 = \frac{20}{[\log(D_{30}) - \log(D_{10})]} \tag{56}$$

$$c_f = 0.26e^{0.758c} + 1.4D_{10} \tag{57}$$

where

$$c = \log\left(m_2^{1.15}\right) - \left(1 - \frac{1}{b_f}\right) \tag{58}$$

$$h_{rf} = 100 \tag{59}$$

Table 16. Information on databases.

Database	Soil Type	No. of SWCCs	Volume Change Correction	Fitting Parameters
NCHRP 9-23	Non-Plastic	36	--	a_f, b_f, c_f, h_{rf}
	Plastic	47	--	a_{fh}, b_{fh}, c_{fh}, h_{rfh}
Zapata's	Non-Plastic	118	--	a_f, b_f, c_f, h_{rf}
	Plastic	16	Yes	a_{fh}, b_{fh}, c_{fh}, h_{rfh}

5.1.8 Correlation Equations for Plastic Soils

$$a_f = 32.835\{\ln(wPI)\} + 32.438 \quad (60)$$

$$b_f = 1.421(wPI)^{-0.3185} \quad (61)$$

$$c_f = -0.2154\{\ln(wPI)\} + 0.7145 \quad (62)$$

$$h_{rf} = 500 \quad (63)$$

where

wPI = weighed Plasticity index equal to the product of P_{200} (expressed as a decimal) and the PI.

5.1.9 Error Analysis

A statistical analysis determined the error associated with the newly proposed functions. In the analysis, the field measured S was compared with the predicted S. The percent mean algebraic error (e_{alg}), the percent mean absolute error (e_{abs}), the sum of the squared error based on measured S (S_e), and the mean squared error based on average measured S (S_y) were computed as follows:

$$e_{\text{alg}} = \frac{\sum\left[\frac{(S_m - S_p)100}{S_m}\right]}{n} \quad (64)$$

$$e_{\text{abs}} = \frac{\sum\left|\frac{(S_m - S_p)100}{S_m}\right|}{n} \quad (65)$$

$$S_{\text{e}} = \sqrt{\frac{\sum(S_m - S_p)^2}{n-p}} \quad (66)$$

$$S_{\text{y}} = \sqrt{\frac{\sum(\bar{S}_m - S_p)^2}{n-p}} \quad (67)$$

where

S_m = measured degree of saturation,
S_p = predicted degree of saturation,
$\bar{S}_m$ = average measured degree of saturation,
n = number of data points,
p = number of parameters associated with the proposed functions.

The corresponding values of S_e/S_y and the adjusted coefficient of correlation (R^2), $1-(S_e/S_y)^2$, are presented in Table 17. For comparison, the same error analysis was performed for the model developed by Zapata (1999); the results are also presented in Table 17.

As Table 17 shows, the percent mean algebraic and absolute errors associated with the proposed model for nonplastic soils were found to be 8.6% and 14.8%, respectively, while the same associated errors were both found to be 88.5% for the Zapata model (1999). Similarly, the percent mean algebraic and absolute errors associated with the proposed model for plastic soils were 0.1% and 9.2%, respectively, while the same errors associated with the Zapata model were 20.4% and 23.9%, respectively. Therefore, the new models provide a far better prediction than those developed by Zapata in 1999. Adjusted R^2 values also reflect the improved predictive capability of the new model. Plots of measured S versus predicted S for nonplastic and plastic soils are shown in Figure 24 and Figure 25, respectively.

5.2 G_s Model Calibration

5.2.1 Gs Model Currently Implemented into the EICM

The Gs Model implemented in the EICM for Level 3 analysis in the MEPDG software Version 0.7 follows the relationship:

$$G_s = 0.041(wPI)^{0.29} + 2.65 \quad (68)$$

where

$$wPI = PI \times P_{200}/100 \quad (69)$$

G_s = Specific gravity of solids
P_{200} = Passing sieve #200 [decimal]
PI = Plasticity index [%]

This correlation was developed using 268 soil data points extracted from literature, where plastic and nonplastic soils were analyzed separately. In order to find a correlation for granular soils with no plasticity (NP), G_s was plotted against D_{60}. The plot is presented in Figure 26, where D_{60} is the GSD from the grain size distribution curve at 60% passing. It was evident from the plot that G_s does not depend on D_{60}. This conclusion was confirmed by statistical analysis, which produced an R^2 of 0.14%. It was also found that the measured

Table 17. Errors associated with SWCC predictions.

Parameter	Non-Plastic Soils		Plastic Soils	
	Proposed Model	Zapata	Proposed Model	Zapata
e_{alg}	8.6%	88.5%	0.1%	20.4%
e_{abs}	14.8%	88.5%	9.2%	23.9%
S_e/S_y	0.65	1.01	0.70	0.91
Adjusted R^2	0.58	-0.02	0.51	0.18

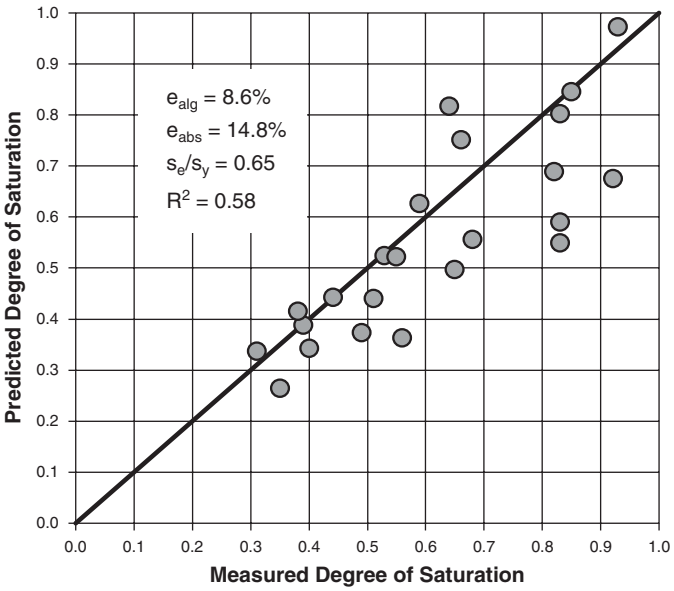

Figure 24. Measured versus predicted S *for nonplastic soils.*

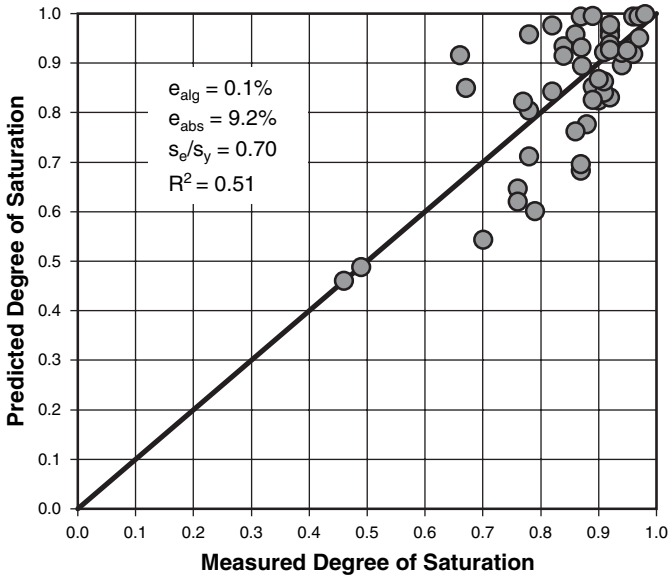

Figure 25. Measured versus predicted S *for plastic soils.*

values of G_s have an average value of 2.65. Therefore, due to the lack of better correlation, G_s was approximated to be 2.65 for the NP soils.

A similar analysis was pursued for the plastic soils. The analysis showed a non-linear relationship between G_s, plasticity index (*PI*), and percent of soil passing sieve # 200 (P_{200}) that is expressed by Equations 68 and 69 above. The relationship between G_s and *wPI* is plotted in Figure 27. Statistical analysis yielded an R^2 of 0.22%, which means that the predicted G_s values correlated very poorly with the measured G_s. Therefore, it was decided that further analysis should be performed to find a better correlation between G_s and other soil parameters for both plastic and nonplastic soils to be used in the Level 3 analysis of the EICM, for implementation in later versions of the MEPDG software.

To calibrate the currently implemented *Gs* Model, a new set of empirical data was gathered from the project field sites. This extended dataset was used to calculate G_s values that were plotted against measured G_s. The results, shown in Figure 28, further confirmed that the *Gs* Model implemented in the EICM in MEDPG Version 0.7 required refining.

5.2.2 New *Gs* Model for Nonplastic Soils

The extended data set, consisting of 136 points, was used in the currently implemented *Gs* Model for nonplastic soils. To determine the predictive capability of the model, G_s calculated was plotted against G_s measured in Figure 29; this plot indicated that the correlation between G_s and D_{60} was not significant. Even though the majority of the soils have a measured G_s value

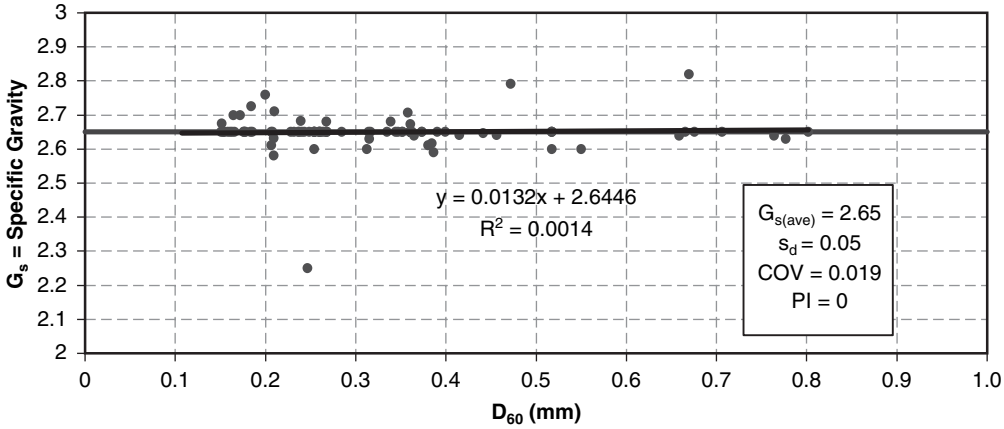

Figure 26. Currently implemented Gs Model *for nonplastic soils using the literature dataset.*

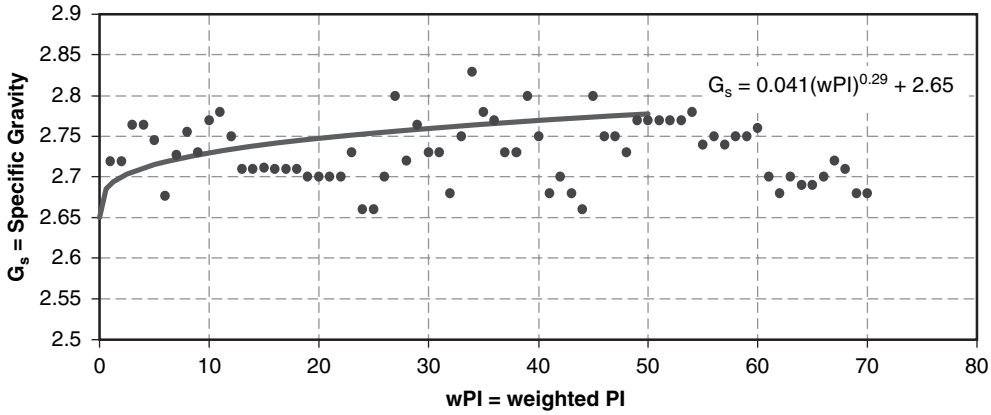

Figure 27. Currently implemented* Gs Model *for plastic soils using the literature dataset.

of 2.65, the remaining values range from 2.57 to 2.88. As a result, the data set plots as a straight line instead of a point [2.65, 2.65]. This finding was confirmed by statistical analysis that yielded an R^2 value of 0.14%.

The acquisition and addition of field or other empirical data into the existing dataset allowed for further study of the relationship between G_s and other soil parameters for the nonplastic soils. It was found that G_s depends linearly on gradation when the gradation variable, g (defined below) varies between 0.5 and 6.0. For values of g larger than 6.0, the specific gravity approaches 2.65. The following equations define the relationship between G_s and gradation presented in Figure 30.

$$G_s = -0.0526 \times g + 2.9243, \qquad 0.5 < g \leq 6.0 \qquad (70)$$

$$G_s = 2.65 \qquad g > 6.0 \qquad (71)$$

$$g = 2.9 - 0.1(P_4/P_{200})^2 + 0.57(P_{40}/P_{200})^2 \qquad (72)$$

where

P_{200} = Percent of soil passing sieve # 200
P_{40} = Percent of soil passing sieve # 40
P_4 = Percent of soil passing sieve # 4

Error analysis of equations 70 through 72 revealed a significant correlation between G_s and gradation with R^2 equal to 74%. The statistical parameters corresponding to the new model are presented in Figure 30. The final number of data points included in the analysis was 103, after removal of outliers.

5.2.3 New *Gs* Model for Plastic Soils

A refined linear correlation was developed for plastic soils assuming G_s is a function of optimal water content (w_{opt}), maximum dry unit weight (γ_{d_max}), and PI based on the following equation:

$$G_s = 2.4528 + 0.006075\, w_{opt} + 0.001486\, \gamma_{d\_max} + 0.001871\, PI \qquad (73)$$

5.2.4 Sensitivity Analysis of Gs Model for Nonplastic Soils

The equations developed for nonplastic soils were subjected to a sensitivity analysis. In the first part of the analysis, two gradation parameters were held constant while the third

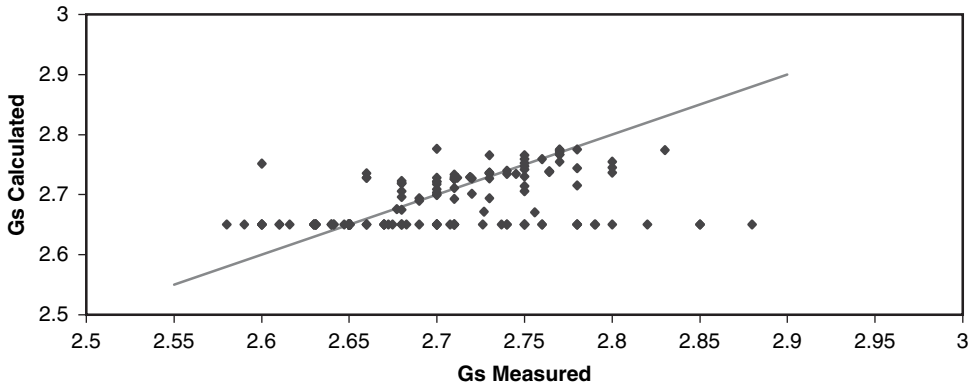

Figure 28. Error analysis of currently implemented* Gs Model *for both NP and plastic soils using the extended dataset.

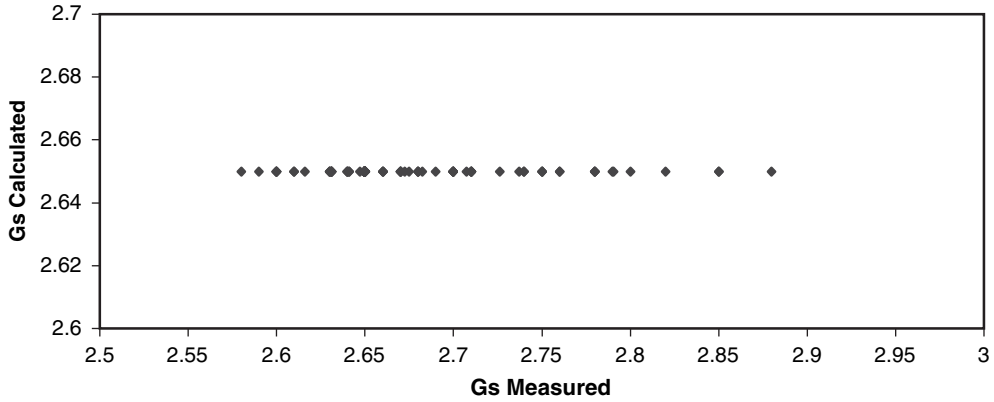

Figure 29. Currently implemented* Gs Model *for nonplastic soils using complete dataset.

parameter was allowed to vary. The gradation variable, *g*, was then used to calculate the specific gravity, which was plotted against the varying gradation parameter. The results were plotted in Figures 31, 32, and 33.

Figure 31 shows that P_4 is a significant parameter when P_{40} and P_{200} are small. However, P_4 makes only a minor contribution to the result when the remaining gradation parameters are very large. It was found that G_s increases as P_4 increases.

Figure 32 shows that G_s increases as P_{40} decreases. P_{40} is a significant parameter when P_4 and P_{200} are small. P_{40} has a minor contribution to variation in G_s when the remaining two parameters are very large.

The variation of G_s with respect to P_{200} was considered last. Figure 33 shows that G_s increases when P_{200} increases. Furthermore, it was found that P_{200} is a very significant parameter for all considered ranges of P_4 and P_{40}.

Based on the results obtained in the parametric study, it was concluded that the new proposed model is technically valid and statistically sound.

5.2.5 Sensitivity Analysis of G_s Model for Plastic Soils

The equation for plastic soils was subjected to a similar sensitivity analysis. In this case, the equation is linear and influenced by three parameters: *PI*, γ_{d_max} and w_{opt}. Therefore, an analysis was performed by holding two of the parameters constant and varying the third. The results are shown in Figures 34 through 39. In addition, a combined effect was studied by holding γ_{d_max} constant and varying the other two parameters. Those results are shown in Figure 40.

5.2.6 Summary

Based on the information presented above, the following conclusions can be drawn:

1. Improvements to the currently implemented G_s *model* resulted in increased R^2 values for both nonplastic and plastic soils.

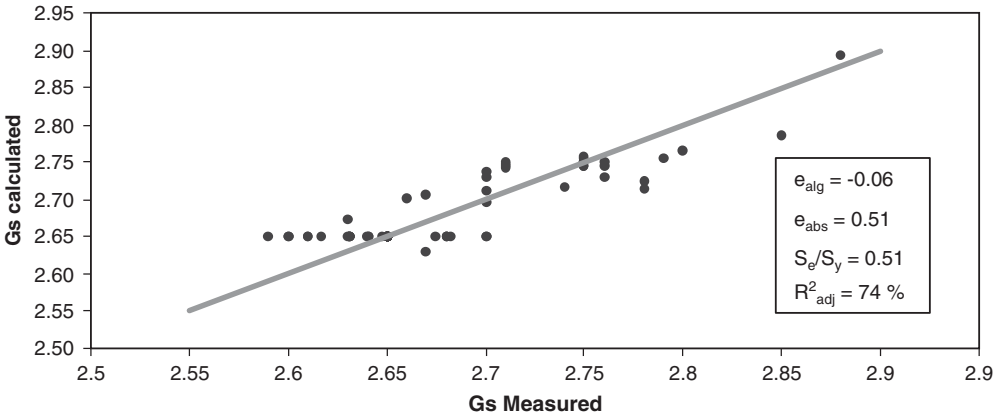

Figure 30. Error analysis of final* Gs Model *for nonplastic soils using complete dataset.

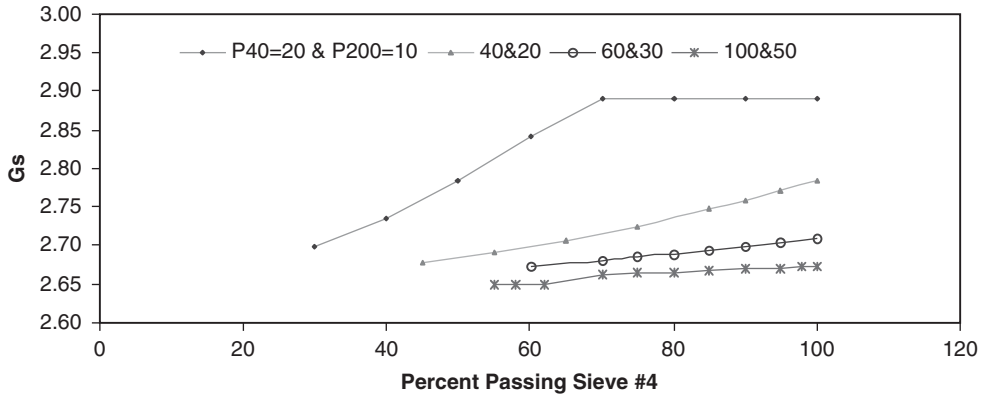

Figure 31. Sensitivity analysis of P_4 for the nonplastic soils.

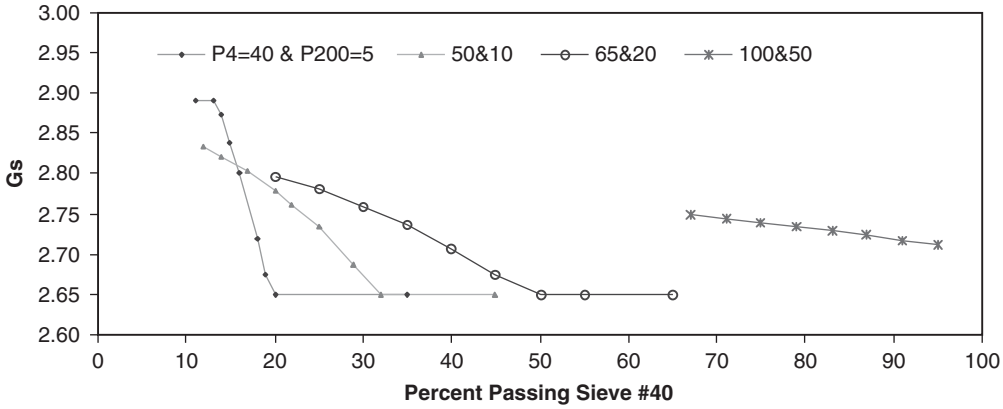

Figure 32. Sensitivity analysis of P_{40} for the nonplastic soils.

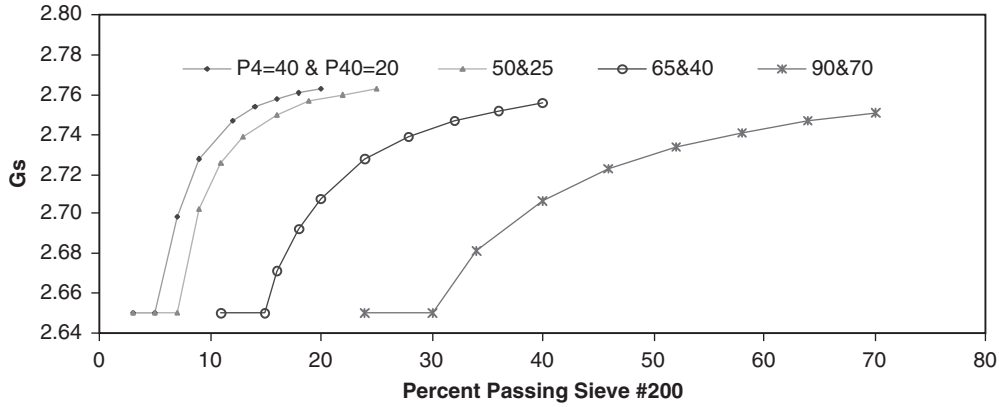

Figure 33. Sensitivity analysis of P_{200} for the nonplastic soils.

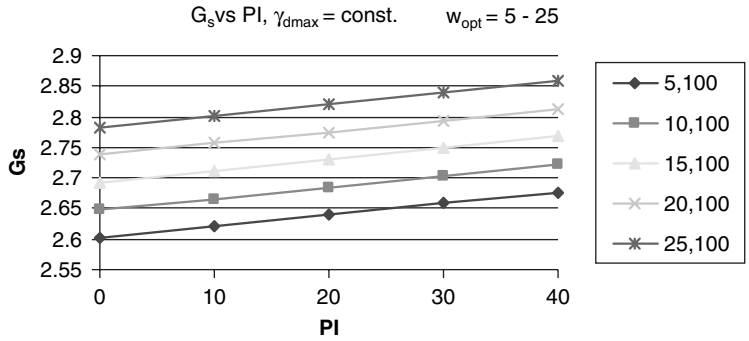

Figure 34. Sensitivity of **Gs Model** *when* **PI** *is varying and γ_{d_max} and w_{opt} are held constant.*

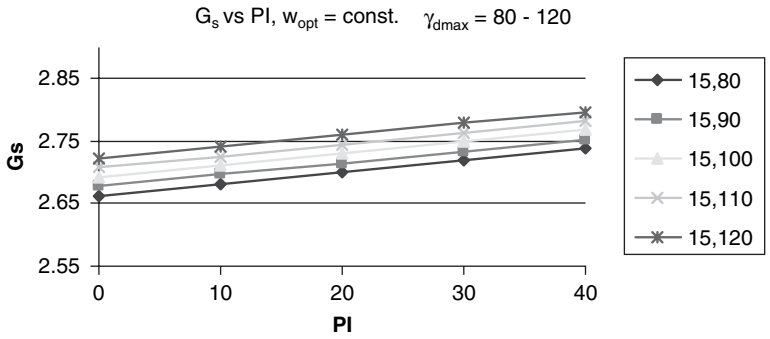

Figure 35. Sensitivity of* Gs Model *when* PI *is varying and* w_{opt} *and* γ_{d_max} *are held constant.

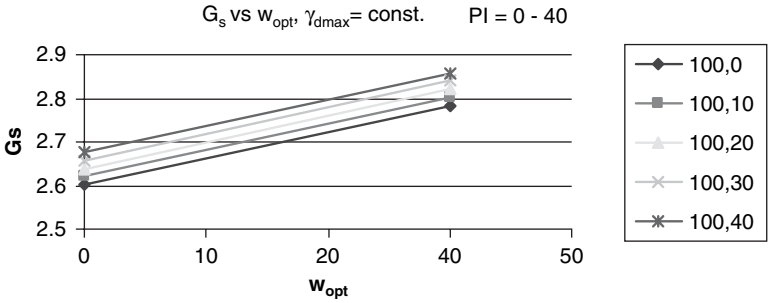

Figure 36. Sensitivity of* Gs Model *when* w_{opt} *is varying and* γ_{d_max} *and* PI *are held constant.

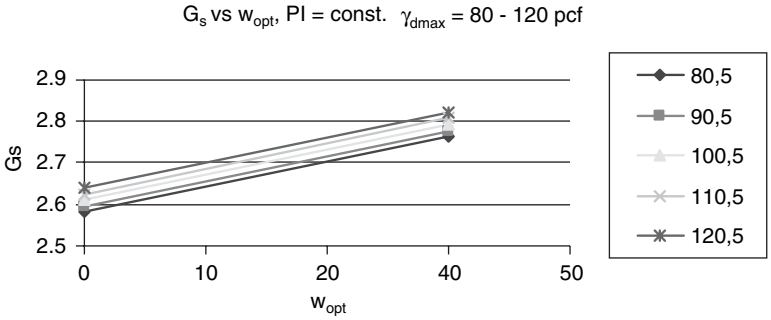

Figure 37. Sensitivity of* Gs Model *when* w_{opt} *is varying and* γ_{d_max} *and* PI *are held constant.

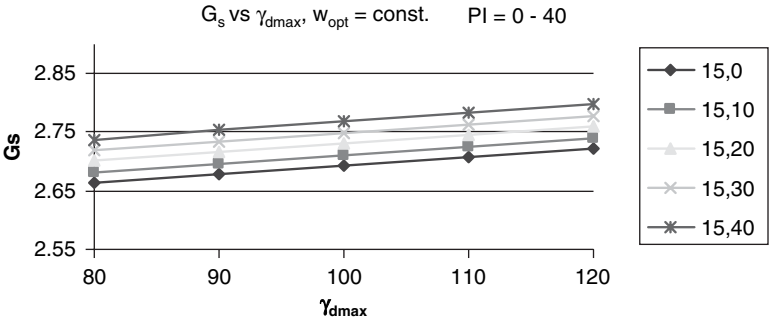

Figure 38. Sensitivity of* Gs Model *when* γ_{d_max} *is varying and* w_{opt} *and* PI *are held constant.

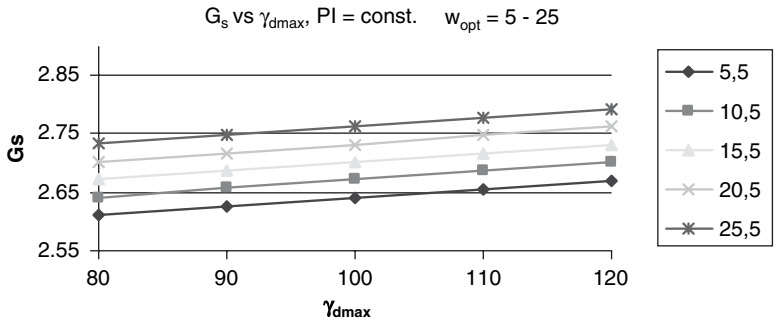

Figure 39. Sensitivity of* Gs Model *when* γ_{d_max} *is varying and* w_{opt} *and* PI *is held constant.

2. For nonplastic soils, the following correlation yielded an R^2 value of 80%:

$$G_s = -0.0526 \times g + 2.9243, \qquad 0.5 < g \leq 6 \tag{74}$$

$$G_s = 2.65 \qquad g > 6 \tag{75}$$

$$g = 2.9 - 0.1\left(\frac{P_4}{P_{200}}\right) + 0.57\left(\frac{P_{40}}{P_{200}}\right)^2 \tag{76}$$

3. All three gradation parameters used in the G_s Model for nonplastic soils were found to be significant, where P_{200} is the most significant of the three for all ranges of P_4 and P_{40} considered. P_4 and P_{40} are significant only when the remaining two parameters are small.
4. For plastic soils, the following correlation was found:

$$G_s = 2.4528 + 0.006075\, w_{opt} + 0.001486\, \gamma_{d\_max} + 0.001871\, PI \tag{77}$$

The sensitivity analysis yielded the expected results as G_s increased when PI, w_{opt}, and γ_{d_max} increased, with PI the most significant parameter in the relationship and γ_{d_max} the least significant. The values found by the relationship vary from 2.65 and 2.85 for most common combinations of parameters.

5.3 K-Sat Model Calibration

5.3.1 K-Sat Model Currently Implemented In EICM Version 2.6

The *k-sat* Model implemented in EICM Version 2.6 is the following:

For nonplastic soils

$$k_{sat} = 118.11 \cdot 10^{\left(-1.1275(\log D_{60}+2)^2 + 7.2816(\log D_{60}+2) - 11.2891\right)} \tag{78}$$

For plastic soils

$$k_{sat} = 118.11 \cdot 10^{\left(0.0004(P_{200}PI)^2 - 0.0929(P_{200}PI) - 6.56\right)} \quad \text{for P200} > 50 \text{ and PI} > 4 \tag{79}$$

where

k_{sat} = Saturated hydraulic conductivity (ft/hr)
D_{60} = Grain size diameter at 60% passing (mm)
P_{200} = Passing sieve #200 (decimal)
PI = Plasticity index (%)

These correlations were developed with a limited database extracted from the literature, where plastic and nonplastic soils were analyzed separately. For nonplastic soils, k_{sat} was found to depend exclusively on D_{60}, where D_{60} is the grain size

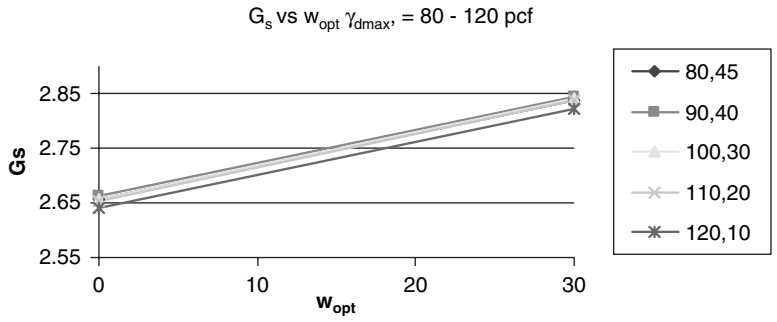

Figure 40. Sensitivity of* Gs Model *when* w_{opt} *and* γ_{d_max} *are varying and* PI *is held constant.

diameter from the GSD curve at 60% passing. It was also found that for plastic soils, k_{sat} yielded reasonable correlations with plasticity index (PI) and P_{200} as defined above.

5.3.2 Validation of the K-Sat Model Implemented in EICM Version 2.6

In order to validate the *k-sat* Model implemented in EICM Version 2.6, a new set of measured data was gathered from the 29 project field sites. The values of k_{sat} were measured on 27 nonplastic soils and 42 plastic soils. Equations 78 and 79 were applied to the newly acquired data set. The calculated values of k_{sat} were plotted against k_{sat} obtained through laboratory testing. The results presented in Figures 41 and 42 suggested that the *k-sat* Model implemented in EICM Version 2.6 was in need of improvement.

5.3.3 Development of a New K-Sat Model

In the development of any new k_{sat} Model, where k_{sat} is correlated with index properties, it is typically necessary to compromise. As a general rule, the more index properties used, the better the correlation is. On the other hand, the more index properties required, the more cumbersome is the model's use and the less likely it is to be used. These tradesoff were kept in mind as new k_{sat} models were developed for the plastic and nonplastic soils.

5.3.3.1 K-sat Model for Plastic Soils

The weighted plasticity index is abbreviated *wPI* and defined by $wPI = P_{200} \times PI$, with P_{200} in decimal and PI in percentage. Within this report, the product $P_{200} \times PI$ is used in lieu of *wPI* with the understanding that P_{200} is always in decimal form when P_{200} and PI are presented as a product. Because of past experience with *wPI*, it was expected to be an important parameter. The percent of clay, $P_{0.002}$, was also expected to be an important parameter, but when it was added, the improvement in the model was marginal to negligible. Because of the added testing burden of acquiring $P_{0.002}$ from laboratory testing, its use was dropped.

The following equation represents the best model for plastic soils. The measured versus predicted hydraulic conductivity data are presented in Figure 43.

$$k_{sat} = 2 * 10^{(-0.1 * P_{200} PI - 6)} \qquad [\text{cm/s}] \qquad (80)$$

An R^2 value of −10 is obviously an extremely poor correlation, although it is an improvement on the old model, which had an R^2 of −15. These poor correlations are believed to be an inherent result of the fact that k_{sat} ranges over so many orders of magnitude that it may be unreasonable to expect a good ($R^2 < 1$) correlation. These results show that if a fairly good estimate of time rate of water movement through soil is to be obtained, k_{sat} must be measured directly. The correlations with index properties proposed in this report will provide only very crude estimates of k_{sat}.

5.3.3.2 K-sat Model for Nonplastic Soils

For nonplastic soils, it was assumed that a full gradation curve down to D_{10} would typically be available. Accordingly, the following parameters were judged important and practical to use: D_{10}, D_{60}, D_{60}/D_{10}, and P_{200}. After trying numerous models with very discouraging results; the following model produced a

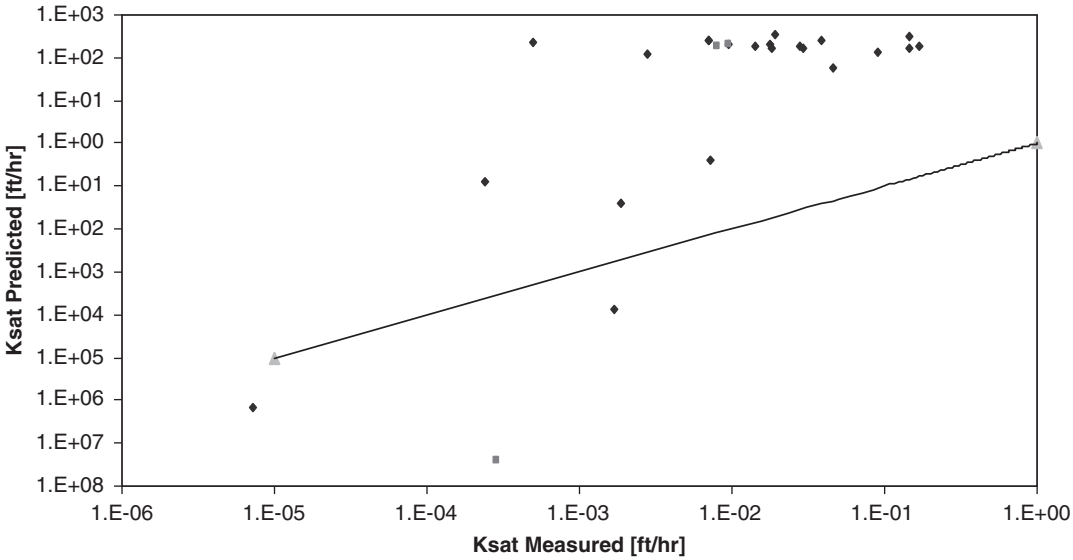

Figure 41. Performance of currently implemented* k-sat Model *for nonplastic soils using the new dataset.

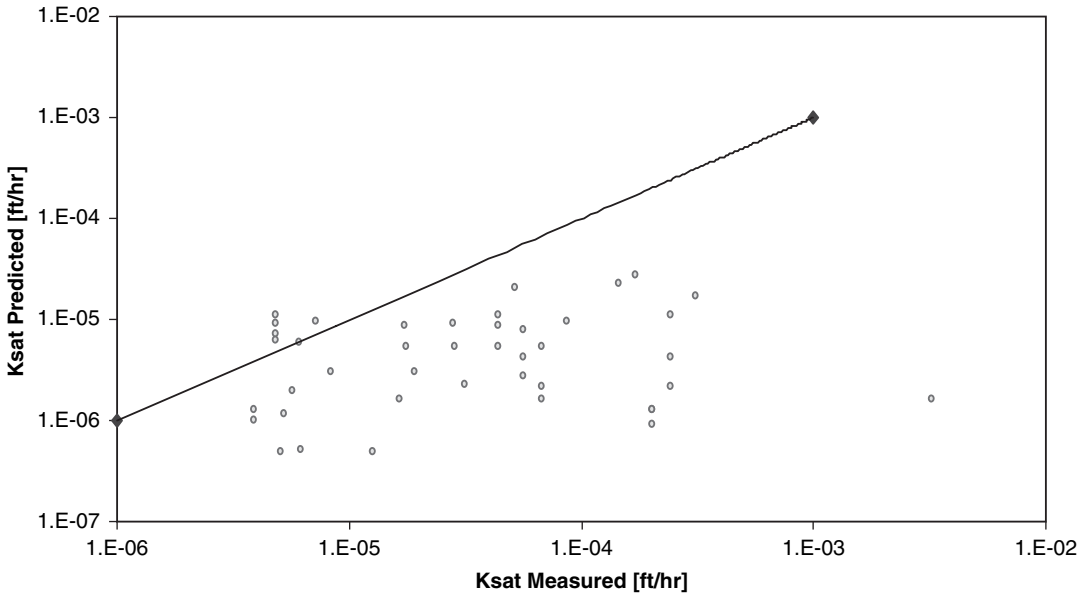

Figure 42. Performance of currently implemented* k-sat Model *for plastic soils using the new dataset.

dramatic increase in R^2_{adj} to 0.82. The measured versus predicted hydraulic conductivity results are shown in Figure 44.

$$k_{sat} = 10^{-6} 10^{\left(5.3D_{10}+0.049D_{60}+0.0092\frac{D_{60}}{D_{10}}-0.1P_{200}+1.5\right)} \quad (81)$$

When the datasets for both plastic and nonplastic soils were combined, there was an apparent improvement in the fitting statistics, as shown in Figure 45. The improvement was primarily due to the expansion of the database wherein the low k_{sat} values for plastic soils were combined with the high k_{sat} values of the non-plastic soils. The final R^2_{adj} was found to be 0.83.

These correlations were judged to be about the best that can be achieved with the currently available database. It should also be noted that time-rate of water flow is not often a critical issue in the MEPDG applications of the EICM. For example, after the moisture contents under pavements reach more or less an equilibrium value (at a distance of 2 m (6 ft) or more from the edge of paved shoulders), further variations

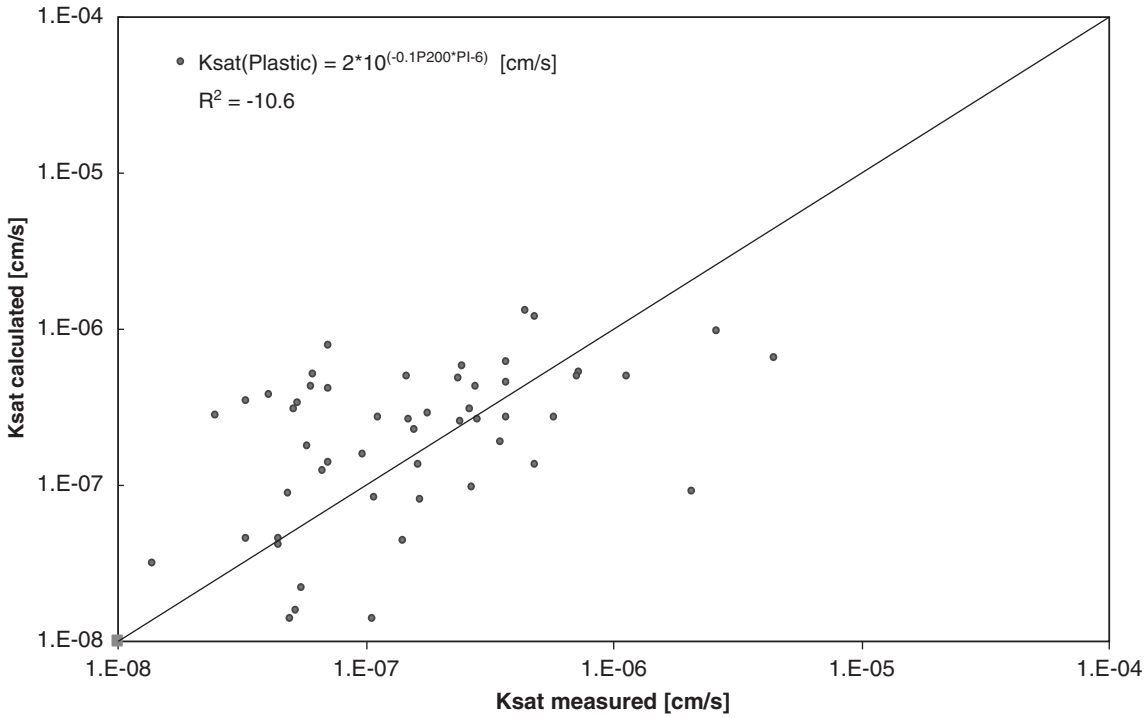

Figure 43. Performance of improved* k-sat Model *for plastic soils using the new dataset.

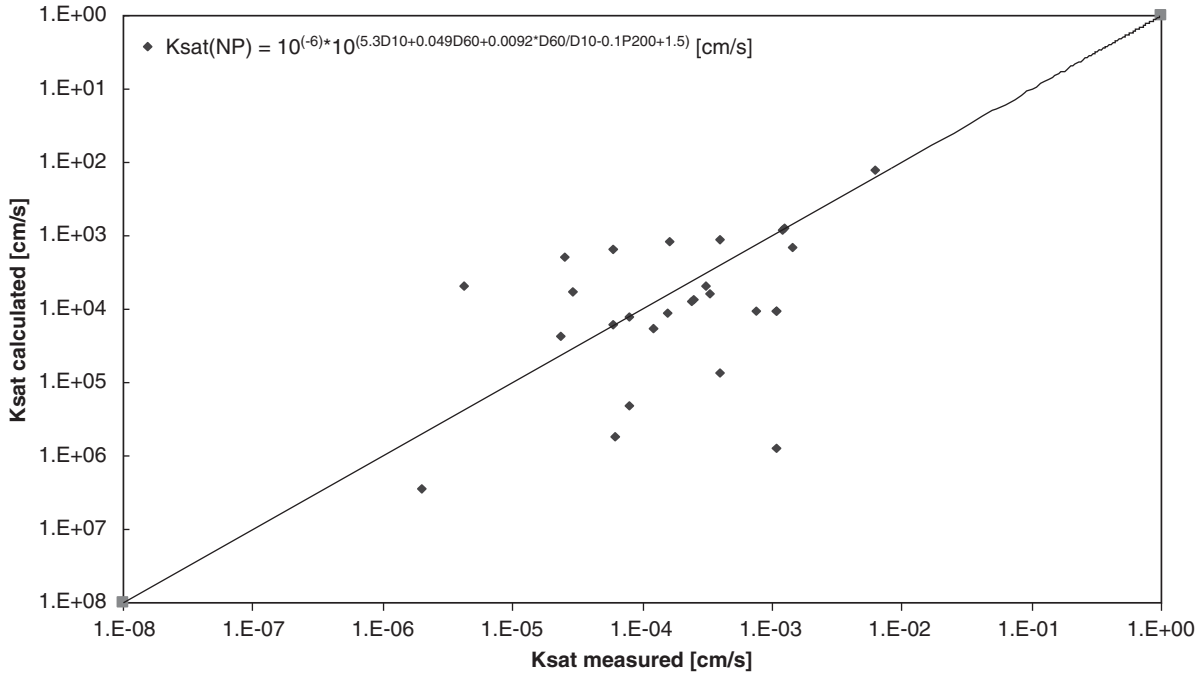

Figure 44. Performance of improved* k-sat Model *for non-plastic soils using the new dataset.

are fairly minor. Exceptions to this generalization usually arise in cases of freezing and frost action.

5.4 Compaction Model Calibration

The last model considered for calibration was the Compaction Model. This model allows estimation of the optimum water content and the maximum dry unit weight for coarse and fine-grained materials in cases where the user does not provide that input data.

Based on an exhaustive statistical analysis of the models in EICM Version 2.6, it was decided that the Compaction Model was satisfactory for prediction with only minor improvements needed.

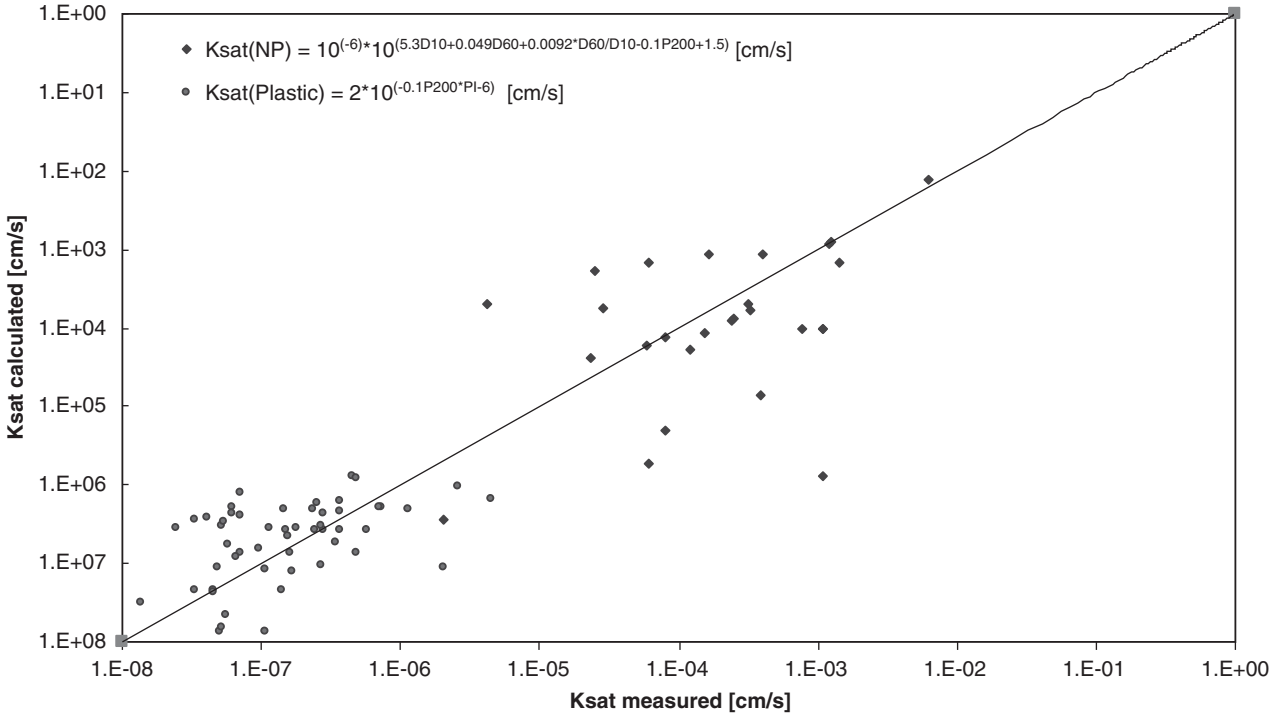

Figure 45. Performance of improved* k-sat Model *for plastic and non-plastic soils using the new dataset.

5.4.1 Compaction Model Currently Implemented in the EICM Version 2.6

The relationships are based on the Passing #200 (P_{200}), Diameter 60 (D_{60}), and Plasticity Index (PI). The following steps constitute the Compaction Model:

1. Identify the layer as a compacted base course, compacted subgrade, or natural in situ subgrade.
2. Calculate the optimum degree of saturation, S_{opt}:

$$S_{opt} = 6.752\ (P_{200}PI)^{0.147} + 78 \tag{82}$$

3. Compute the optimum gravimetric moisture content, w_{opt}:
   a) If $P_{200}PI > 0$ (plastic materials):

$$w_{opt} = 1.3\ (P_{200}PI)^{0.73} + 11 \tag{83}$$

   b) If $P_{200}PI = 0$ (granular, non-plastic materials):

$$w_{opt\,(T99)} = 8.6425\ (D_{60})^{-0.1038} \tag{84}$$

      i. If layer is not a base course

$$w_{opt} = w_{opt\,(T99)} \tag{85}$$

      ii. If layer is a base course

$$\Delta w_{opt} = 0.0156[w_{opt(T99)}]^2 - 0.1465 w_{opt(T99)} + 0.9 \tag{86}$$

$$w_{opt} = w_{opt\,(T99)} - \Delta w_{opt} \tag{87}$$

4. Compute $\gamma_{d\,max}$ for compacted materials, $\gamma_{d\,max\,comp}$

$$\gamma_{d\,max\,comp} = \frac{G_s \gamma_{water}}{1 + \dfrac{w_{opt} G_s}{S_{opt}}} \tag{88}$$

5. Compute $\gamma_{d\,max}$
   a) If layer is a compacted material

$$\gamma_{d\ \max} = \gamma_{d\ \max\,comp} \tag{89}$$

   b) If layer is a natural in situ material

$$\gamma_d = 0.90 \gamma_{d\ \max\,comp} \tag{90}$$

   EICM uses γ_d for $\gamma_{d\,max}$.
6. Compute the volumetric water content, θ_{opt}

$$\theta_{opt} = \frac{w_{opt} \gamma_{d\ \max}}{\gamma_{water}} \tag{91}$$

5.4.2 Improvement to the Compaction Model

Analysis of the Compaction Model conducted in this project found that for natural in situ materials, the approximation used in Equation 90 could be improved. The following equation to estimate the unit weight of the in situ materials was found to be better than the equation previously used:

$$\gamma_d = 0.81944 \gamma_{d\ \max\,comp} + 18.485 \tag{92}$$

where

γ_d = Unit weight of the in situ material (pcf)
$\gamma_{dmax\,comp}$ = Maximum dry unit weight of the compacted material (pcf)

This equation replaces $\gamma_d = 0.9 \gamma_{d\ \max\,comp}$

CHAPTER 6

Summary and Conclusions

This report has presented the results of the research conducted under NCHRP Project 9-23, "Environmental Effects in Pavement Mix and Structural Design Systems," with the objective of evaluating, calibrating, and validating the EICM. The EICM is a one-dimensional, coupled heat and moisture flow model originally developed for FHWA and adopted as the climatic model in the MEPDG software (Version 0.7, released July 2004) developed under NCHRP Project 1-37A. The EICM is intended to help predict or simulate the changes in behavior and characteristics of pavement and unbound materials in conjunction with varying environmental conditions over years of service.

In order to evaluate and calibrate the EICM, 30 sites were selected for field investigation; these included 28 LTPP sites, the MnRoad test facility, and the WesTrack test facility. At each site, three locations, 3 feet apart, located along the center of the outer lane of the pavement were cored, and soil samples were collected representing each unbound layer beneath the pavement. At 18 LTPP SMP sites, the three locations were cored near the TDR instrumentation hole just outside the respective test section, in the transition zone either at the start or end of the section. At non-SMP sites, there was no TDR instrumentation and, therefore, sampling was performed in one of the two transition zones approximately 8 to 10 feet from the test section. Typically, three sand cone tests and samples from the granular base and six tube samples from the subgrade were obtained from each site. In addition, a tube sample or a grab sample was collected from the side of the highway away from the shoulder. If cracks were present in the pavement, one of the three locations (or a fourth location) was chosen in proximity to the crack. A total of 84 sand cone tests were performed in situ. Eighty-four HMA cores were taken, along with 165 tube samples for asphalt and soil characterization.

The laboratory testing program included 257 moisture content determination tests, 251 dry density determinations, 144 grain size distribution curves, 148 Atterberg limits tests, 104 specific gravity tests, 64 saturated hydraulic conductivity tests, and 85 SWCC determinations.

Table 18 presents the mean, maximum, minimum, and coefficient of variation of the soil properties for non-plastic and plastic soils. In addition to the tests performed on soil samples, 22 hydraulic conductivity tests were performed on the HMA cores obtained from the HMA pavement sites.

In addition to the data collected at the project field sites, parameters and information needed to complete the input set to run the EICM, as well as parameters to validate the models were extracted from the following existing databases: LTPP Database, MnRoad, WesTrack, and ADOT Database.

The hydraulic conductivity of 22 large cores of HMA material was measured. Hydraulic conductivity was found to be too low to account for any significant water infiltration through the HMA mix layers. Very few cracks were found at the 30 sites. In a few cases where cracks were found, the water content adjacent to the crack was measured and found to be not statistically significantly higher than other locations away from the crack.

The equilibrium moisture condition in the EICM Version 2.6 was originally based on a suction model that depends on the water table depth and on a SWCC model that is functionally dependent on simple soil properties. This project found that sources of error in the prediction of moisture content were primarily related to the suction model. Further analysis led to a much more accurate approach for suction computations through the use of the specific models discussed in this report.

The new Suction model eliminates the use of the water table depth as the basis for the prediction and incorporates an approach based on the TMI. To a significant degree, this index balances lateral infiltration and evaporation for a particular region. Although the recommended TMI methodology (new Suction models) has an empirical component, the new model has been found to improve the prediction of the equilibrium moisture for the granular bases significantly.

Table 18. Summary of laboratory results on unbound materials.

Parameter	Nonplastic soils			Plastic soils		
	Range	Mean	COV (%)	Range	Mean	COV (%)
Moisture content (%)	2 – 20	7	50	3 - 55	19	38
Dry density (pcf)	100 - 146	129	10	65 - 146	108	12
Plasticity Index	NP	NP	--	1 – 42	15	57
Degree of saturation (%)	27 – 100	74	29	16 – 100	81	20
Matric suction (kPa)	3 - 150	28	109	20 - 1100	179	122
Specific gravity	2.60 – 2.88	2.73	2.3	2.64 – 2.87	2.74	1.7
Hydraulic conductivity (ft/hr)	3E-5 – 0.7	7	2	4E-6 – 1E-2	6E-4	340

In addition to the new Suction Model, new or re-calibrated models such as the SWCC models, the specific gravity model (Gs Model), the saturated hydraulic conductivity model (*k-sat* Model), and the Compaction Model were developed based on the extensive database gathered from the field. The EICM with improved, more accurate models is incorporated in the MEPDG software Version 1.0 (released June 2007).

References

Ahuja, L. R., J. W. Naney, and R. D. Williams (1985) "Estimating Soil Water Characteristics from Simpler Properties or Limited Data," *Soil Science Society of America Journal,* Vol. 49, No. 5, pp. 1100-1105.

Aitchison, G. D. (ed.) (1965) *Moisture Equilibria and Moisture Changes in Soils Beneath Covered Areas,* A Symposium in Print, Australia Butterworths.

Aitchison, G. D., and B. G. Richards (1965) A Broad Scale Study of Moisture Conditions in Pavement Subgrades throughout Australia – Factors in Planning a Regional Study of Moisture Variation in Pavement Subgrades. *Moisture Equilibria and Moisture Changes in Soils Beneath Covered Areas*, A Symposium in Print, Australia Butterworths, pp. 184 to 190.

Aitchison, G. D., and B. G. Richards (1965) A Broad Scale Study of Moisture Conditions in Pavement Subgrades throughout Australia – Techniques Adopted for the Measurements of Moisture Variables. *Moisture Equilibria and Moisture Changes in Soils Beneath Covered Areas*, A Symposium in Print, Australia Butterworths, pp. 191 to 204.

Aitchison, G. D., and B. G. Richards (1965) A Broad Scale Study of Moisture Conditions in Pavement Subgrades throughout Australia – Field Studies. *Moisture Equilibria and Moisture Changes in Soils Beneath Covered Areas,* A Symposium in Print, Australia Butterworths, pp. 205 to 225.

Aitchison, G. D., and B. G. Richards (1965) A Broad Scale Study of Moisture Conditions in Pavement Subgrades throughout Australia – The Selection of Design Values for Soil Suction Equilibria and Soil Suction Changes in Pavement Subgrades. *Moisture Equilibria and Moisture Changes in Soils Beneath Covered Areas*, A Symposium in Print, Australia Butterworths, pp. 226 to 232.

Barbour, S. L., et al. (1996) Prediction of Moisture Movement in Highway Subgrade Soils. *Proceedings of the 45th Canadian Geotechnical Conference: Innovation, Conservation, and Rehabilitation,* Paper No. 41A, October 1996, pp. 41A-1 to 41A-13.

Basma, A. A., and T. I. Al-Suleiman (1991) "Climatic Consideration in New AASHTO Flexible Pavement Design," *Journal of Transportation Engineering,* Vol. 117, No. 2, March/April 1991, pp. 210 to 223.

Climatic Atlas of USA, Disk 1–Contiguous 48 States (CD-ROM). (2000) National Climatic data Center, National Oceanic and Atmospheric Administration, September 2000.

Coleman, J. D. (1965) Geology, Climate and Vegetation as Factors Affecting Soil Moisture. *Moisture Equilibria and Moisture Changes in Soils Beneath Covered Areas*, A Symposium in Print, Australia Butterworths, pp. 93 to 99.

Cresswell, H. P. and Z.Paydar (1996) "Water Retention in Australian Soils. 1. Description and Prediction Using Parametric Functions," *Australian Journal of Soil Research,* Vol. 34, No. 2, pp. 195–212.

De Bruijn, C. M. A. (1965). Annual Redistribution of Soil Moisture Suction and Soil Moisture Density Beneath Two Different Surface Covers and the Associated Heaves at the Onderstepoort Test Site near Pretoria. *Moisture Equilibria and Moisture Changes in Soils beneath Covered Area*s, A Symposium in Print, Australia Butterworths, pp. 122–134.

De Bruijn, C. M. A. (1965) Some Observations on Soil Moisture beneath and Adjacent to Tarred Roads and Other Surface Treatments in South Africa. *Moisture Equilibria and Moisture Changes in Soils beneath Covered Areas,* A Symposium in Print, Australia Butterworths, pp. 135–142.

Eigenbrod, K. D., G. J. A. Kennepohl. (1996) "Moisture Accumulation and Pore Water Pressures at Base of Pavements," *Transportation Research Record 1546*, November 1996, pp. 151–161.

Epps, J., et al. (2002) *NCHRP Report 455*: *Recommended Performance-Related Specification for Hot-Mix Asphalt Construction: Results of the WesTrack Project*. Transportation Research Board, National Research Council. Washington, D.C.

Farouki, O. (1982). *Evaluation of Methods for Calculating Soil Thermal Conductivity*. US Army Corps of Engineers, Cold Regions Research & Engineering Laboratory (CRREL). Hanover, N. H. Report 82–8.

Fredlund, D. G. and H. Rahardjo (1993) *Soil Mechanics for Unsaturated Soils*. John Wiley & Sons, Inc.

Fredlund, D. G. and A. Xing (1994) "Equations for the Soil-Water Characteristic Curve," *Canadian Geotechnical Journal*, Vol. 31, No. 4, pp. 521–532.

Fredlund, D. G., et al. (1995) "The Relationship of the Unsaturated Shear Strength to the Soil-Water Characteristic Curve," *Canadian Geotechnical Journal*, Vol. 32, pp. 440–448.

Ghosh, R. K. (1980) "Estimation of Soil-Moisture Characteristics from Mechanical Properties of Soils," *Soil Science,* Vol. 130, No. 2, pp. 60–63.

Kern, J. S. (1995) "Evaluation of Soil–Water Retention Models Based on Basic Soil Physical Properties," *Soil Science Society of America Journal,* Vol. 59, No. 4, pp. 1134–1141.

Klemunes, Jr., J. A. (1995) *Determining Soil Volumetric Moisture Using Time Domain Reflectometry*. MS Thesis, University of Maryland, Maryland.

Larsen, David C., ed. (1982) *Thermal Conductivity 16*. Also in *Proceedings of Sixteenth International Thermal Conductivity Conference*. IIT Research Institute. Nov 7–9, 1979, Chicago, Illinois.

Leong, E. C. and H. Rahardjo (1996) "A Review on Soil-Water Characteristic Curve Equations," *Geotechnical Research Report*, NTU/GT/96-5,

Nanyang Technological University, NTU-PWD Geotechnical Research Center, Singapore.

LTPP Information Management System Data, Release 15.0, Version 2002.11. (2003). Primary Data Set All QC Levels, Vol. 1, January 2003.

LTPP Seasonal Monitoring Program: Instrumentation, Installation, and data Collection Guidelines. (1994). U. S. Department of Transportation, Federal Highway Administration, FHWA-RD-94–110, April 1994.

McKeen, R. G. and L. D. Johnson (1990) "Climate-Controlled Soil Design Parameters for Mat Foundations," *Journal of Geotechnical Engineering*, Vol. 116, No. 7, July 1990, pp 1073–1094.

Moats, C. D. (1994) *Satellite Estimates of Shortwave Surface Radiation and Atmospheric Meteorology for the BOREAS Experiment Region*. National Aeronautics and Space Administration. Microform.

Nandagiri, L. and R.Prasad (1997) "Relative Performances of Textural Models in Estimating Soil Moisture Characteristics," *Journal of Irrigation and Drainage Engineering–ASCE,* Vol. 123, No. 3, pp. 211–214.

NCHRP 2002 Design Guide – Pavement Analysis and Design System. ERES Division, Applied Research Associates and Arizona State University, NCHRP 1-37a, Version 0.089, January 2003.

Pellinen, T.K. (2001). *Investigation of the Use of Dynamic Modulus as an Indicator of Hot-Mix Asphalt Performance*. Ph.D. Dissertation, Arizona State University, Tempe Arizona.

Rawls, W. J., L. R. Ahuja, and D. L. Brakensiek (1992) Estimating Soil Hydraulic Properties from Soils Data. *Proceedings of the International Workshop on Indirect Methods for Estimating the Hydraulic Properties of Unsaturated Soils,* van Genuchten, M. Th., Leij, F. J., and Lund, L. J., editors. University of California. Riverside, California. pp. 329–340.

Richards, B. G. (1965) Measurement of the Free Energy of Soil Moisture by the Psychrometric Technique Using Thermistors. *Moisture Equilibria and Moisture Changes in Soils Beneath Covered Areas*, A Symposium in Print, Australia Butterworths, pp. 39–46.

Richards, B. G. (1965) An Analysis of Subgrade Conditions at the Horsham Experiment Road Site using the Two-Dimensional Diffusion Equation on a High-speed Digital Computer. *Moisture Equilibria and Moisture Changes in Soils Beneath Covered Areas*, A Symposium in Print, Australia Butterworths, pp. 243–258.

Richards, B. G. (1967) Moisture Flow and Equilibria in Unsaturated Soils for Shallow Foundations. *Permeability and Capillarity of Soils*, ASTM Special Technical Publication No. 417, American Society for Testing and Materials, 1967, pp. 4–34.

Robertson, Eugene C. and B. S. Hemingway (1995) *Estimating Heat Capacity and Heat Content of Rocks.* U.S. Geological Survey. Microfiche.

Russam, K. (1965) The Prediction of Subgrade Moisture Conditions for Design Purposes. *Moisture Equilibria and Moisture Changes in Soils Beneath Covered Areas*, A symposium in Print, Australia Butterworths, pp. 233–236.

Russam, K. and J. D. Coleman (1969) "The Effect of Climatic Factors on Subgrade Moisture Conditions," *Geotechnique*, Vol. XI, No. 1, March 1961, pp 22–28.

Smettem, K. R. J., and P. J. Gregory (1996) "The Relation Between Soil Water Retention and Particle Size Distribution Parameters for Some Predominantly Sandy Western Australian Soils," *Australian Journal of Soil Research*, Vol. 5, No. 38, pp 695–708.

Soil Vision User's Guide, Version 2, 1st Edition. (2000). Soil Vision Systems Ltd., Saskatoon, Saskatchewan, Canada.

Tomasella, J. and M. G. Hodnett (1998) "Estimating Soil Water Retention Characteristics from Limited Data in Brazilian Amazonia," *Soil Science,* Vol. 163, No. 3, pp. 190–202.

Tye, R.P. (1969) *Thermal Conductivity*. Academic Publishers, London, New York.

University Of Minnesota – Center for Transportation Studies (1997) *Investigation of Hot Mix Asphalt Mixtures at MnRoad*, Report Number 97–06.

Von Quintus, H. (2001) *Calibration and Validation of the Fatigue Cracking and Rutting Prediction Models for the 2002 Design Guide*. NCHRP 1-37A Interim report. March 20, 2001.

Way, G. (1980) *Environmental Factor Determination from In-Place Temperature and Moisture Measurements under Arizona Pavements.* FHWA/AZ Report 80/157. September 1980.

Williams, J., et al. (1983) "The Influence of Texture, Structure and Clay Mineralogy on the Soil Moisture Characteristic," *Australian Journal of Soil Research*, Vol. 21, pp. 15–32.

Williams, R. D. and L. R. Ahuja (1992) Estimating Soil Water Characteristics Using Measured Physical Properties and Limited Data. *Proceedings of the International Workshop on Indirect Methods for Estimating the Hydraulic Properties of Unsaturated Soils,* van Genuchten, M. Th., Leij, F. J., and Lund, L. J., editors. University of California. Riverside, California, pp. 405–416.

van Genuchten, M. Th. and F. J. Leij (1992) On Estimating the Hydraulic Properties of Unsaturated Soils. *Proceedings of the International Workshop on Indirect Methods for Estimating the Hydraulic Properties of Unsaturated Soils.* van Genuchten, M. Th., Leij, F. J., and Lund, L. J., editors. University of California. Riverside, California. pp. 1–14.

Yaws, C. L. (1997) *Handbook of Thermal Conductivity*. Gulf Pub. Co. Houston, Texas.

Zapata, C. E. (1999) *Uncertainty in Soil-Water Characteristic Curve and Impacts on Unsaturated Shear Strength Predictions.* Ph. D. Dissertation, Arizona State University, Tempe, Arizona.

Zapata, C. E., et al. (2000) Soil-Water Characteristic Curve Variability. In: C. D. Shackelford, S. L. Houston, and N-Y Chang (eds). *Advances in Unsaturated Geotechnics.* ASCE – GEO Institute Geotechnical Special Publication, No. 99. Also *Proceedings of Sessions of Geo-Denver 2000,* Aug. 5-8, 2000, Denver, Colorado. pp. 84–124.

Abbreviations and acronyms used without definitions in TRB publications:

AAAE	American Association of Airport Executives
AASHO	American Association of State Highway Officials
AASHTO	American Association of State Highway and Transportation Officials
ACI–NA	Airports Council International–North America
ACRP	Airport Cooperative Research Program
ADA	Americans with Disabilities Act
APTA	American Public Transportation Association
ASCE	American Society of Civil Engineers
ASME	American Society of Mechanical Engineers
ASTM	American Society for Testing and Materials
ATA	Air Transport Association
ATA	American Trucking Associations
CTAA	Community Transportation Association of America
CTBSSP	Commercial Truck and Bus Safety Synthesis Program
DHS	Department of Homeland Security
DOE	Department of Energy
EPA	Environmental Protection Agency
FAA	Federal Aviation Administration
FHWA	Federal Highway Administration
FMCSA	Federal Motor Carrier Safety Administration
FRA	Federal Railroad Administration
FTA	Federal Transit Administration
IEEE	Institute of Electrical and Electronics Engineers
ISTEA	Intermodal Surface Transportation Efficiency Act of 1991
ITE	Institute of Transportation Engineers
NASA	National Aeronautics and Space Administration
NASAO	National Association of State Aviation Officials
NCFRP	National Cooperative Freight Research Program
NCHRP	National Cooperative Highway Research Program
NHTSA	National Highway Traffic Safety Administration
NTSB	National Transportation Safety Board
SAE	Society of Automotive Engineers
SAFETEA-LU	Safe, Accountable, Flexible, Efficient Transportation Equity Act: A Legacy for Users (2005)
TCRP	Transit Cooperative Research Program
TEA-21	Transportation Equity Act for the 21st Century (1998)
TRB	Transportation Research Board
TSA	Transportation Security Administration
U.S.DOT	United States Department of Transportation